

**X-linked inhibitor of apoptosis protein in intestinal
homeostasis and the pathogenesis of inflammatory
bowel disease**

Dissertation

in fulfilment of the requirements for the degree “Dr. rer. nat.”
of the Faculty of Mathematics and Natural Sciences
at Kiel University

Submitted by
Shreya Gopalakrishnan
Kiel, 2018

First referee:	Prof. Dr. med. Sebastian Zeissig
Second referee:	Prof. Dr.Dr.h.c. Thomas C. G. Bosch
Date of the oral examination:	29.08.2018
Approved for publication:	

Table of Contents

1. Introduction	1
1.1 The lower gastrointestinal tract.....	1
1.1.1 Microbial components in the lower GI tract	1
1.1.2 The intestinal epithelium	2
1.1.3 Paneth cells and their functions in the gut.....	6
1.1.3.1 Paneth cell antimicrobial peptides as chemical barriers of the gut	7
1.1.3.1.1 Types of Paneth cell antimicrobial peptides.....	7
1.1.3.1.2 Paneth cell-dependent regulation of commensal microbiota and host immunity.....	11
1.1.3.2 Regulation of the intestinal stem cell niche by Paneth cells	13
1.2 Inflammatory bowel disease	14
1.2.1 The microbiota in IBD.....	15
1.2.2 Genetic factors in IBD	18
1.2.2.1 X chromosome-linked inhibitor of apoptosis protein variants in early-onset Crohn's disease	20
1.2.3 Paneth cell dysfunction in Crohn's disease.....	21
1.3 X chromosome-linked inhibitor of apoptosis protein	23
1.3.1 XIAP structure.....	24
1.3.2 XIAP in the regulation of TNF-dependent cell death pathways.....	25
1.3.2.1 TNFR1 signaling.....	25
1.3.2.2 XIAP-dependent regulation of ripoptosome	27
1.3.2.3 XIAP-dependent regulation of caspases	29
1.3.3 XIAP in the regulation of innate and adaptive immunity	31
1.3.3.1 XIAP-dependent regulation of the inflammasome pathway	31
1.3.3.2 XIAP-dependent induction of the TGF- β and BMP signaling	33
1.3.3.3 XIAP-dependent control of Dectin-1 signaling	34
1.3.3.4 XIAP-dependent regulation of NOD1/2 signaling.....	36
1.3.3.5 XIAP-dependent control of adaptive immunity.....	37
1.4 Purpose of the current study.....	38
2. Materials and methods.....	39

2.1 Materials	39
2.1.1 List of antibodies	39
2.1.2 List of probes and primers.....	40
2.1.3 Buffers, solutions and media	42
2.1.4 Kits	44
2.1.5 Reagents and chemicals.....	44
2.1.6 Instruments	46
2.1.7 Consumables	47
2.1.8 Software.....	48
2.2 Methods.....	49
2.2.1 Mice	49
2.2.2 <i>Helicobacter hepaticus</i> infection.....	49
2.2.3 Immunofluorescence staining.....	50
2.2.4 Hematoxylin and eosin staining and histopathological evaluation.....	51
2.2.5 Fluorescence <i>in situ</i> hybridization staining.....	51
2.2.6 RNA extraction and quantitative polymerase chain reaction	52
2.2.7 Bacterial killing assay.....	52
2.2.8 Flow cytometry	54
2.2.9 16S rRNA sequencing for detection of bacteria in tissues	55
2.2.10 Dextran sulfate sodium-induced colitis.....	55
2.2.11 Colon explant culture and enzyme-linked immunosorbent assay.....	56
2.2.12 Image capture and analysis	56
2.2.13 Statistical analysis.....	56
3. Results	57
3.1 XIAP regulates Paneth cell homeostasis.....	57
3.2 Microbial-dependent TNF signaling mediates PC death in <i>Xiap</i> ^{-/-} mice	60
3.3 XIAP is required for control of the commensal intestinal microbiota	64
3.4 Absence of spontaneous intestinal inflammation in <i>Xiap</i> ^{-/-} mice	67
3.5 Deficiency in <i>Xiap</i> is associated with susceptibility to microbiota-induced intestinal inflammation	69
3.6 Increased susceptibility to chemically-induced colitis in <i>Xiap</i> ^{-/-} mice.....	71

3.6.1 Increased colitis susceptibility in <i>Xiap</i> ^{-/-} mice is maintained in the absence of the adaptive immune system	74
3.7 Intestinal epithelial- or myeloid-specific deletion of <i>Xiap</i> is not sufficient to elicit PC death or susceptibility to intestinal inflammation	75
4. <i>Discussion and outlook</i>	80
5. <i>Conclusion</i>	86
<i>Summary</i>	87
<i>Zusammenfassung</i>	89
6. <i>References</i>	91
<i>Appendix</i>	120
List of Abbreviations	120
List of figures	123
List of tables	124
<i>Declaration</i>	125
<i>Curriculum Vitae</i>	126
<i>Acknowledgements</i>	128

1. Introduction

1.1 The lower gastrointestinal tract

The lower gastrointestinal (GI) tract is the region of the digestive system that extends to about 200-400 m² and is composed of the small intestine and the large intestine, lined by epithelial surfaces called columnar intestinal epithelial cells (IECs). Anatomically, from the proximal to the distal end, the small intestine comprises the duodenum, the jejunum, and the ileum, and the large intestine consists of the caecum, the colon, and the rectum. Acting as gatekeepers, the IECs separate vast numbers of resident microbes known as the commensal microbiota (also called commensal bacteria, commensal microbes or commensals), in the lumen from the host. Tightly regulated interactions occur between the host and the commensal microbiota which forms the critical feature of intestinal homeostasis. Breach of such homeostatic environment is commonly observed in diseases such as inflammatory bowel disease (IBD).

1.1.1 Microbial components in the lower GI tract

The density of intestinal microbes in the human lower GI tract collectively sums to 10¹³-10¹⁴.¹ The concentration of these microbes progressively increases from the small intestine to the large intestine. Within the duodenum and the jejunum of the human small intestine, the concentration of luminal and mucosa-associated microbes is about 10³-10⁵, in the ileum it is about 10⁸ and in the large intestine, about 10¹⁰-10¹².² The microbial ecosystem along the lower GI tract consists of several diverse species belonging to Eukarya, Archea, and Eubacteria.³ Amongst these, two different bacterial phyla, the Bacteroidetes and the Firmicutes, are the most abundant in the gut. However, other bacterial phyla that are commonly present but less abundant include the Proteobacteria, Actinobacteria Verrucomicrobia, Tenericutes, Deferribacteres, and Fusobacteria.^{3,4} Collectively, in healthy individuals, the different commensal microbiotas co-exist in a symbiotic relationship with the host to help mediate proper physiological functioning of the host and prevent the dominance of gut-associated microbes capable of causing pathogenesis (pathobionts) or invading pathogens. There are several ways by which the commensal microbiota prevents the dominance of the pathobionts and pathogens. The commensal microbes produce toxins, which act against pathogenic members of their own or similar species. For instance, bacteriocins

produced by indigenous *Escherichia coli* of the Proteobacteria phylum, inhibit the growth of enterohaemorrhagic *E. coli* O157:H7.⁵ The commensal microbiota can also alter the local pH in the intestine to inhibit the growth of selective pathogens. In particular, the *Bifidobacterium* spp., of the Actinobacteria phylum acidify the intestinal environment to inhibit the growth of *E. coli* O157:H7.⁶ Moreover, commensals also consume amino acids and nutrients required for the growth of pathogens leading to the starvation of pathogens, thereby restricting the expansion of the pathogens. For example, the indigenous *E. coli* consumes proline that is needed for the growth of *E. coli* O157:H7, thus limiting the abundance of *E. coli* O157:H7.⁷

The commensal microbiotas also prevent pathogen domination by promoting host immunity. The commensals express microbiota-associated molecular patterns (MAMPs) which are recognized by receptors present in the host cells called pattern recognition receptors (PRRs).^{8,9} The different families of PRRs include the Toll-like receptors (TLRs), the nucleotide-binding domain and leucine-rich repeat containing receptors (NLRs), and the retinoic acid-inducible gene-I (RIG-)-like receptors (RLRs).¹⁰ The initial recognition of MAMPs by the PRR allows for signaling mechanisms involving nuclear factor kappa-light-chain-enhancer of activated B cells (NF- κ B) in the host. These signaling mechanisms subsequently lead to the expression and production of various host factors that further control the abundance of commensal microbiota to prevent pathogen invasion.¹¹ For example, MAMP-PRR interactions are important to generate efficient quantities of host chemical barriers called anti-microbial peptides (AMPs), that further shape the abundance and communities of commensals to prevent pathogen invasion.¹² Notably, although certain AMPs are expressed at germ-free (GF) conditions, some of these AMPs require PRR stimulation by MAMPs to be expressed.¹² Thus, the commensal microbiotas play key roles in keeping pathogens at bay and the commensal-host interactions shape the host immunity which further regulates the commensal microbiota to inhibit pathogen intrusion.¹³

1.1.2 The intestinal epithelium

The IECs that connect the host and environment in the gut are structurally organized as glandular invaginations, called the crypts of Lieberkühn, which are intercalated with protrusions of villi and microvilli, specifically in the small intestine. Extensive chemical and nutrient absorption from food occurs in the small intestine that is mediated by the

presence of these villi and microvilli. In contrast, the large intestine lacks villi, forming a flat mucosal surface that allows little absorption of food and aids in the movement of the stool.

The IECs undergo rapid turnover that takes in average about 3-5 days in the small intestine and 6-7 days in the colon. This process is driven by the intestinal stem cells (ISCs) that lie at the bottom of small intestinal crypts (**Fig. 1.1**).¹⁴ The ISCs exist as crypt base columnar cells (CBCs), that express leucine-rich repeat-containing G protein-coupled receptor 5 (*Lgr5*), and generate rapidly proliferating progenitor cells called transit-amplifying (TA) cells.^{15,16} These TA cells which are localized to the central region of the crypts differentiate into either the absorptive or secretory cell lineage. Absorptive enterocytes, secretory goblet, enteroendocrine, tuft cells and M cells migrate upwards, mature and live to approximately 3-5 days. In contrast, Paneth cells (PCs) that are present only in the small intestine, reside intermingled with CBCs and are long-lived, for about 20 days (**Fig. 1.1**).^{15,17,18} There also exists a quiescent stem cell population residing four positions from the crypt base (+4 position) directly above PCs, which is believed to restore the CBC stem cells upon damage.^{14,19,20}

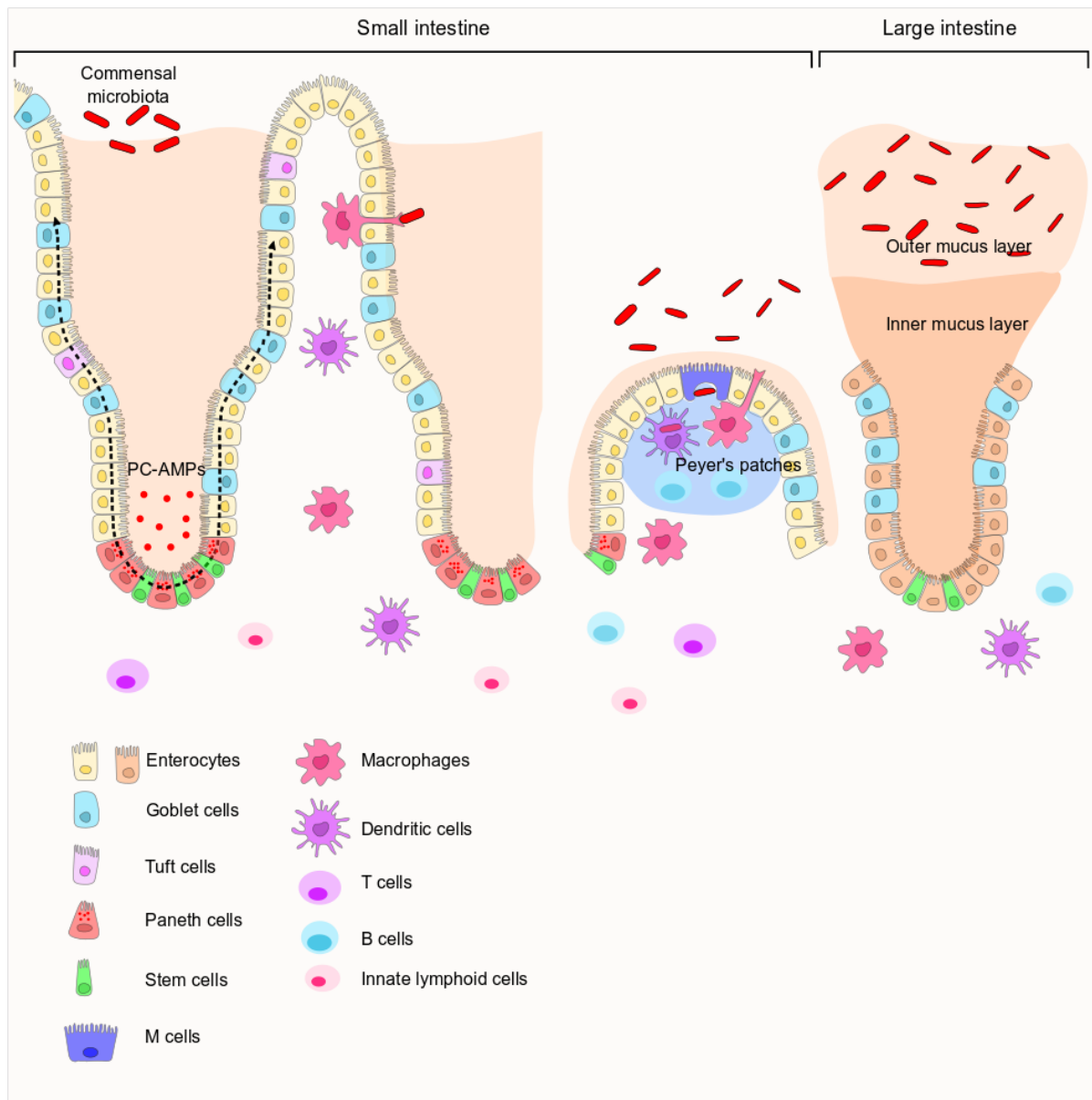


Figure 1.1 The intestinal epithelium

IECs in the lower GI tract act as gatekeepers, separating vast numbers of commensal microbiota in the lumen from the host. IECs undergo rapid turnover driven by ISC, which lie adjacent to PCs at the bottom of the crypts. IECs with the exception of PCs, migrate upwards, indicated by black dashed arrows. The PCs and goblet cells secrete PC-AMPS and mucus which regulate the commensal microbiota and act as host chemical barriers. Amongst all the IECs, the M cells in particular are involved in active transportation of luminal contents to the myeloid and the lymphoid cells present in the underlying Peyer's patches and lamina propria. The host and resident microbes have regulated interactions which forms the central feature of intestinal homeostasis. Adapted from Peterson *et al.*, (2014).²¹

The absorptive enterocytes, which make up over 80% of the IECs, aid in nutrient and water absorption from the luminal contents. The enterocytes contain closely placed microvilli that comprise the filamentous brush border glycocalyx, which is a group of

carbohydrate moieties of glycolipids and glycoproteins.^{15,22,23} The presence of microvilli on the surface of IECs not only aids in the absorption process, but is also vital for sampling the commensal microbes in the lumen to mediate immune tolerance in the host.^{24,25}

Certain IECs are responsible for secreting factors that physically protect the host. The goblet cells secrete mucus that is composed of glycoproteins called mucins and gastric peptides known as trefoil factors.^{26,27} The mucus layer plays dual roles of barrier protection to the host from luminal contents and lubricant to the mucosal surface.^{27,28} The mucus layer in the small intestine exists as a thin layer which is penetrated by microbes. However, in the large intestine, it exists as two different layers, where the outer layer is penetrable by microbes and the inner layer is non-penetrable and firmly attached to the colonic epithelium (**Fig. 1.1**).^{29,30}

The epithelium also offers chemical barriers at the mucosal surface in the form of AMPs, which are predominantly secreted by PCs. As mentioned above, the AMPs are responsible for regulating the microbial numbers and shaping microbial communities in the gut.³¹ In addition to protecting the host, the gut produces hormones that play key roles in the modulation of the appetite, regulation of metabolite production in the microbiota and enablement of cross-talk with the brain immune cells.^{32–34} The hormone production in the lower GI tract in response to meal-related stimuli is carried out by the secretory enteroendocrine cells (EECs) (**Fig. 1.1**).³⁵

A unique population of IECs called the tuft cells (also known as brush, caveolated or solitary chemosensory cells) share close morphology to taste-receptor cells and are a subject of investigation in intestinal homeostasis.³⁶ They are predicted to be involved in allergy control, which is based on the key observation that they initiate type-2 mediated adaptive immune responses and produce cytokines like interleukin (IL-) 25 (IL-25) and IL-13, in response to helminth infections in the gut.^{37,38}

A special type of IECs called follicle-associated epithelium (FAE) lie over isolated and organized lymphoid follicles called Peyer's patches in the small intestine. Under constitutive conditions, about 10% of this FAE comprises M cells (**Fig. 1.1**) that actively sample the luminal contents and transport them to the myeloid and lymphoid cells

present in the underlying follicles and lamina propria compartments via the process of phagocytosis and transcytosis to initiate immune tolerance.^{39,40}

Following maturation and migration towards the villi, the IECs shed off into the lumen with age and die due to programmed cell death or apoptosis. Maintenance of intestinal homeostasis requires a constant balance between cell proliferation and cell loss. The expulsion of IECs occurs by a regulated mechanism where the tight junction and cytoskeletal proteins in the cell membrane undergo re-arrangement.⁴¹ This is followed by the expulsion of cells due to tension build-up by the action of proteins called Rho-associated kinases.⁴² Once the IECs are released from the villus tip, a spatial gap in the epithelium is formed that is sealed by the tight junction proteins thereby not compromising the barrier integrity under basal conditions in the intestine.⁴¹ Thus, the different IECs offer protection to the host from the lumen as well as mediate tightly regulated interactions with the commensal microbiota and the underlying immune system of the host that eventually leads to a homeostatic environment in the gut.

1.1.3 Paneth cells and their functions in the gut

PCs were discovered by Gustav Schwalbe in 1869 but later named and described by Josef Paneth in 1884.^{43,44} The PCs are characterized by a unique morphology defined by pyramidal shape with the presence of granules in their cytoplasm. The extensive network of endoplasmic reticulum and Golgi bodies in the PC, reflects their secretory property and directs the large granules present in the cytoplasm to the apical side of the cells.¹² The contents of the PC granules remained elusive until 1967 when the discovery of lysozyme in the PC granules led to the first idea that PCs may have a role in defense function of the host.⁴⁵ With time, the discovery of several families of AMPs in these granules confirmed the central role of PCs in innate defenses in the gut.

PCs can be identified by histochemical stains such as eosin or periodic acid Schiff's stain that stains the secretory granules, in accordance with the cationic charge of the granules.^{46,47} More recently, antibodies against the AMPs are used to detect the PCs by means of immunostaining. PCs in humans start to appear at 13.5 weeks post-gestation period in both the small intestine and in the colon, however, by 17 weeks of gestation, the PCs are confined to the small intestine.⁴⁸ In rodents, PCs appear from the day of birth only in the small intestine and increase in the number between 14 to

28 days after birth, yet they do not appear in the colon.⁴⁹ While PCs are usually confined to the small intestine of healthy adults, they may occur unusually in the stomach or the colon during chronic inflammation where they are called metaplastic PCs.^{50,51} The metaplastic PCs are structurally identical to normal PCs, and secrete AMPs to protect damaged epithelium during inflammation against microbial invasion.⁵¹⁻⁵⁴

1.1.3.1 Paneth cell antimicrobial peptides as chemical barriers of the gut

At constitutive conditions, most IECs are capable of synthesizing AMPs, however, maximum production of different families of AMPs is observed by PCs.^{55,56} In the small intestine, the amount of AMPs produced by the PCs (PC-AMPs) increases from the proximal end to the distal end. In the large intestine low amounts of PC-AMPs in the lumen protect the host and regulate the microbiota.^{57,58} Investigations on GF mice have revealed that certain PC-AMPs are expressed independently of microbial stimulation whereas other PC-AMPs require microbial stimulus for their normal expression.⁵⁹ Importantly, the expression of all PC-AMPs is elevated following microbial stimulation.⁶⁰ Subsequent to stimulation with microbial products or pharmacological agonists, secretion of the granules containing AMPs is accompanied by increased levels of cytosolic calcium ions (Ca^{2+}) from within the cells as well as inflow of extracellular Ca^{2+} .^{61,62} The increase of Ca^{2+} levels associated with the granule release is enabled by the Ca^{2+} -dependent potassium channel KCa3.1 that is encoded by the gene *KCNN4*.⁶² Upon the release of the AMPs into the crypt lumen, the granules are moved further upwards by cystic fibrosis transmembrane regulator protein that is expressed on the apical side of the crypt cells present adjacent to the PCs.⁶³⁻⁶⁵

1.1.3.1.1 Types of Paneth cell antimicrobial peptides

PC-AMPs are cationic and confer protection against different bacteria, viruses, fungi, and parasites in the gut as described below and summarized in **table 1.1**. The different AMPs produced by PCs include α -defensins, cathelicidins, lysozyme C, group IIA phospholipase A2 (sPLA2), C type lectins and host defense-related ribonucleases.¹²

Table 1.1 Types of PC-AMPs

Name of the PC-AMP (humans)	Name of the PC-AMP (murine)	Mechanism of action	Antimicrobial activity
α -defensins	Cryptdin and Cryptdin-related sequence	Pore-inducing, long fibrils (nanonets)	Gram-negative and Gram-positive bacteria, fungi, parasites and viruses
Cathelicidin- LL-37	Cathelicidin-related antimicrobial peptide	Pore-inducing	Gram-positive and Gram-negative bacteria, fungi and some enveloped virus
C-type lectin-regenerating islet-derived protein III α (REGIII α)	(REGIII γ)	Pore-inducing	Gram-positive bacteria
sPLA2	sPLA2	Hydrolysis of phospholipids in cell membrane	Gram-positive bacteria
Lysozyme C	Lysozyme C (Lyz1)	Hydrolysis of peptidoglycan	Gram-positive, less extent Gram-negative bacteria
Angiogenin	Angiogenin 4	-	Gram-positive and Gram-negative bacteria

 α -defensins

The α -defensins are amongst the first antimicrobials to be described in mammals, which are constitutively expressed and comprise six conserved cysteine residues, stabilized by disulfide bonds.^{66,67} α -defensins are highly expressed by PCs in the intestinal epithelium and the α -defensin gene expressed by PCs spans over two

exons.^{68,69} The PC- α -defensins are of six types in humans: α -1, α -2, α -3, α -4 and human defensin 5 (HD5) and 6 (HD6), out of which HD5 and HD6 are the most characterized. In mice, α -defensins are known as crypt defensins or cryptdins, of which 27 isoforms dominate the small intestine of the mice.^{46,70,71} There exists enormous variability between the closely-related yet different cryptdin forms across the different strains of mice that makes the study of α -defensins in mice challenging.⁷² In mice, most enteric α -defensins are expressed as biologically inactive precursors called pro α -defensins. The pro α -defensins undergo cleavage by a protease enzyme called matrilysin or matrix metalloproteinase 7 (MMP-7) to form mature α -defensins, which are released from the PCs into the crypt lumen.⁷³ In compliance with the central role of MMP-7 in regulating α -defensins, studies on mice which carry deletions of *Mmp7* (*Mmp7*^{-/-} mice) have shown that these mice lack mature α -defensins in the small intestine due to which they display microbial imbalances also known as dysbiosis in their gut. Dysbiosis in *Mmp7*^{-/-} mice makes them more susceptible to infection with pathogens when compared to the wildtype (WT) mice.^{73,74} Although these mice lack mature α -defensins in the small intestine, investigations revealed the presence of mature forms of α -defensins in the colon and caecum of these mice, indicating possible alternative mechanisms of α -defensin processing in the large intestine.⁵⁸ The processing of immature α -defensins in humans follows a similar mechanism, however, this is carried out by the enzyme trypsin and not MMP-7.⁷⁵

In both mice and humans, α -defensins are secreted in response to lipopolysaccharide (LPS), and muramyl dipeptide (MDP), present on the cell wall of bacteria.⁶⁰ There are different mechanisms by which α -defensins induce bacterial killing. *In vitro* studies have revealed that when α -defensins associate with artificial lipid bilayer membranes, they form anionic permeable channels for conducting ions that induces microbial killing.⁷⁶ Accordingly, human defensin α -1 induces membrane pores and DNA fragmentation in the protozoan *Trypanosoma cruzi* which subsequently leads to the death of the protozoan.⁷⁷ Moreover, the α -defensin HD-6 also entraps bacteria and prevents bacterial entry into the epithelium by forming long fibrils.⁷⁸ As such, defensins offer wide antimicrobial activity against a variety of microbes including Gram-positive and Gram-negative bacteria, viruses, fungi and parasites.^{12,59,79–82}

In addition to the cryptdins, cryptdin-related sequences (CRS) are produced by PCs in mice whose pro-form has over 95% sequence similarity to the pro-form of α -defensins.⁸³ Six different CRS peptides are found in mice and exhibit similar antimicrobial activity when compared to α -defensins.⁸⁴ GF mice have very low levels of CRS peptides when compared to conventionally raised mice suggesting that CRS peptides require microbial stimulation to be expressed.⁸³

Cathelicidins

Another family of antimicrobials called cathelicidins are secreted by PCs which are polypeptides that comprise α -helical structures along with N-terminal cathepsin L inhibitor-like domain that is conserved across different vertebrates and a variable C-terminal region that carries the domain for antimicrobial activity.^{85,86} In humans, cathelicidins have two leucine amino acid residues among the 37 amino acids present, hence the name LL-37, and in mouse they are called cathelicidin-related antimicrobial peptide (mCRAMP).^{87,88} Their expression is induced by short chain fatty acids such as butyrate which is commonly found in fermentation products of undigested fiber from bacteria.⁸⁹ Similar to the defensins, they induce pores in the cell membrane of microbes and have antimicrobial activity towards a range of Gram-positive, Gram-negative bacteria, fungi and some enveloped virus.⁹⁰⁻⁹³

C-type lectins

PCs also secrete AMPs that belong to the family of C-type lectins, which in humans is called hepatocarcinoma-intestine-pancreas/pancreatitis-associated protein (HIP/PAP) and in mice is called regenerating islet-derived protein 3 γ (REG3 γ).^{94,95} The C-type lectins comprise a carbohydrate recognition domain and an N-terminal signal peptide which can bind peptidoglycan, a component of the bacterial cell wall.⁹⁴ Upon binding, the AMPs form a hexameric membrane-permeabilizing pore on the cell wall of Gram-positive bacteria that induces the bacterial killing.⁹⁶ C type lectins are induced by the TLR-myeloid differentiation primary response protein 88 (MyD88; an adaptor protein critical for TLR signaling) signaling following MAMP-PRR interactions. Their antimicrobial action occurs in the mucus layer of the gut, induced by the cleavage of their pro-peptide anionic N-terminal sequences by trypsin.⁹⁷⁻⁹⁹ Studies on *Reg3 γ ^{-/-}* mice revealed that this lectin is crucial for spatial segregation of microbes from the epithelium in the ileum. In the absence of Reg3 γ , mice display mucosal inflammation

with upregulation of cytokine Il-22 suggesting that PC-AMPs can also impact immune signaling.^{100,101}

sPLA2 and lysozyme C

PCs constitutively secrete antimicrobial enzymes such as sPLA2 and lysozyme C (LyzC), which have potent antimicrobial activities mediated by specific enzymatic mechanisms. sPLA2 has a preferential bactericidal activity towards Gram-positive bacteria. It penetrates through the cell wall and hydrolyses phospholipids in the cell membrane of bacteria, therefore destroying the membrane integrity.^{102–104} LyzC is a glycoside hydrolase enzyme that exists only in one form in humans, but in mice, are expressed by macrophages (encoded by *Lyz2* gene) and PCs (encoded by *Lyz1* gene).¹² LyzC hydrolyses the glycosidic bonds between N-acetylglucosamine and N-acetyl-muramic acid of peptidoglycan in the cell wall of the microbes to kill them.^{12,105–107}

Defense-related ribonucleases (Angiogenin)

A distinct and an important class of antimicrobials known as the defense-related ribonucleases (RNase) have recently been discovered. The murine angiogenin 4 (ANG4) and the human angiogenin (ANG) protein belong to the RNase superfamily, which is exclusively expressed by PCs and displays antimicrobial activity against a wide variety of Gram-positive and Gram-negative microbes.¹⁰⁸ The antimicrobial mechanism of ANG4 is still under investigation. The expression of *Ang4* from PCs is induced by microbial stimulation, and more specifically, previous studies have shown *Ang4* is expressed upon colonization with the microbe *Bacteroides thetaiotaomicron*.^{59,108}

1.1.3.1.2 Paneth cell-dependent regulation of commensal microbiota and host immunity

Years of study in mice models have helped us understand how PCs regulate the commensal microbiota (**Fig. 1.2**). Aforementioned, PCs play a key role in controlling microbial abundance in the gut. This has been demonstrated in mice which carry deletions of the NLR nucleotide-binding oligomerization domain-containing protein 2 (*Nod2*^{-/-} mice) that have defective expression of α -defensins, and therefore are unable to control the amounts of commensal microbiota in the ileum. In particular, *Nod2*^{-/-} mice

display increased abundance of mucosa-adherent bacteria in the ileum when compared to WT mice and the crypts isolated from *Nod2*^{-/-} mice show defects in bacterial killing *in vitro* when compared to crypts isolated from WT mice.¹⁰⁹ PCs also tightly shape the composition of the gut microbiota (**Fig. 1.2**). Accordingly, increased amounts of Firmicutes, more particularly, increased segmented filamentous bacteria (SFB), as well as low amounts of Bacteroidetes are detected in *Mmp7*^{-/-} mice that lack mature α -defensins. Whereas, an opposite trend is observed in mice that have transgenic expression of the human defensin HD5 (*DEFA5*-TG mice).⁷⁴

PC-AMPs also tightly shape the host immunity. Commensal bacteria in the lumen are recognized and taken up by the host myeloid dendritic cells which migrate to the mesenteric lymph nodes where they initiate adaptive immune tolerance.^{110–113} Ablation of PCs using mice that express diphtheria toxin under the control of the cryptdin-2 promoter, led to defective microbial killing in the gut and increased microbial translocation into the mesenteric lymph nodes, suggesting that PC-AMPs are critical in regulating bacterial translocation to mesenteric lymphnodes.^{60,114} Furthermore, as mentioned previously, *Mmp7*^{-/-} mice have increased abundance of SFB while *DEFA5*-TG mice have low abundance of SFB.⁷⁴ SFB are microbes capable of initiating pro-inflammatory IL-17 responses from adaptive T cells (T_H17 cells), and in accordance with abovementioned alterations of SFB in *Mmp7*^{-/-} and *DEFA5*-TG mice, high amounts of T_H17 cells are present in *Mmp7*^{-/-} mice, while T_H17 cells are absent in *DEFA5*-TG mice.^{74,115,116} Thus, the PC-AMPs also tightly modulate the host immune system by regulating the commensal microbiota in the gut.

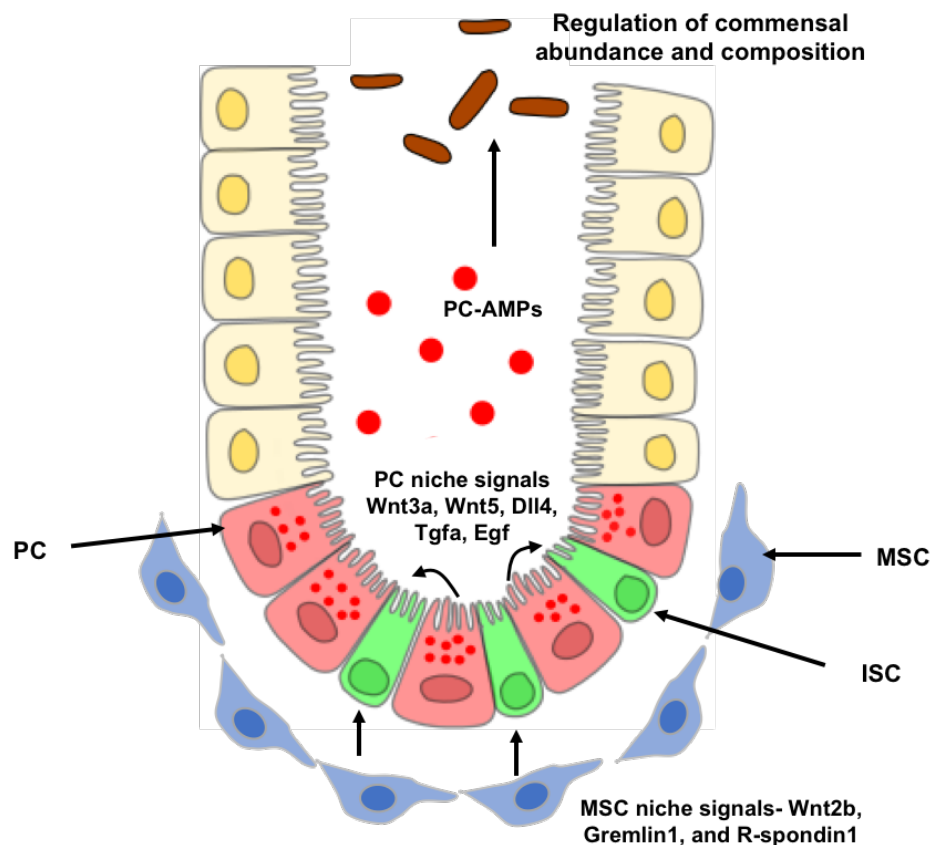


Figure 1.2 PC functions in the gut

The PCs (in red) that lie at the bottom of the small intestinal crypts are important producers of AMPs in the gut, which play key roles in regulating the quantities and communities of the commensal microbiota. PCs also provide niche signals for ISC (in green) differentiation, which are critical *in vitro* but may be dispensable *in vivo* due to ISC niche signals provided by mesenchymal cells (MSC; in blue) in the underlying lamina propria. Adapted from Stzpourginski *et al.*, (2017).¹¹⁷

1.1.3.2 Regulation of the intestinal stem cell niche by Paneth cells

The ISCs and the crypt environment are tightly controlled by different signaling pathways such as the Wntless/Int (WNT) pathway, NOTCH pathway and the epidermal growth factor (EGF) pathway.¹¹⁸ The WNT signaling pathway is critical for the proliferation and differentiation of both the TA progenitors as well as the ISCs, and plays a central role for post-natal crypt development in the gut including the maturation of PCs.^{119–122} The NOTCH signaling pathway is also important for the ISC proliferation and differentiation.^{123,124} Further, the WNT and NOTCH pathway together monitor the lineage specification of differentiated cells in the intestinal epithelium.^{125,126} The EGF signaling pathway was also demonstrated to regulate ISC proliferation, and activation of the EGF pathway, promotes ISC proliferation and inhibits ISC apoptosis (a form of cell death).^{127,128}

ISC differentiation in the intestinal crypt is regulated by niche signals that are comprised of the ligands that activate the WNT, NOTCH and EGF pathways.¹¹⁸ The expression of some of these ligands, particularly those that activate the WNT and the NOTCH pathways, may require cell to cell contact.^{124,125,129} Accordingly, expression profiling of ISCs and PCs revealed that PCs which lie adjacent to ISCs express the WNT ligands *Wnt3a* and *Wnt5*, NOTCH ligand delta-like 4 (*Dll4*) and EGF receptor ligands *Egf* as well as transforming growth factor alpha (*Tgfa*) that support ISC differentiation and formation of *ex vivo* intestinal organoids (**Fig. 1.2**). Importantly, *in vitro* culturing of single-cell sorted PCs along with ISCs, led to organoid formation that was 10 fold more effective than those formed by culturing ISCs alone.¹³⁰ However, contradictory *in vivo* studies in mice have suggested that IEC-specific deletion of the transcription factor atonal bHLH transcription factor 1 (*Math1*), responsible for driving the formation of secretory cell lineage in the intestinal epithelium, led to complete loss of PCs in mice but revealed functional ISCs that undergo successful proliferation and differentiation, suggesting that PC-niche signals are not required *in vivo*.^{129,131,132} Accordingly, recent studies have now demonstrated that mesenchymal cells which exists below the IECs in the lamina propria also provide other niche signals to ISCs that can compensate for the loss of PC-specific niche signals (**Fig. 1.2**).^{133,134} Thus, while the PC-specific niche signals may be indispensable in an *in vitro* system, these are not required for the regulation of ISC *in vivo*.

1.2 Inflammatory bowel disease

As described above, the host and microbiota shape each other to maintain a symbiotic relationship. Disruption of this physiological cross-talk and breaching of the essential host barriers in the gut, allows for direct and inappropriate immune responses towards the commensal microbiota that form the basis of intestinal inflammation as observed in diseases such as IBD. IBD encompasses a group of disorders that are characterized by chronic relapsing inflammation of the GI tract. The symptoms of IBD includes intestinal bleeding, bloody diarrhea, abdominal pain and fever that can often lead to undernourishment in children and at some cases, a risk of developing colon cancer.¹³⁵ The most prevalent forms include ulcerative colitis (UC) and Crohn's disease (CD). In UC, the inflammation typically originates in the rectum and proceeds to affect the mucosa of the colon in a continuous manner. CD is most commonly associated with inflammation in the small intestine and the colon, however, may affect the entire GI

tract. CD is accompanied by transmural inflammation in patches, with non-necrotizing granulomas as the defining histological hallmark.¹³⁶ Around 3 million people in Europe have been documented with IBD with increasing incidence of the disease observed throughout the world.^{137–139} Most patients with IBD display clinical onset between 16–35 years.¹⁴⁰ However, IBD can also manifest at childhood and is then referred to as pediatric or early-onset IBD. Treatment regimes in IBD are based on immunosuppression, and include the use of corticosteroids, thiopurines and biologicals such as anti-tumor necrosis factor (TNF) antibodies.¹⁴¹ These treatments inhibit inflammation and suppress IBD symptoms but do not provide cure to the disease. Furthermore, many patients are refractory to these treatments. Although the precise etiology of IBD is unknown, altered host-environmental interactions are a hallmark of IBD and contribute to the disease pathogenesis in genetically susceptible hosts.^{142,143}

1.2.1 The microbiota in IBD

In the last couple of decades, our understanding of the complex roles of the commensal microbiota in IBD has vastly improved due to the advent of high throughput microbial sequencing studies. Furthermore, critical contributions of the microbiota have been documented in many IBD-associated mouse models where intestinal inflammation is often ameliorated or abrogated upon administration of antibiotics or GF rederivation of the mice. For example, mice with a deletion of the regulatory cytokine interleukin *110* display spontaneous intestinal inflammation. However, when they are treated with antibiotics such as neomycin-metronidazole or ciprofloxacin from birth or when rederived GF, these mice show no inflammation.^{144–146}

In line with the contributions of the microbiota to IBD pathogenesis, early life administration of antibiotics can however lead to persistent alteration of commensal communities and is associated with an increased incidence of IBD later in life.^{147–150} As such, a study conducted by Shaw SY *et al.*, identified that the use of antibiotics during the first year of life was associated with a three-fold risk of developing IBD in adults.¹⁵¹ Another study also described an increased risk of pediatric CD related to early antibiotic use.¹⁵² Studies to delineate the mechanistic basis of these observations have shown that the presence of commensal bacteria and their products during early life has persistent effects on immune cell composition and function in the intestine. For instance, the presence of *Bacteroides fragilis* or isolated products from this microbe

such as glycosphingolipid GSL-Bf717 inhibits the proliferation of lipid-recognizing invariant natural killer T (iNKT) cells that protects the mice from NKT cell-mediated colitis at adult age.¹⁵³ Thus, appropriate commensal colonization and development of specific microbial communities in neonatal life, can have an impact on the development of IBD in adult life.

With the aim of understanding which kind of microbial alterations are involved in IBD, studies have identified specific microbes, some of which are associated with promoting intestinal inflammation while others are associated with protective effects. For example, studies in rodents have recognized certain microbial symbionts of the Bacteroidetes phylum capable of promoting intestinal inflammation. These include, *Bacteroides vulgatus*, *Bacteroides thetaiotaomicron* and *Bacteroides unifirmatis* that are capable of inducing colitis in mice.^{154–156} Conversely, *Clostridium* spp., and the commensal microbiota *Faecalibacterium prausnitzii* belonging to the Firmicutes phylum, can alleviate inflammation by promoting anti-inflammatory signaling and regulatory adaptive T cell development.^{157–160} In accordance with these alterations, IBD patients present with altered abundances of the Bacteroidetes and the Firmicutes phyla.^{161–165} More importantly, altered Bacteroidetes and reduced Firmicutes in IBD patients are often accompanied by increased abundance of the Proteobacteria phylum, known to actively promote intestinal inflammation.^{157,163,164,166–169} For instance *B. wadsworthia*, a Deltaproteobacterium is capable of inducing intestinal inflammation in WT as well as *Il10^{-/-}* mice.^{170,171} Similarly, several members of *Helicobacter* spp. and *Enterobacteriaceae* spp. can induce intestinal inflammation in mice and humans as described in the paragraphs below.^{172–174}

While microbial alterations are evident in IBD, whether or not dysbiosis contributes to disease pathogenesis or whether intestinal inflammation causes secondary microbial alterations is still under discussion. Nevertheless, dysbiosis may be accompanied by increased abundance of specific pathobionts that are capable of initiating intestinal inflammation or providing susceptibility to intestinal inflammation, irrespective of the genetic background of the mice. Garrett *et al.*, made these observations in mice that are double deficient for T-box protein 21 of (*T-bet^{-/-}*) and recombination-activating gene (*Rag2^{-/-}*) (also known as the TRUC mice model) which present with spontaneous colitis.¹⁵⁶ Analysis of the microbial communities in the gut revealed that spontaneous

colitis in TRUC mice was driven by *Klebsiella pneumoniae* and *Proteus mirabilis* from the Proteobacteria phylum, which usually exist in low amounts. Moreover, colitis was transferrable from the TRUC mice to normal WT mice upon co-housing. Although these microbes induced inflammation in WT mice, it is key to note that colonization of *K. pneumoniae* and *P. mirabilis* alone into GF TRUC mice did not initiate inflammation, suggesting that presence of the endogenous commensal microbiota was required for eliciting intestinal inflammation.¹⁵⁶ Similarly, mice that carry deletions of NLR family, pyrin domain containing 6 (*Nlrp6*^{-/-} mice) are characterized by increased abundance of *Prevotellaceae* spp., belonging to the Bacteroidetes phylum, that make them susceptible to chemically-induced colitis, which is transferrable to WT mice on co-housing.¹⁷⁵ Moreover, antibiotic treatment abrogated colitis to the same extent in the co-housed WT and *Nlrp6*^{-/-} mice that was associated with similar levels of *Prevotellaceae* spp., in these mice, thus demonstrating that *Prevotellaceae* spp., may drive colitis irrespective of the genetic background.¹⁷⁵

Dysbiosis may also be present as a consequence of genetic defects in the absence of inflammation. This has been demonstrated in *Mmp7*^{-/-} mice which present with aforementioned alterations in microbial communities but do not have any spontaneous inflammation. Similarly, *Nod2*^{-/-} mice that have defective expression of PC α -defensins display increased abundance of *Bacteroides* (of the phylum Bacteroidetes) in the small intestine but do not have spontaneous inflammation.^{109,176}

Intestinal inflammation may be induced by specific opportunistic microbes exclusively in certain IBD mouse models that do not affect WT mice. For example, infection with the opportunistic microbe *Helicobacter hepaticus* that exists in many animal facilities does not initiate inflammation in WT mice but elicits granulomatous ileitis in *Nod2*^{-/-} mice and colitis in *Il10*^{-/-} mice.^{172,177} Similar observations were also made in mice that are hypermorphic (HM) for autophagy-related gene *Atg16l1* (*Atg16l1*^{HM} mice) which present with PC granule abnormalities.¹⁷⁸ Infection of the *Atg16l1*^{HM} mice with the opportunistic microbe *Murine norovirus* (MNV) leads to changes in PC morphology and gene expression, and exposure of MNV-positive *Atg16l1*^{HM} mice to dextran sulfate sodium (DSS; a chemical colitogen) is associated with pathology in the ileum resembling CD that is not observed in WT mice or MNV-negative *Atg16l1*^{HM} mice.¹⁷⁹

Inflammation itself may also cause secondary alterations in microbial communities which promotes the growth of pathogens and pathobionts. Previous studies by Lupp *et al.*, showed that during chemically-, microbially- or genetically-induced inflammation in mice that leads to a reduction in the abundance of commensal microbiota, the *Enterobacteriaceae* spp., of the Proteobacteria phylum take advantage of the reduced abundance of the commensal microbiota to enhance their growth.¹⁷⁴ These secondary alterations that enhance the abundance of microbes belonging to the Proteobacteria phylum, can further promote the inflammation.^{169,170,172,174,175,180} Similarly, *Helicobacter rodentium*-induced colitis in *Il10^{-/-}* mice worsened when the mice were exposed to the Proteobacterium *Helicobacter troglodytes* and the inflammation was associated with reduced abundance of several anaerobic microbes with beneficial roles in the gut.¹⁸¹ The reduced abundance of these anaerobic microbes was further associated with enhanced damage and permeability of the intestinal mucosa, and translocation of *Enterobacteriaceae* into the liver that caused sepsis in the *Il10^{-/-}* mice.¹⁸¹ Inflammation-associated microbial alterations are also observed in patients with IBD. Ileal biopsies of CD patients contain elevated amounts of the adherent-invasive *E. coli* (AIEC).¹⁸² AIEC binds and adheres to the adhesion receptor carcinoembryonic antigen-related cell adhesion molecule 6 (CEACAM6), present on the surface of the IECs, in order to invade the IECs. *In vitro* studies revealed that stimulation of IECs with TNF- α or interferon gamma (IFN- γ) or infection of cultured IECs with AIEC, leads to the upregulation of CEACAM6, which further promotes the binding of more AIEC.¹⁸³ The upregulation of CEACAM6 is associated with secondary promotion of intestinal inflammation and faster disease progression.^{142,183}

Together, microbial alterations that may either precede and promote inflammation in genetically susceptible hosts or occur secondary to intestinal inflammation, form the basis of IBD pathogenesis.

1.2.2 Genetic factors in IBD

IBD may appear in a sporadic or familial form, the former occurring considerably more frequently. Several studies in monozygotic twins have vastly improved our understanding of the heritability factor in IBD, which is about 15-50% in CD and around 10-20% in UC.¹⁸⁴ The complexity of the genetic factors in IBD has been illustrated by genome-wide association studies (GWAS) which have documented over 230 genetic

loci associated with IBD.^{143,185,186} The predominant focus of GWAS are common single nucleotide polymorphisms (SNPs) with moderate to high allele frequencies and low to moderate effect size. GWAS have offered critical insight about the genetic basis of IBD. Examples of these include the identification of the autophagy-related gene *ATG16L1*, the intracellular receptor *NOD2* and interleukin 23 receptor *IL23R* mutations in CD.^{187–190} However, as mentioned above, most of these SNPs are of low to moderate risk effect size and are not located within the coding regions of genes, both of which has limited our understanding of how these SNPs functionally contribute to IBD.^{142,191}

On the other hand, next-generation sequencing (NGS) and whole exome sequencing (WES), have allowed to identify rare and exonic variants that are typically associated with loss or severe impairment of gene function that can give rise to monogenic forms of IBD. Identification of these rare Mendelian disorders, which typically manifest at young age, has provided important novel insight to pathways critical for control of intestinal inflammation and the pathogenesis of IBD.^{185,191} For example, loss-of-function mutations in the genes encoding the regulatory cytokine IL-10 protein and its receptor subunits *IL10RA* and *IL10RB* leads to very early-onset CD, which invariably manifests within the first year of life.^{192,193} Accordingly, mice with constitutive deletion of the *Il10* gene or its receptor subunit *Il10rb* display spontaneous colonic inflammation in the presence of the commensal microbiota, confirming that loss of this gene or its receptor form is sufficient to induce intestinal inflammation.¹⁹⁴ Similarly, loss-of-function mutations in other genes critical for the regulatory branch of adaptive immunity, such as *FOXP3* and *CTLA4*, are also associated with IBD.^{195,196}

In addition to defects in regulatory and adaptive immunity, mutations in genes essential for intestinal epithelial barrier function can give rise to monogenic forms of IBD. As an example, a disintegrin and metalloprotease 17 (ADAM-17) is a protein responsible for cleaving TGF- α ligand from the cell membrane to bind to its receptor EGF receptor (EGFR), which is critical for the maintenance of IEC barrier integrity and patients with ADAM-17 deficiency present with early-onset IBD.^{197–199} In accordance with this, studies on mice with a reduced activity of ADAM-17 (*Adam17^{ex/ex}* mice) have revealed that these mice demonstrate increased gut permeability and susceptibility to chemically-induced colitis.²⁰⁰ Moreover, the *Adam17^{ex/ex}* mice had improved

regeneration of the epithelial cells in the chemically-induced colitis model upon the administration of exogenous TGF- α , suggesting that ADAM-17 deficiency leads to the incapacity to shed off EGFR ligands, thus compromising epithelial barrier integrity.²⁰⁰ Another example is, patients with mutations in the gene encoding for the inhibitor of NF- κ B kinase subunit gamma (*NEMO*), present with IBD.²⁰¹ In accordance with this observation, mice which have IEC-specific deficiency of NEMO display spontaneous intestinal inflammation, highlighting that the absence of NEMO in the intestinal epithelium contributes to intestinal inflammation.²⁰²

Monogenic forms of IBD may also arise due to mutations in genes associated with innate immunity. IBD, particularly early-onset IBD is often observed in patients with chronic granulomatous disease (CGD).²⁰³⁻²⁰⁵ CGD is an immunodeficiency disorder that is associated with defective phagocytic killing of microbes that invade the host. It is observed in patients with mutations in genes that encode for proteins that are a part of the phagocyte NADPH oxidase (phox) complex (responsible for generating reactive oxygen species) such as neutrophil cytosolic factor 1 (NCF1), neutrophil cytosolic factor 2 (NCF2) or neutrophil cytosolic factor 4 (NCF4).

In addition to providing insights into pathways leading to intestinal inflammation, studies on rare monogenic forms of IBD have also identified the successful use of novel personalized therapies to induce remission of intestinal inflammation in patients with IBD.²⁰⁶ For instance, patients with *IL10* mutations or CGD patients with IBD who have defects in the hematopoietic cells, achieve disease remission upon allogeneic stem cell transplantation.²⁰⁷⁻²¹¹ Together, these studies demonstrate the importance of studying rare monogenic forms of IBD that have high effect size that provide insights to the disease pathogenesis and novel treatment options in IBD.

1.2.2.1 X chromosome-linked inhibitor of apoptosis protein variants in early-onset Crohn's disease

IBD is closely associated with immunodeficiency, and several primary immunodeficiencies (PIDs) often present with IBD-like pathology and phenotypes.²⁰⁶ For example, as mentioned in the previous section, CGD is often accompanied by early-onset IBD. Furthermore, another PID called X-linked lymphoproliferative syndrome type 2 (XLP-2) elicited by Epstein-Barr virus (EBV) infection, is characterized by excessive production of cytokines resulting from over-activation of

macrophages and lymphocytes also known as hemophagocytic lymphohistiocytosis (HLH). XLP-2 is caused by mutations in the gene encoding X chromosome-linked inhibitor of apoptosis protein (*XIAP*). In line with the association of PID and IBD mentioned above, early studies on the description of families with XLP-2, have described cases of IBD in these studies.^{212–214} Moreover, Worthey *et al.*, reported a pediatric male patient with severe CD manifesting at the age of 15 months, in whom WES revealed a loss of function mutation in *XIAP*. Importantly, this patient showed IBD in the absence of any signs of lymphoproliferation.²¹⁵ Upon investigation of such rare pediatric-onset CD patients through WES, research work by Zeissig *et al.*, also identified a hemizygous, *de novo* nonsense mutation in the *XIAP* gene in a 9-month-old male patient who presented with CD but not XLP-2,. This patient showed severe colitis which ameliorated upon ileostomy, but he continued to have mild persistent discontinuous colitis and did not respond to immunomodulatory or biological treatment.²¹⁶ Subsequently, Sanger sequencing in cohorts of 780 patients with adult-onset UC, 1900 patients with adult-onset CD and 275 patients with pediatric IBD revealed three additional, novel variants of *XIAP*, all of which occurred in male patients with early-onset CD in the absence of XLP-2.²¹⁶ Together, 4% of male patients with early-onset CD in this cohort harbored *XIAP* variants. Furthermore, studies by Speckmann *et al.*, described that six out of twenty five (24%) patients with *XIAP* mutations presented with CD and amongst the six CD patients, five did not have HLH and the sixth patient had partial HLH.²¹⁷ Similarly, studies by Schmid JP *et al.*, demonstrated that five out of thirty (17%) patients with *XIAP* mutations had chronic hemorrhage colitis and amongst these five patients, three did not present with HLH.²¹⁴ Thus, these studies show an association of genetic variants in *XIAP* with CD that can occur independent of lymphoproliferative disease. Numerous studies have now described novel *XIAP* mutations in male pediatric patients, and a few have reported adult CD cases independent of lymphoproliferative disease, indicating the importance of screening for *XIAP* mutations, especially in patients presenting with early-onset CD.^{217–224}

1.2.3 Paneth cell dysfunction in Crohn's disease

Several studies in humans and mice have described functional and morphological alterations in PC which are central to the pathophysiology of CD. The CD susceptibility gene *NOD2*, one of the first genes to be discovered in CD, is associated with defective

expression of PC-AMPs.^{189,225} Many reports have established that ileal CD patients with *NOD2* mutations have reduced α -defensin expression, and ileal crypts isolated from these patients show defective killing of bacteria.^{226–228} This concept is further supported in *Nod2*^{-/-} mice which aforementioned, show reduced α -defensin expression when compared to the WT mice.¹⁷⁶

Previous reports by Wehkamp *et al.*, showed that ileal CD patients with decreased α -defensin expression have defective expression of the WNT signaling pathway transcription factor -T cell-specific transcription factor 4 (TCF4) and correspondingly, mice which lack *Tcf4* (*Tcf4*^{-/-} mice) show reduced levels of cryptdins.²²⁷ This may be explained by the role of WNT signaling in the regulation of PC-AMPs.¹²² Activation of WNT signaling by its ligands results in the accumulation of β -catenin (a transcription co-activator) in the cytoplasm which then translocates into the nucleus of the cells to bind to TCF4.^{119,229} This binding regulates the expression of target genes encoding for MMP-7 and cryptdins, thus explaining the reduction of cryptdins in the absence of TCF4.¹²² Moreover, the deteriorated expression of α -defensins in the absence of TCF4 occurs independently of *NOD2*, which led to the notion that TCF4 may directly be associated with ileal CD. In line with this, sequencing studies of three IBD cohorts led to the discovery of *TCF4* as a CD susceptibility gene.²³⁰

Mutations in *KCNN4*, which encode for the potassium channel KCa3.1 that regulates the PC granule secretion, is also associated with CD.²³¹ Supporting this observation, mice which carry deletion of KCa3.1 (*KCa3.1*^{-/-} mice) show increased sensitivity to T-cell induced colitis.²³² Although there were no direct implications of PC defects in the *KCa3.1*^{-/-} mice, previous reports have indeed demonstrated that defects in the KCa3.1 channel can lead to improper PC-AMP secretion.^{62,232} This allows for a speculation that the reduction in PC-AMPs due to defective PC-AMP secretion, may also contribute to increased sensitivity to intestinal inflammation in the absence of KCa3.1 channel.

Apart from alterations in levels of PC-AMPs, CD is also associated with defects in PC morphology. CD patients who have mutations in an autophagy-related gene *ATG16L1*, present with disorganized and diffused PC granules when compared to control patients, also confirmed in *Atg16l1*^{HM} mice.¹⁷⁸ Likewise, mutations in the immunity-related GTPase (IRG) M (*IRGM*) which is another protein that regulates autophagy,

are associated with CD.^{233,234} In accordance with this observation, studies on *Irgm1*-deficient mice have revealed that the size of the PC granules in these mice are irregular and the granules are less dense when compared to the WT mice.²³⁵ Thus, CD is associated with PC morphological alterations.

While functional or morphological PC defects in the above-mentioned mice models do not lead to spontaneous intestinal inflammation, studies on the CD-susceptibility gene X-box binding protein-1 (*XBP1*) have revealed that PC dysfunction can itself induce intestinal inflammation.²³⁶ *XBP1* is a protein that is required for the transcription of several genes involved in a process called unfolded protein response (UPR), which ensures proper management of proteins emerging from the ER of stressed cells.²³⁷ Amongst the different cellular compartments of IECs, PCs particularly have high susceptibility to ER stress due to their increased secretory properties. Accordingly, studies have shown that the constitutive or IEC- or PC-specific deletion of *Xbp1* in mice leads to PC loss that induces inflammation in the ileum (ileitis).²³⁸ Similarly, IEC-specific deletion of protein kinase C iota (a protein critical for PC differentiation; PKC λ/ι) in mice, leads to the loss of PCs that drives spontaneous intestinal inflammation due to increased IEC apoptosis driven by microbiota.²³⁹ Thus, PC dysfunction may also lead to intestinal inflammation. In conclusion, these different studies establish that functional and morphological defects in PC are central to CD and genetic defects inducing PC dysfunction can either provide increased susceptibility to inflammation or directly cause inflammation.

1.3 X chromosome-linked inhibitor of apoptosis protein

Apoptosis or programmed cell death is a form of regulated cell death where cells undergo morphological and biochemical changes that allows for their removal by adjacent phagocytic cells.^{240,241} Several virus in order to replicate efficiently have evolved to obstruct this process of cell death in the host.²⁴² Screening for genes involved in the inhibition of apoptosis led to the discovery of the inhibitor of apoptosis (IAP) family of proteins in baculovirus-infected insect cell lines.²⁴³ Subsequently, many IAPs were discovered in organisms ranging from viruses to mammals. One of the first mammalian IAPs that was found to inhibit apoptosis was called MIHA (mammalian homologues of IAP), later termed XIAP, as it was X chromosome-linked.^{244–248} Overall,

eight mammalian IAPs exist, with XIAP having gained much attention due to its pivotal roles in the regulation of immunity and cancer.^{249–251}

1.3.1 XIAP structure

A common feature of all IAP family members is the presence of baculoviral IAP repeat (BIR) motifs on their N-terminus, derived from the initial discovery of the IAPs in baculovirus-infected insect cell lines.²⁴³ IAPs are characterized by the presence of one to three BIR domains (**Fig. 1.3**), each of which contains approximately 70 amino acids that fold to form four α -helices surrounding and linking three stranded- β sheets. These structures generate a central core of hydrophobic residues along with a zinc-binding fold which is tetrahedrally coordinated by three cysteines and a histidine amino acid residue.^{252–254} The presence of three BIR domains in XIAP allows for strong interactions with different proteins which is of functional relevance to their involvement in several signaling pathways.²⁵⁵ The three BIR domains are categorized under two types. Type I BIR domain consists of the BIR1 domain that is implicated in TGF- β and bone morphogenetic protein (BMP) signaling, essential for mesoderm development in early *Xenopus* embryos.^{256,257} The BIR2 and BIR3 domains are grouped under the type II BIR domain that contain a deep peptide-binding hydrophobic cleft (absent in type I BIR domain) called IAP-binding motif (IBM) through which IAPs mediate interactions with tetrapeptides on caspases.^{258–262} The BIR2 domain is also implicated in NOD2-dependent NF- κ B signaling important in regulating innate immunity. In addition to the BIR domains, some of the IAPs including XIAP, share a carboxy-terminal ubiquitin (Ub)-associated domain (UBA) (**Fig. 1.3**), through which they add mono- or poly-Ub molecules to a target protein, allowing them to participate in the proteasome-dependent degradation process.²⁶³ Ub-dependent protein degradation by proteasomes is essential for signaling events such as cell cycle control, discarding misfolded or damaged proteins.^{264,265} The addition of Ub molecules occurs via a multi-step process that involves different ubiquitination enzymes such as E1, E2 and E3 which activate, conjugate and ligate the Ub molecules respectively to target proteins.²⁶⁶ The ubiquitination process is carried out together with the adjacent C-terminal RING finger domain of XIAP (**Fig. 1.3**), which confers E3-ligase activity (that further depends on the E1 and E2 enzymes).^{264,267} XIAP thus functions as an ubiquitin ligase which is critical for mediating NF- κ B signaling to promote cell survival.^{256,263} Together, the

different domains of XIAP carry out several important roles in cell death and immunity as highlighted in the following sections.



Figure 1.3 Schematic representation of the different domains of XIAP

XIAP interacts with different proteins via its BIR domains (BIR1-3) present on its N-terminal. The C-terminal UBA and RING domains are responsible for the ubiquitin ligase function of XIAP.

1.3.2 XIAP in the regulation of TNF-dependent cell death pathways

1.3.2.1 TNFR1 signaling

TNF is a pro-inflammatory cytokine which binds to its receptor TNFR1 to initiate either NF- κ B-dependent signaling to promote cell survival and inflammation, or cell death. Following ligation of TNF and TNFR1, complex I formation is initiated by the recruitment of TNF receptor associated via death domain (TRADD) and receptor interacting serine/threonine kinase 1 (RIPK1). These molecules subsequently recruit the signal transducers TNF receptor-associated factor 2 (TRAF2) and TRAF5 as well as cellular inhibitor of apoptosis proteins (cIAPs) that belong to the family of IAPs (**Fig. 1.4**).^{268–271} Further, ubiquitination of RIPK1 by cIAPs and recruitment of linear ubiquitin chain assembly complex (LUBAC) to the complex I activates NF- κ B signaling to promote cell survival and inflammation.²⁷² However, depending on the cellular status and the fate of RIPK1, and in the absence of IAPs, particularly XIAP, cell death pathways can be activated (**Fig. 1.5**).^{273,274}

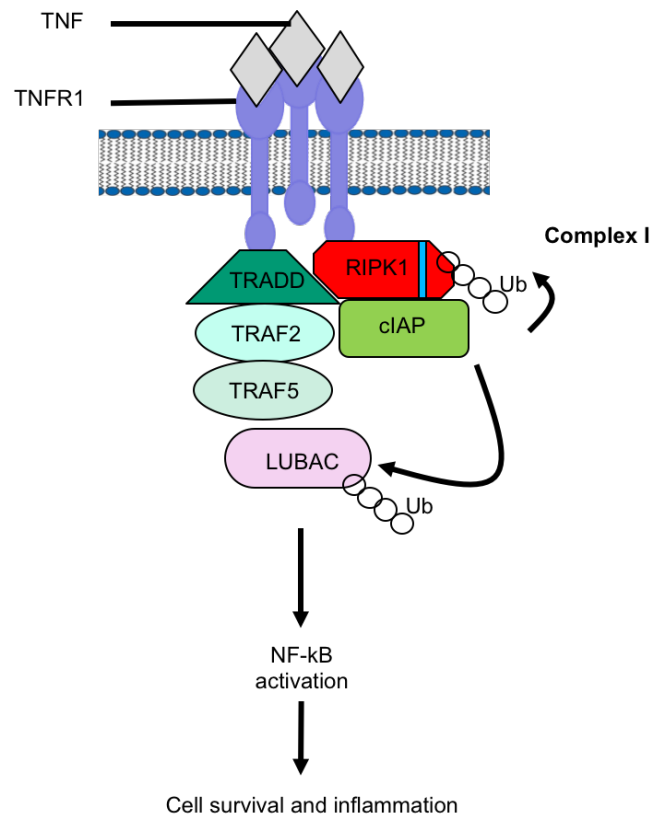


Figure 1.4 TNFR1-dependent cell survival pathway

When TNF engages with its receptor form TNFR1, complex I (which contains TRADD, RIPK1, TRAF2, TRAF5, cIAP, LUBAC) is formed, leading to the activation of NF-κB signaling to promote cell survival and inflammation. Adapted from Lawlor *et al.*, (2015).²⁷⁵

Destabilization of complex I leads to the formation of complex II that promotes cell death pathways (**Fig. 1.5**).^{271,276} Complex II may occur in the presence or absence of RIPK1. Accordingly, when RIPK1 levels are low, complex IIa is formed, which is composed of TRADD (dissociated from complex I), adaptor molecule Fas-Associated protein with Death Domain (FADD), the anti-apoptotic regulator Fas-associated death domain-like interleukin-1β converting enzyme inhibitory protein (cFLIP) and the cysteine protease caspase-8.²⁷⁷ In the presence of active caspase-8, the apoptotic form of cell death is carried out.^{278,279,279,280} Cell death signaling in the presence of high levels of RIPK1, leads to the formation of complex IIb also known as the ripoptosome, which consists of the same components of complex IIa along with RIPK1 and RIPK3.^{277,278,281,282} When caspase-8 is active, apoptosis is carried out similar to in complex IIa, however, when caspase-8 levels are low, RIPK1 associates with RIPK3 to phosphorylate the RIPK3 substrate mixed lineage kinase domain-like (MLKL) and

forms a complex called the necrosome, therewith initiating another form of cell death called necroptosis (**Fig. 1.5**).^{281,283–285}

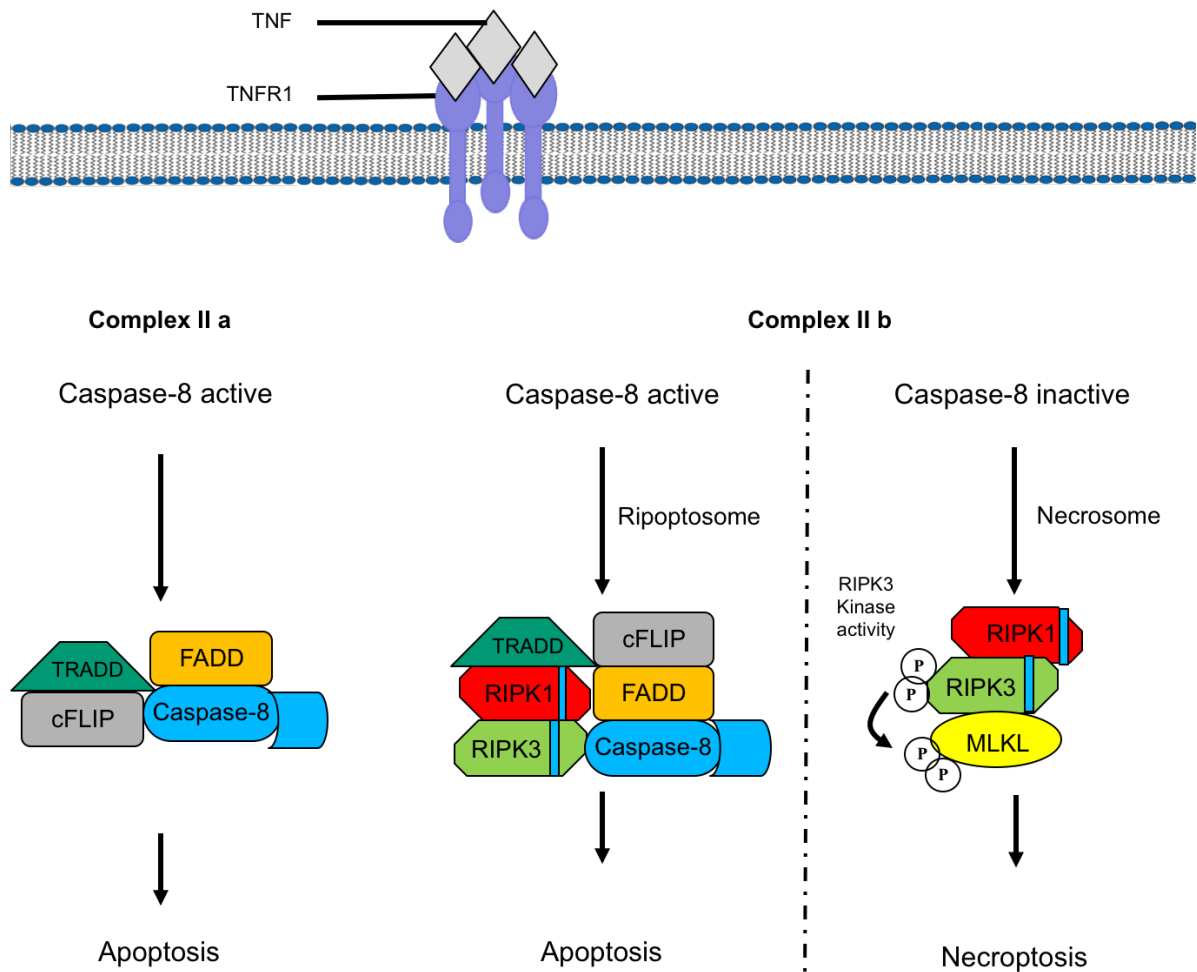


Figure 1.5 TNFR1-dependent cell death pathway

The cell death pathway downstream to TNFR1 signaling is activated based on the cellular status, the fate of RIPK1, and in the absence of IAPs. Upon engagement of TNF with TNFR1, Complex IIa (consisting of TRADD, FADD, cFLIP and caspase-8) is formed in the absence of RIPK1 when caspase-8 is activated, which leads to the initiation of apoptosis. In the presence of RIPK1, complex IIb is formed, which based on the RIPK1 and RIPK3 activity that can either induce ripoptosome formation (comprised of TRADD, cFLIP, RIPK1, RIPK3 and caspase-8) leading to apoptosis, or necrosome formation (comprised of RIPK1, RIPK3 and MLKL) leading to necroptosis. Adapted from Lawlor *et al.*, (2015).²⁷⁵

1.3.2.2 XIAP-dependent regulation of ripoptosome

The ripoptosome complex is known to be activated by different signals such as TLR stimulation, TNF binding to its receptor TNFR1, or genotoxic stress.^{273,282} The cIAPs play an important role in the ubiquitination of RIPK1 upstream which is critical in diverging the pathway from ripoptosome formation, to NF-κB signaling that promotes

cell survival (**Fig. 1.4**).^{263,270,286–288} Interestingly, studies have proven that XIAP inhibits ripoptosome formation upon TLR stimulation of myeloid cells by blocking RIPK3-dependent induction of cell death downstream to TNFR1 signaling.²⁷³ More comprehensive investigation by Lawlor *et al.*, revealed that in the absence of XIAP in myeloid cells, stimulation of TLRs allowed for MyD88 signaling that induced the production of TNF which upon binding to its receptor form TNF-receptor 2 (TNFR2), led to degradation of cIAP1 and TRAF2 (**Fig. 1.6**). Further, degradation of cIAP1 and TRAF2 in the absence of XIAP switched the pathway from NF- κ B-dependent cell survival to RIPK3- and caspase-8-dependent cell death pathway, downstream to TNFR1 signaling.²⁸⁹ While myeloid cell death in these studies was shown to occur downstream of caspase-8, previous studies by Yabal *et al.*, showed that RIPK3-dependent activation of cell death upon TLR stimulation in XIAP-deficient myeloid cells occurs independent of caspase-8, suggesting that cell death could be mediated by the necroptotic pathway.²⁷³ Consistent with this observation, Wicki *et al.*, have shown that TNF stimulation of neutrophils in mice led to necroptosis of the neutrophils in the absence of XIAP.²⁹⁰ Taken together, XIAP inhibits ripoptosome formation and regulates both apoptotic and necroptotic pathways.

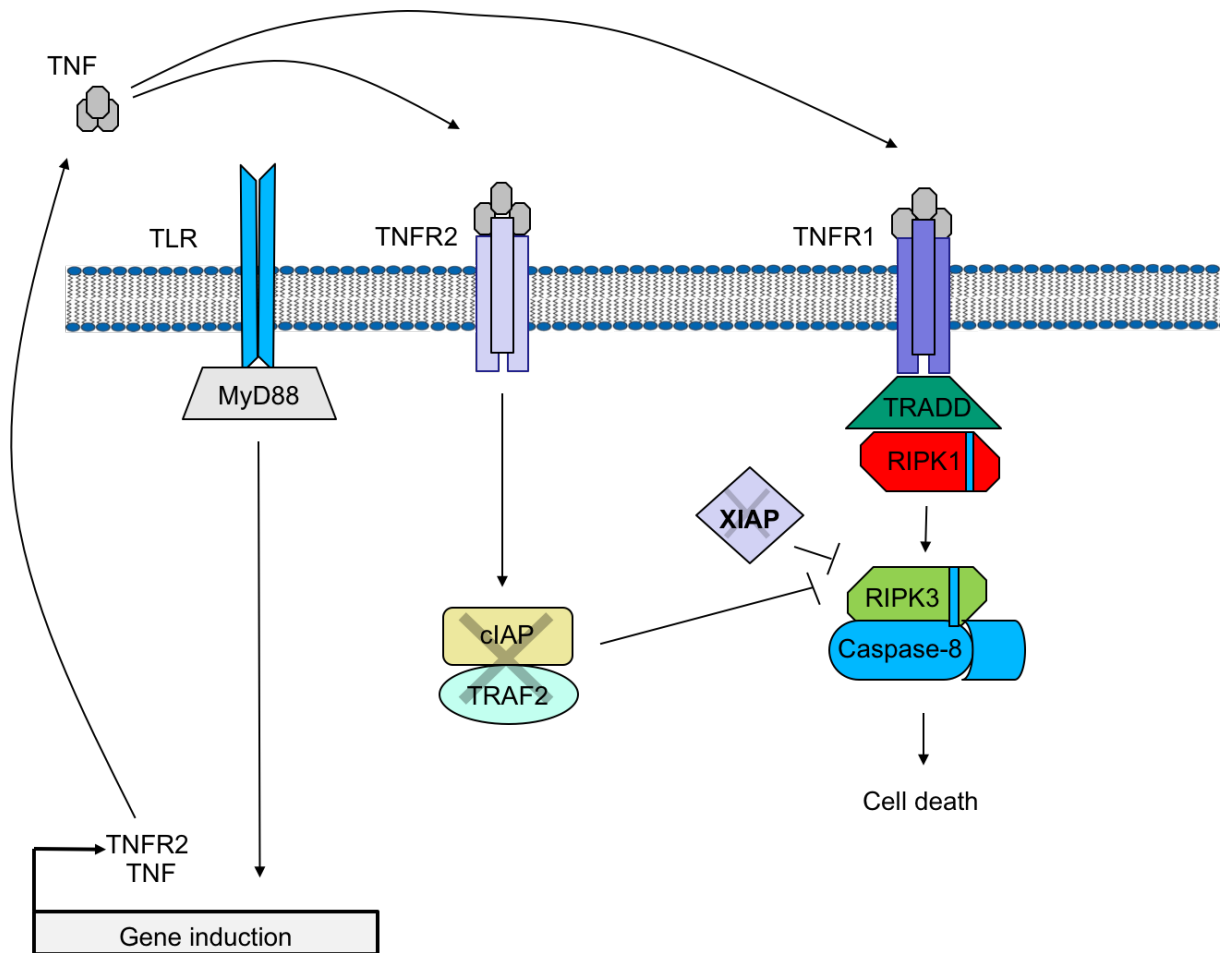


Figure 1.6 XIAP- dependent control of the ripoptosome

Stimulation of TLRs allows for MyD88 signaling that induces the production of TNF that upon binding to its receptor TNFR2 further induces degradation of cIAP1 and TRAF2. The degradation of cIAP1 and TRAF2 in the absence of XIAP is associated with caspase-8 and RIPK3-dependent apoptotic cell death in the ripoptosome complex. Adapted from Lawlor *et al.*, (2017).²⁸⁹

1.3.2.3 XIAP-dependent regulation of caspases

Apoptosis is carried out by a regulated cascade that involves proteolytic enzymes called cysteine aspartases or caspases.²⁹¹ There are two categories of caspases which perform different roles in the process of apoptosis. The first category of caspases called initiator includes caspase-2, -8, -9 and -10 which are responsible for the initiation of apoptosis. The second type called effector caspases comprises caspase-3, -6 and -7 and play a role in the actual execution of apoptosis.²⁹¹ Internal and external death signals trigger the recruitment, dimerization and autocatalytic processing of inactive initiator caspases to activate them. The internal death signals are induced by the mitochondrial signaling pathway, which activate caspase-9, while external death signals such as TNF ligands and Fas ligands induce the activation of caspase-8 and

caspase-10.^{280,292} These active initiator caspases further allow for proteolytic cleavage and activation of execution caspases such as caspase-3 and caspase-7.^{291,293,294} The execution caspases then cleave several downstream proteins, some of which are responsible for regulating DNA fragmentation, that leads to the phagocytosis of the cells.^{295–298}

XIAP plays a central role in inhibiting effector caspases downstream to caspase-8 activation.^{248,260,299,300} It is the only IAP family member capable of directly inhibiting caspase-3, -7 and to a lesser extent caspase-9, by interfering with the proteolytic activity of the caspases (**Fig. 1.7**).^{248,260,299,300} More specifically, the BIR2 domain of XIAP, belonging to the type II BIR domain, mediates interaction with different downstream caspases through the IBM motif.^{253,259,261,301} While the BIR2 domain is involved only in binding to caspases, the insertion of the linker region between BIR1 and the BIR2 domain of XIAP into the catalytic groove of the effector caspases, facilitates the caspase inhibition activity.^{260,261,301} The BIR3 domain (belongs to the type II BIR domain) bearing approximately 40% homology with BIR2 domain, binds and inhibits caspase-9, but the mechanism by which caspase-9 is inhibited is fundamentally different. The BIR3 domain binds to caspase-9 through a small distal helix present at the C-terminus of XIAP and monomerizes caspase-9, leaving the protein in an inactive form.^{300,302} The RING domain of XIAP was also implicated in regulating cell death *in vivo*. An interesting observation by Yang *et al.* was that XIAP is capable of self-ubiquitination through its RING domain, regulating itself to allow for apoptosis in cells. This *in vitro* study was carried out on thymocytes which upon treatment with glucocorticoid or etoposide (to induce apoptosis) and when co-transfected with XIAP that lacks the RING domain, displayed less apoptosis in comparison to apoptotic thymocytes that were co-transfected with the whole XIAP protein.³⁰³ However, contradicting *in vivo* studies on mice that have a truncated RING domain (*Xiap*^{ΔRING}) revealed that these mice have an increased caspase-3 activity and impaired ubiquitination of active caspase-3 that led to increased apoptosis of embryonic stem (ES) cells and fibroblasts in these mice when compared to the ES cells and fibroblasts isolated from wildtype mice.³⁰⁴ This suggests that the RING domain may be important to inhibit apoptosis efficiently *in vivo*. Thus, XIAP plays a central role in regulating caspases to inhibit apoptosis.

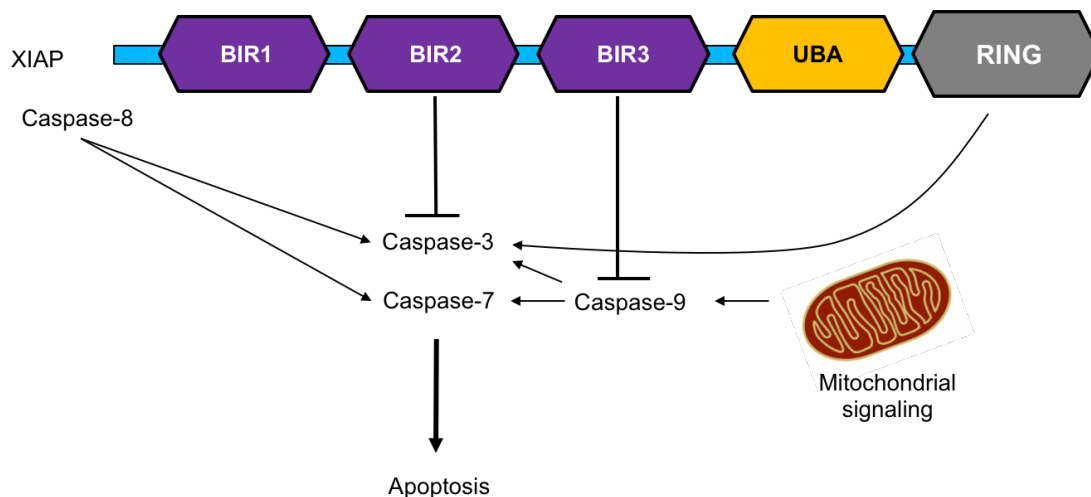


Figure 1.7 XIAP-dependent control of caspase-mediated apoptosis

XIAP acts on effector caspases such as caspase-3, -7, and -9 to promote apoptosis. XIAP through its BIR2 domain binds to caspase-3, and caspase-7 and it interferes with the proteolytic activity of these caspases thereby inhibiting apoptosis. XIAP also binds to caspase-9 through its BIR-3 domain and leaves caspase-9 in an inactive form thus inhibiting caspase-9 mediated apoptosis. The RING domain has also been shown to interfere with caspase-3 activity although it is speculated that this mechanism may be due to the ubiquitin ligase function of the RING domain. Adapted from Filipovich *et al.*, (2010).²¹³

1.3.3 XIAP in the regulation of innate and adaptive immunity

XIAP and its closely related forms cIAP1 and cIAP2, together coordinate different signaling pathways involved in immunity including cell death inhibition, ubiquitin ligase function, or NF- κ B signaling.²⁶² While XIAP so far has not been directly implicated in the NF- κ B signaling downstream to TNFR1 pathway, it signals through various other pathways to promote NF- κ B signaling (highlighted in the paragraphs below).

1.3.3.1 XIAP-dependent regulation of the inflammasome pathway

As described above, XIAP inhibits ripoptosome formation upon TLR stimulation of myeloid cells by blocking RIPK3-dependent induction of cell death downstream to TNFR1 signaling.^{273,289} However, an interesting observation is that ripoptosome formation also lead to the activation of the NACHT, LRR and PYD domains-containing protein 3 (NLRP3) inflammasome pathway (**Fig. 1.8**). The activation of NLRP3 inflammasome occurs when the N-terminus of the NLRP3 interacts with a bipartite adaptor protein called apoptosis-associated speck-like protein containing a caspase recruitment domain (ASC) which further bridges the cysteine aspartase caspase-1 to form the NLRP3 inflammasome complex. These processes subsequently allow for the

production of the proinflammatory cytokine IL-1 β (**Fig. 1.8**).^{305,306} The NLRP3 inflammasome pathway also controls the production of cytokine IL-18, a process that occurs in a similar manner to the production of IL-1 β .³⁰⁷ Both these cytokines have effector roles in inflammatory diseases including IBD and their effector functions require the conversion from an inactive pro-form to an active form which is carried out by the enzyme caspase-1 in the inflammasome pathway.³⁰⁸ Importantly, patients with XIAP mutations that have XLP-2, present with elevated levels of IL-18³⁰⁹, and XLP-2 in these patients is often accompanied by EBV infection.^{212,214,217,310–312} In accordance with this, since EBV does not cause infection in mice, Yabal *et al.*, adopted murine γ -herpesvirus 68 (MHV-68) and infected the mice which carry deletions of XIAP (*Xiap*^{-/-} mice) as well as *Xiap* ^{Δ RING} mice with MHV-68, that led to hyperinflammation with increased IL-1 β production in these mice, mimicking XLP-2 pathology. in humans²⁷³ These studies suggest that increased inflammasome responses that contribute to the XLP-2 pathology in patients with XIAP deficiency are likely mediated by EBV infections. Although studies by Yabal *et al.*, suggested that XIAP-dependent regulation of IL-1 β may occur independent of the other IAP forms cIAP1 and cIAP2, another study has shown that XIAP can coordinate with cIAPs to regulate the inflammasome pathway and production of IL-1 β .^{273,274} Nevertheless, both these studies have highlighted the importance of XIAP in regulating myeloid homeostasis by controlling the inflammasome pathway.

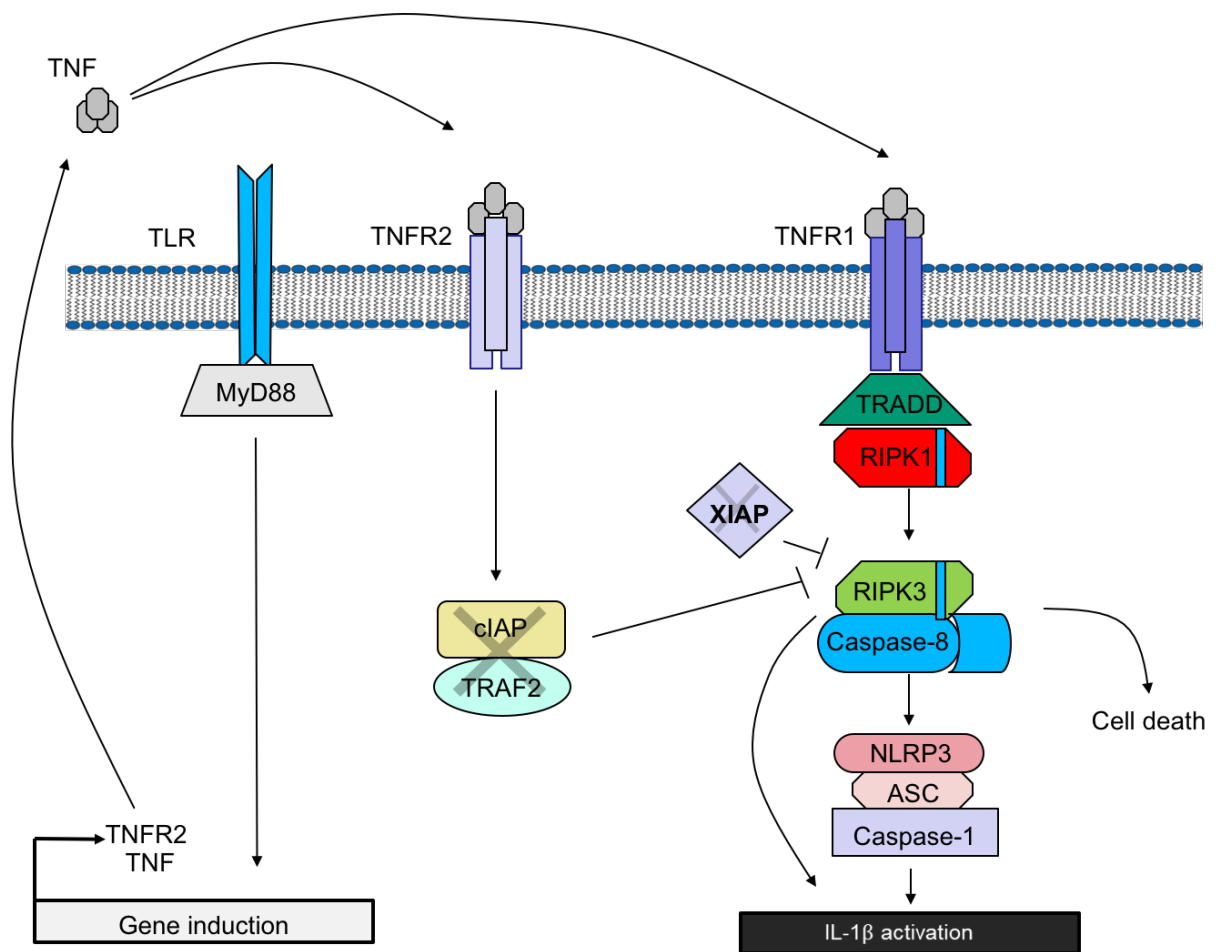


Figure 1.8 XIAP-dependent control of the inflammasome pathway

Ripoptosome formation in the absence of XIAP is associated with apoptotic cell death as well as the activation of NLRP3 inflammasome pathway. The activation of NLRP3 inflammasome occurs when NLRP3 interacts with the ASC adaptor protein which further associates with caspase-1 to form the NLRP3 inflammasome. These processes subsequently allow for the production of the proinflammatory cytokine IL-1 β . Adapted from Lawlor *et al.*, (2017).²⁸⁹

1.3.3.2 XIAP-dependent induction of the TGF- β and BMP signaling

As mentioned above, TGF- β and BMP signaling is essential for mesoderm development in early *Xenopus* embryos and XIAP plays a central role in regulating this pathway.^{256,257} Following the binding of TGF- β /BMP ligand to its respective receptor forms, the protein TGF- β activating kinase 1 (TAK1), an ubiquitin-dependent mitogen-activated protein kinase kinase kinase, is recruited to the TGF- β /BMP signaling pathway. The binding and activation of TAK1 requires the interaction with TGF- β activated Kinase 1 also known as TAB1.^{313,314} Previous studies have shown that XIAP via its BIR1 domain bridges TAB1 to TAK1 allowing for the activation of TAK1 (**Fig.**

1.9).^{256,257,315} This process further activates the MAP kinases downstream, leading to NF- κ B transcription to promote inflammation and cell survival.^{315,316}

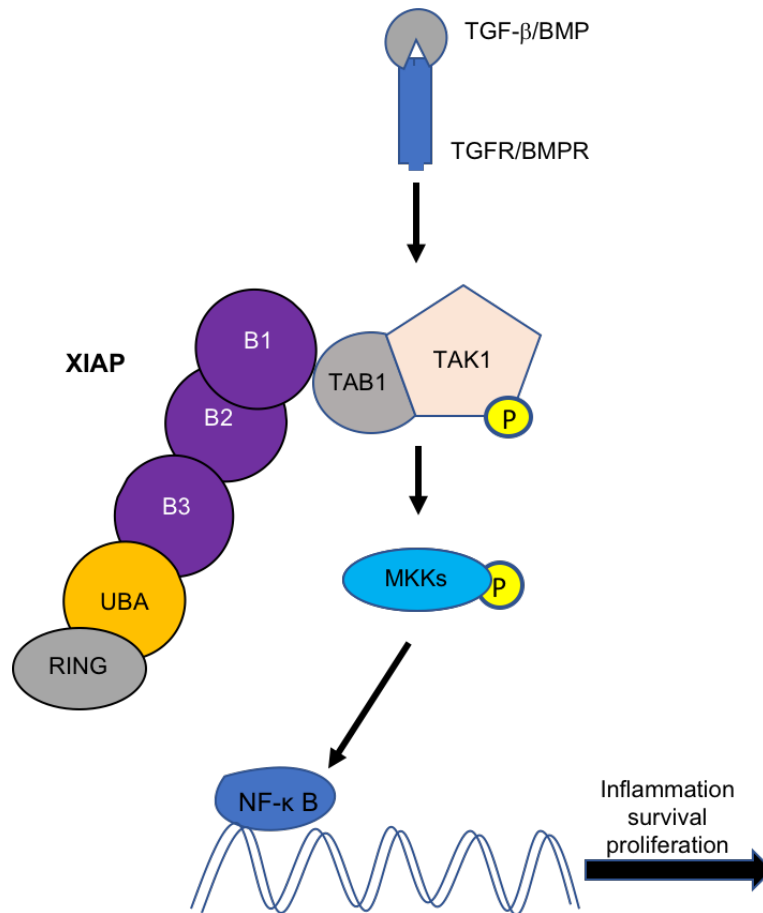


Figure 1.9 XIAP-dependent regulation of TGF- β and BMP signaling

XIAP interacts with TAB1 via its BIR1 domain and bridges TAB1 to the TGF- β /BMP signaling pathway. TAB1 binds and activates TAK1, which that further leads to the activation of NF- κ B signaling. Adapted from Yusuke *et al.*, (2017).³¹⁷

1.3.3.3 XIAP-dependent control of Dectin-1 signaling

XIAP also plays an important role in eliciting responses towards fungal infections.³¹⁸ Recognition of β -glucan which is a polysaccharide present in the cell wall of several microbes including fungi by the PRR Dectin-1, is critical for NF- κ B-dependent innate immune responses against fungal infections.³¹⁹ Previous studies have demonstrated that following Dectin-1 stimulation by β -glucan, XIAP was required for recruiting, binding and ubiquitinating B-cell chronic lymphocytic leukemia/lymphoma 10 (BCL10), that activates NF- κ B signaling, allowing for the initiation of effective innate responses against fungal infections (**Fig. 1.10**).^{318,320} In accordance with this, the *Xiap*^{-/-} mice when infected with the fungus *Candida albicans*, had defects in the production of pro-

inflammatory cytokines at acute stages due to defective NF- κ B signaling. Moreover, XIAP-dependent recruitment of BCL10 was also required for carrying out phagocytosis of *C. albicans* (Fig. 1.10). When NF- κ B-dependent innate immunity is compromised at initial stages and phagocytosis does not occur efficiently in *Xiap*^{-/-} mice following *C. albicans* infection, the pathogen accumulates in macrophages which at later stages causes hyperactivation of macrophages that leads to inflammation in the *Xiap*^{-/-} mice.³²⁰ These processes may also describe the mechanism behind XLP-2 that is associated with hyperactivation of macrophages and excessive production of cytokines observed during chronic inflammation.³²¹

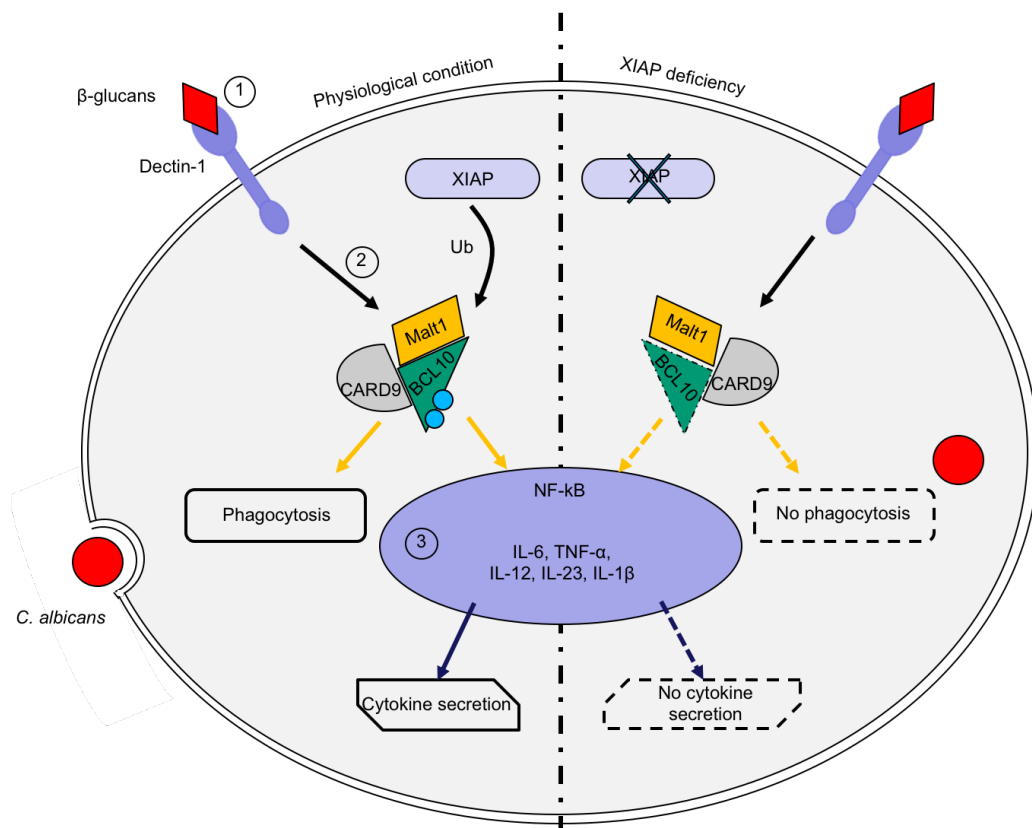


Figure 1.10 XIAP-dependent control of the fungal infections

Following *C. albicans* infection (on the left) where Dectin-1 stimulation occurs (1), XIAP binds to and ubiquitinates BCL10 (2) which subsequently leads to phagocytosis to remove *C. albicans* from macrophages as well as activation of NF- κ B signaling to produce pro-inflammatory cytokines that mediate effective innate responses against *C. albicans* infection (3). On the right, XIAP deficiency leads to improper NF- κ B signaling that causes defective production of cytokines as well as impaired phagocytosis, allowing for the accumulation of *C. albicans* at acute stages of infection in the macrophages. Adapted from Chiocchetti A (2014).³¹⁷

1.3.3.4 XIAP-dependent regulation of NOD1/2 signaling

XIAP also gained much attention, when it was discovered to play a crucial role in the NOD1/2 signaling pathway. At a molecular level, in response to the bacterial ligands L-Ala- γ -D-Glu-mDAP (Tri-DAP; recognized by NOD1) or MDP (recognized by NOD2), XIAP is recruited to the NOD1/2 signaling pathway where it polyubiquitinates the downstream receptor-interacting protein kinase- 2 (RIPK2).³²² This event further leads to the recruitment of a trimeric protein complex called linear ubiquitin chain assembly complex (LUBAC) that consists of the catalytic subunits HOIP and two regulatory subunits called HOIL-1 and SHARPIN. The recruitment and ubiquitination of proteins in the LUBAC complex by XIAP subsequently enables NF- κ B transcription that leads to the production of pro-inflammatory cytokines (**Fig. 1.11**).^{323,324}

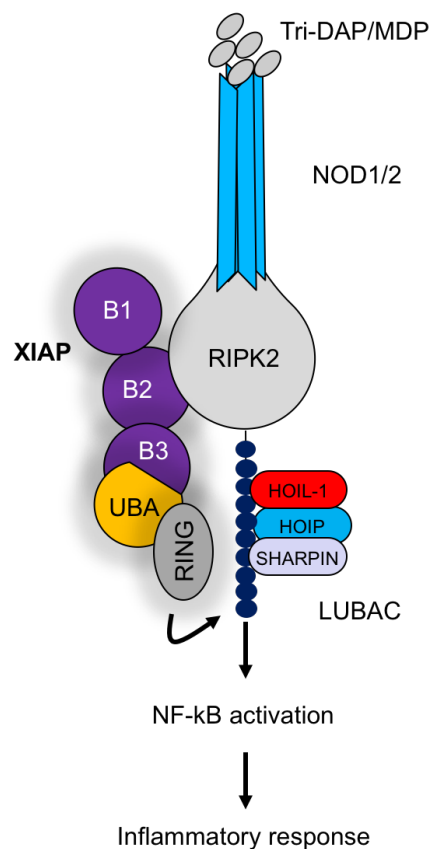


Figure 1.11 XIAP-dependent control of the NOD1/2 signaling pathway

Activation of NOD1/2 by its ligands leads to the recruitment of XIAP which binds to RIPK2 through its BIR2 domain to allow for RIPK2 ubiquitination. Ubiquitination of RIPK2 subsequently leads to the recruitment of the LUBAC complex. In addition, XIAP also ubiquitinates proteins in the LUBAC complex to promote NF- κ B signaling, which induces inflammatory responses. Adapted from Damgaard *et al.*, (2012).³²³

Numerous studies in mice and humans have demonstrated that loss of XIAP is directly associated with defective NOD1/2 signaling. For example, *Xiap*^{-/-} mice show an increased bacterial burden, decreased survival and compromised NF-κB transcription, upon infection with pathogen *Listeria monocytogenes*.³²⁵ The infected mice also display defective expression of cytokines *Il6* and *Tnfa* by macrophages, known to be secreted following the activation of the NOD2.^{176,325,326} Moreover, a subset of CD patients with *XIAP* mutations also have impaired NOD1/2 signaling.^{215,216,223} More specifically, studies performed by Zeissig *et al.*, showed that peripheral blood mononuclear cells (PBMCs) from a subset of the patients with *XIAP* mutations were unable to bind to RIPK2 and demonstrated defective NF-κB signaling followed by diminished secretion of cytokine IL-8, only in response to NOD1/2 ligands but not in other TLR ligands.²¹⁶ Hence, XIAP plays a central role in the NOD1/2 signaling to carry out efficient NF-κB transcription and production of pro-inflammatory cytokines.

1.3.3.5 XIAP-dependent control of adaptive immunity

Apart from its vital roles in innate immunity, XIAP was also shown to regulate adaptive immunity. Previous studies demonstrated that pulmonary macrophages isolated from *Xiap*^{-/-} mice infected with *Chlamydomphila pneumoniae*, undergo increased apoptosis and have low levels of NF-κB when compared to the WT mice after stimulation with LPS, TNF-α or IFN-γ.³²⁷ In addition to these innate defects from macrophages, loss of XIAP in mice was associated with reduced proliferation of adaptive T cells and low numbers of CD8 positive cytotoxic T cells when compared to WT mice.³²⁷ These defects are likely mediated by increased effector caspase-mediated apoptosis of T cells as well as defective NF-κB signaling due to the absence of XIAP.^{248,260,299,300,323} Compromised adaptive immunity observed during XIAP deficiency, also affects anti-viral responses. Previous studies in mice by Gentle *et al.*, have demonstrated that XIAP cooperates with cIAP1 to regulate T cell loss during lymphocytic choriomeningitis virus (LCMV) infection. The loss of CD8 positive T cells during LCMV was shown to be due to the combined loss of XIAP and cIAP1 that induced TNF-dependent T cell death.²⁸⁷ In accordance with this observation, *in vitro* studies showed that T cells from patients with XIAP deficiency have an increased susceptibility to apoptosis and this phenotype is rescued by the expression of WT XIAP.²¹² In addition to regulating T cell survival, loss of XIAP has also been associated with defects in innate-like T lymphocyte such as invariant NKT cells (iNKT cells) and Mucosal-associated invariant T (MAIT) cells.³²⁸

XIAP-deficient patients with HLH who present with EBV infection were shown to have low numbers of iNKT and MAIT cells.³²⁸ However, these alterations were observed only in certain patients with XIAP deficiency and can also occur in HLH patients with EBV infection who do not carry *XIAP* mutations.^{328,329} Therefore, low numbers of iNKT and MAIT cells accompanying EBV infection may occur due to increased apoptosis of these cells triggered as a consequence of excessive inflammation observed in HLH, but may not be due to XIAP deficiency.³²¹

1.4 Purpose of the current study

The Zeissig group and others have recently described novel *XIAP* mutations in male children with early-onset Crohn's disease (CD).^{215-218,220,223} While the only curative treatment regime currently available for CD patients with *XIAP* mutations is allogeneic hematopoietic stem cell transplantation, significant mortality associated with the outcome of this procedure calls for alternative therapies.³³⁰ Investigation of alternative therapies requires a better understanding of the mechanism of CD pathogenesis in patients with *XIAP* mutations. To provide insight into the pathways that link *XIAP* mutations to IBD, we have investigated the role of XIAP in intestinal homeostasis and pathogenesis of IBD, by studying mice with constitutive and cell-specific deletions of *Xiap*.

2. Materials and methods

2.1 Materials

2.1.1 List of antibodies

Table 2.1 List of antibodies

Antibody	Host	Company	Concentration	Catalog number
4',6-diamidino-2-phenylindole (DAPI)		Sigma-Aldrich, Seelze, Germany	1:1000	D9542-1MG
Anti-chromogranin A (H-300)	rabbit	Santa Cruz, Heidelberg, Germany	1:200	sc-13090
Anti-cleaved Caspase-3 (Asp175)	rabbit	Cell Signaling Technology®, Frankfurt, Germany	1:300	9664S
Alexa Fluor 594 anti-goat	donkey	Life Technologies, Darmstadt, Germany	1:1000	A11058
Alexa Fluor 488 anti-rabbit	donkey	Life Technologies, Darmstadt, Germany	1:1000	A21206
Anti- GFP (D5.1) XP®	rabbit	Cell Signaling Technology®, Frankfurt, Germany	1:75	2956
Anti- lysozyme C (C-19)	goat	Santa Cruz, Heidelberg, Germany	1:100	sc-27958
Anti- mucin 2 (H-300)	rabbit	Santa Cruz, Heidelberg, Germany	1:100	sc-15334

2.1.2 List of probes and primers

Table 2.2 List of probes and primers

Gene name	Sense	Antisense
Cy3-Bact338	5'-GCTGCCTCCCGTAGGAGT-3'	
<i>Il1β</i>	5'-GATGATAACCTGCTGGTGTGTGA-3'	5'-TTTGTCGTTGCTTGGTTCTCC-3'
<i>Il6</i>	5'-TAGTCCTTCCTACCCCAATTTCC-3'	5'-TTGGTCCTTAGCCACTCCTTC-3'
<i>Tnfα</i>	5'-CCACCACGCTCTTCTGTCTACTG-3'	5'-GCCATAGAACTGATGAGAGG-3'
<i>Il8</i>	5'-CTGGGATTCACCTCAAGAACA TC-3'	5'-CAGGGTCAAGGCAAGCCTC-3'
<i>Ifny</i>	5'-AGCAAGGCGAAAAAGGATGC-3'	5'-TCATTGAATGCTTGGCGCTG-3'
<i>Il22</i>	5'-GTTGACACTTGTGCGATCTCT-3'	5'-TTGCACCGGGTGTGACG-3'
<i>Il10</i>	5'-GAGAGCTGCAGGGCCCTTTGC-3'	5'-CTCCCTGGTTTCTTTCCCAAGACC-3'
<i>Lyz1</i>	5'-AATGGATGGCTACCGTGGTGT-3'	5'-TAGTCGGTGCTTCGGTCTC-3'
<i>Xiap</i>	5'-TGCAAATACCTATTGGATGAG AAGG-3'	5'-AAAGATTCCTCAAGTGAATGGGT-3'
<i>Defa1</i>	5'-AAGAGACTAAAACTGAGGAGCAGC-3'	5'-CGACAGCAGAGCGTGTA-3'

<i>Defa3</i>	5'- TCGCTGAACATGGAGACCAC- 3'	5'-CGAGGTAGTCATCAGGCACC- 3'
<i>Defa5</i>	5'- AGGCTGATCCTATCCACAAAA CAG-3'	5'- TGAAGAGCAGACCCTTCTTGGC- 3'
<i>Reg3y</i>	5'- CTGTGGTACCCTGTCAAGAGC -3'	5'-TTGGGATCTTGCTTGTGGCTA- 3'
<i>Mmp7</i>	5'- ACAAAGGACGACATTGCAGG- 3'	5'-AGTGAGTGCAGACCGTTTCT-3'
<i>Ang4</i>	5'- TAGACTCGTCCCCAGTTGGA- 3'	5'-AGGAATCACAACCAGACCCAG- 3'
<i>bactin</i>	5'- GCCATGTACGTAGCCATCCA- 3'	5'-CGGAGTCCATCACAATGCCT-3'
Total bacteria (<i>Eub338</i>)	5'- ACTCCTACGGGAGGCAGCAG- 3'	5'-ATTACCGCGGCTGCTGG-3'
<i>Basophila wadsworthia</i>	5'-CCAACATGCACGGYTCCA- 3'	5'- CGTCGAACTTGA ACTTGA ACTTG TAGG-3'
<i>Helicobacter hepaticus</i>	5'- GCATTTGAACTGTTACTCTG- 3'	5'-CTGTTTTCAAGCTCCCCGAAG- 3'
16S-V6-784 (forward)	5'-AGGATTAGATACCCTGGTA- 3'	
16S-V6- 1061 (reverse)		5'-CRRCACGAGCTGACGAC-3'

2.1.3 Buffers, solutions and media

Name	Composition
1,4-piperazinediethanesulfonic acid (PIPES) buffer	10 mM PIPES 150 mM Sodium Chloride (NaCl) pH 7.4
Acid ethanol (EtOH)	99.75 % Absolute EtOH 0.25 % 37% Hydrochloric acid
Carnoy's fixative	46 % EtOH 46 % Glacial acetic acid 8 % Chloroform
Coating Buffer for enzyme-linked immunosorbent assay (ELISA)	0.1 M Sodium hydrogen carbonate (NaHCO ₃) 0.03 M Sodium carbonate (Na ₂ CO ₃) pH 9.5
Citrate buffer	1.8 % 0.1 M Citric acid 8.2 % 0.1 M Sodium citrate pH 6.0
Eosin stain	8 g Eosin Y 5 ml Deionized water 940 ml 96% EtOH
Flow cytometry buffer	1 % Fetal calf serum (FCS) in phosphate buffered saline (PBS)
<i>Helicobacter hepaticus</i> growth media	39 g Columbia agar 1000 ml Deionized water (sterile) 4 mg Amphotericin B

	2 Vials Skirrow Campylobacter selective supplement 100 ml Lysed horse blood
Hybridization buffer for fluorescence <i>in situ</i> hybridization staining	18 % 5 M NaCl 2 % 1 M Tris-hydrochloric acid (Tris-HCl) 0.5 % Sodium dodecyl sulfate (SDS) pH 7.4
PBS (10X)	1.37 M NaCl 27 mM Potassium chloride (KCl) 100 mM Di-Sodium hydrogen phosphate (Na ₂ HPO ₄) 18 mM Potassium dihydrogen phosphate (KH ₂ PO ₄) pH 7.4
RPMI 1640 complete 50	500 ml RPMI 1640 10 % FCS (v/v) 2 mM L-glutamine 1 % Penicillin-streptomycin (v/v)
Sodium phosphate buffer	31.6 % 1 M Sodium dihydrogen phosphate monohydrate (NaH ₂ PO ₄ · H ₂ O) 68.4 % 1 M Di-Sodium hydrogen phosphate dihydrate (Na ₂ HPO ₄ · 2H ₂ O) pH 7.2
Stop Solution for ELISA	2 N Sulfuric acid (H ₂ SO ₄)
Tryptic soy agar medium	40 g Tryptic soy agar

	1000 ml Deionized water (sterile)
Tryptic soy broth	30 g Tryptic soy broth 1000 ml Deionized water (sterile)
Wash Buffer for ELISA	PBS (1X) 0.05 % Tween-20 (v/v)
Washing Buffer for fluorescence <i>in situ</i> hybridization staining	900 mM NaCl 2 % 1 M Tris-HCl 0.06 % SDS pH 7.4

2.1.4 Kits

Kits	Company
Mouse IL-6 ELISA Kit	BioLegend®, London, UK
Mouse MCP-1 ELISA Kit	BioLegend®, London, UK
RNeasy Mini Kit	QIAGEN, Hilden, Germany
AllPrep DNA/RNA Mini Kit	QIAGEN, Hilden, Germany
DNeasy Blood & Tissue Kit	QIAGEN, Hilden, Germany
High-Capacity cDNA Reverse Transcription Kit	Applied Biosystems™, Darmstadt, Germany
Maxima SYBR Green/ROX qPCR Master Mix (2X)	Thermo Fisher Scientific, Waltham, Massachusetts, USA
MiSeq V3 sequencing kit	Illumina®, Inc., San Diego, California, (USA)

2.1.5 Reagents and chemicals

Reagents and chemicals	Company
2-Mercaptoethanol	Carl Roth, Karlsruhe, Germany
7-Amino-actinomycin D	BD Biosciences, Heidelberg, Germany
37 % Hydrochloric acid	VWR, Darmstadt, Germany

Absolute EtOH	VWR, Darmstadt, Germany
Amphotericin B	Biochrom, Berlin, Germany
Bovine serum albumin (BSA)	Sigma-Aldrich, Seelze, Germany
Chloroform	Merck, Darmstadt, Germany
Columbia agar	Oxoid Germany GmbH, Wesel, Germany
Dextran sulfate sodium	MP Biomedicals, Santa Ana, California, USA
Di-Sodium hydrogen phosphate	Merck, Darmstadt, Germany
Di-Sodium hydrogen phosphate dihydrate	Merck, Darmstadt, Germany
DNase enzyme	Sigma-Aldrich, Seelze, Germany
EDTA 0.5 M solution pH 8.0	Applied Biosystems, Darmstadt, Germany
Entellan®	VWR, Darmstadt, Germany
Eosin Y	University clinic Dresden pharmacy, Dresden, Germany
FCS	Merck, Darmstadt, Germany
FluorSave™ Reagent	Merck, Darmstadt, Germany
Formalin	SAV Liquid Production GmbH, Flintsbach am Inn, Germany
Glacial acetic acid	Merck, Darmstadt, Germany
Horse blood	Oxoid Germany GmbH, Wesel, Germany
L-Glutamine	Merck, Darmstadt, Germany
Mayer's hemalum solution	VWR, Darmstadt, Germany
Penicillin-Streptomycin (P/S)	Merck, Darmstadt, Germany
Potassium chloride	Merck, Darmstadt, Germany
Potassium dihydrogen phosphate	Merck, Darmstadt, Germany
RNA/ater RNA Stabilization Reagent	QIAGEN, Hilden, Germany
RPMI 1640 medium	Thermo Fisher Scientific, Waltham, Massachusetts, USA
SDS	AppliChem, Darmstadt, Germany
SignalStain® Antibody Diluent	Cell Signalling Technology®, Frankfurt, Germany
Skirrow Campylobacter selective supplement	Oxoid Germany GmbH, Wesel, Germany

Sodium carbonate	Merck, Darmstadt, Germany
Sodium chloride	Sigma-Aldrich, Seelze, Germany
Sodium dihydrogen phosphate monohydrate	Merck, Darmstadt, Germany
Sodium hydrogen carbonate	Merck, Darmstadt, Germany
Sulfuric acid	VWR, Darmstadt, Germany
TrypLE™ Express Enzyme	Life Technologies, Darmstadt, Germany
Trypsin (10X)	Merck, Darmstadt, Germany
Tris	Calbiochem (Merck), Darmstadt, Germany
Tris base	Calbiochem (Merck), Darmstadt, Germany
Tryptic soy broth (TBE) medium	BD Biosciences, Heidelberg, Germany
TBE agar	BD Biosciences, Heidelberg, Germany
Tween® 20	Serva, Heidelberg, Germany
Xylene	VWR, Darmstadt, Germany

2.1.6 Instruments

Instrument	Company
-80° C freezer	New Brunswick™, Eppendorf AG, Hamburg, Germany
-20° C freezer	Liebherr, Bieberach an der Riß, Germany
4° C refrigerator	Liebherr, Bieberach an der Riß, Germany
Anaerobic pot	Oxoid Germany GmbH, Wesel, Germany
BD 115 Incubator	BINDER, Tuttlingen, Germany
BDTM LSR II Flow Cytometer	BD Biosciences, Franklin Lakes, New Jersey, USA
FlexStation 3 Multi-Mode Microplate Reader	Molecular Devices, Sunnyvale, California, USA

Heraeus™ Fresco™ 21 Microcentrifuge (rotor-75003424)	Thermo Fisher Scientific, Waltham, Massachusetts, USA
Heraeus™ Megafuge™ 16R Centrifuge (rotor-75003629, 75003181)	Thermo Fisher Scientific, Waltham, Massachusetts, USA
Illumina® MiSeq system	Illumina®, Inc., San Diego, California, (USA)
NanoDrop™ 2000 Spectrophotometer	Thermo Fisher Scientific, Waltham, Massachusetts, USA
OD600 DiluPhotometer™	Implen, Munich, Germany
QIAxcel Advanced System	QIAGEN, Hilden, Germany
Rocking platform	Carl Roth, Karlsruhe, Germany
Rotary Microtome HM 340 E	Thermo Fisher Scientific, Waltham, Massachusetts, USA
Stratagene Mx3005P QPCR System	Agilent Technologies, Santa Clara, California, USA

2.1.7 Consumables

Consumables	Company
5 ml FACS tube	Sarstedt, Nümbrecht, Germany
Corning® 40 and 70 µm cell strainer	Sigma-Aldrich, Seelze, Germany
96 well qPCR plate	Agilent Technologies, Santa Clara, California, USA
Corning® 96 Well Clear Polystyrene Microplate, round bottom with lid	Sigma-Aldrich, Seelze, Germany
Corning® 96 well EIA/RIA plate, flat bottom	Sigma-Aldrich, Seelze, Germany
Corning® serological pipette, 5 ml/10 ml/25 ml/50 ml	Sigma-Aldrich, Seelze, Germany
Falcon™ Conical Centrifuge Tubes, 15 ml/50 ml	Thermo Fisher Scientific, Waltham, Massachusetts, USA
Microtest Plate 96 Well, F	Sarstedt, Nümbrecht, Germany
PCR tubes 0.5 ml	Sarstedt, Nümbrecht, Germany
Pipet tips, 10 µl, 200 µl, 1000 µl,	Sarstedt, Nümbrecht, Germany

Reaction tube 1.5 ml	Engelbrecht GmbH, Edermünde, Hesse, Germany
SafeSeal Micro Tube 1.5 ml and 2 ml	Sarstedt, Nümbrecht, Germany
Shredder	QIAGEN, Hilden, Germany
SuperFrost Plus™ slides	Thermo Fisher Scientific, Waltham, Massachusetts, USA
Syringe (10 ml)	B. Braun Melsungen AG, Hessen Germany

2.1.8 Software

Software	Company
Fast Length Adjustment of Short reads (FLASH)	Center for Computational Biology, Johns Hopkins University, Baltimore Maryland, USA
FlowJo software	Tree Star Inc., Ashland, Oregon, USA
FIJI software	National Institutes of Health, Maryland, USA
GraphPad Prism 6	GraphPad Software, San Diego, California, USA
R Software	R foundation, Vienna, Austria

2.2 Methods

2.2.1 Mice

All mice were handled and experiments were conducted with the approval and in compliance with the institutional guidelines and respective authorities at Kiel University, Technical University of Dresden and Hannover Medical School. The germ-free (GF) C57BL/6J and GF *Xiap*^{-/-} mice were generated and housed at the gnotobiotic facility at the Hannover Medical School. The *Xiap*^{-/-} mice³³¹ were crossed with *Tnfr1*^{-/-}³³², the recombination activating gene 1 (*Rag1*^{-/-})³³³, *Nod2*^{-/176-}, or *Lgr5-EGFP-IRES-CreER*^{T2 16} mice (all mice lines obtained from The Jackson Laboratory (Bar Harbor, Maine, USA) and *Ripk3*^{-/-} mice³³⁴ (gift of Prof. Stefan Krautwald, University Hospital Schleswig-Holstein, Kiel, Germany) to obtain the respective double knockout mice. Furthermore, mice with a floxed *Xiap* allele (*Xiap*^{fl/fl}) were generated as mentioned before³³⁵, by crossing with transgenic mice that express Flp recombinase.³³⁵ *Xiap*^{fl/fl} mice were either crossed with Villin-*Cre*³³⁶ (The Jackson Laboratory), LysM-*Cre*³³⁷ (The Jackson Laboratory) or Defa6-*Cre*²³⁸ (gift of Prof. Dr. Richard S. Blumberg, Harvard Medical School, Boston, Massachusetts, USA, and Prof. Dr. Arthur Kaser, University of Cambridge, United Kingdom), to generate IEC-specific, myeloid cell-specific or PC-specific *Xiap* knockouts, respectively. All experiments were conducted with sex- and age-matched mice. All mice were weaned at three weeks of age and housed as per regulations of the specific institutes. Mice were maintained at specific pathogen-free (SPF) barrier facilities and were either from a C57BL/6J background (all single and double knockout mice) or a mixed background of C57BL/6J and C57BL/6N (all conditional knockout mice).

2.2.2 *Helicobacter hepaticus* infection

Helicobacter hepaticus was cultured and grown in the laboratory of Prof. André Bleich (Hannover Medical School, Germany). *H. hepaticus* was isolated from the caecum of a male mouse (BC-R4-1110^{-/-}) from The Jackson Laboratories, aged 24 weeks³³⁸ and plated on Columbia agar with supplements (refer to materials section for the composition). The agar plates were cultured under microaerophilic conditions and placed in an anaerobic pot at 37°C. To generate the microaerophilic conditions in the anaerobic pots, a gas mixture consisting of 10 % CO₂, 10 % H₂ and 80 % N₂ was exchanged four times from -0.2 bar pressure to 0.2 bar pressure. The bacteria were re-inoculated and expanded onto a new plate every 3 to 4 days and cultured at the

same conditions until the amounts required for infecting mice were generated. For the infection, mice were gavaged with either PBS or 1×10^8 colony forming units (CFU) of *H. hepaticus* in 100 μ l PBS. Following gavage, mice were sacrificed and tissues were collected for different downstream analysis either two or twelve weeks after infection as indicated in **Fig. 2.1**.

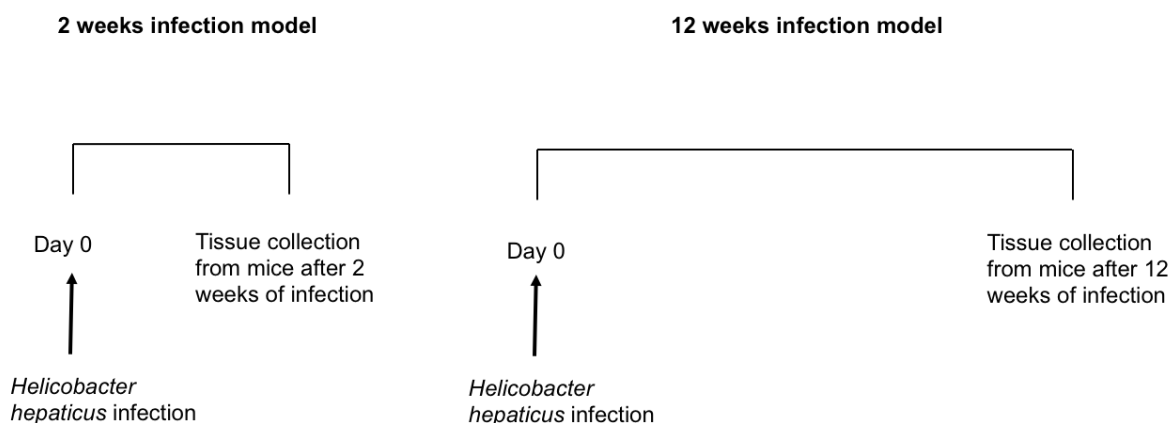


Figure 2.1 Acute and chronic infection models of *H. hepaticus* infection

Schematic representation of acute model (2 weeks) and chronic model (12 weeks) of *H. hepaticus*.

2.2.3 Immunofluorescence staining

Small and large intestinal 'Swiss rolls' were fixed overnight in formalin at 4°C and all samples were dehydrated and embedded in paraffin. Sections of four micrometer (μ m) thickness were cut using a microtome and dehydrated as mentioned in the **table 2.3**.

Table 2.3 Dehydration steps for staining

Dehydration steps	Reagent	Duration (minutes)	Number of times the washing step was carried out
1	Xylene	5	3
2	Absolute EtOH	3	2
3	95% EtOH	3	2
4	70% EtOH	3	2

Thereafter, slides were washed 3 times in PBS for 5 minutes. Antigen retrieval was performed by boiling the slides for 20 minutes in citrate buffer. Following antigen

retrieval, slides were cooled down to 40-50°C, washed 3 times in PBS for 5 minutes each and blocked in 1 % BSA in PBS-Tween® 20 for 30 minutes at room temperature (RT). The slides were incubated with SignalStain Antibody Diluent containing the primary antibodies (see section 2.1.1 for antibody details and dilutions used) for one hour at RT. This was followed by washing the slides 3 times in PBS for 5 minutes each and incubating with respective fluorescence labeled secondary antibodies (see section 2.1.1) and DAPI for 1 hour at RT. The slides were then washed 3 times in PBS for 5 minutes each and embedded in FluorSave™ Reagent.

2.2.4 Hematoxylin and eosin staining and histopathological evaluation

Small and large intestinal 'Swiss rolls' were fixed overnight in formalin at 4°C and all samples were dehydrated and embedded in paraffin. Sections of four µm thickness were cut using a microtome and were dehydrated using a series of xylene and EtOH as described in section 2.2.3. The slides were washed thrice in PBS for 5 minutes each, incubated for 2 minutes in Mayer's hemalum solution (diluted 1:2 with PBS), and rinsed in deionized water. The slides were then incubated for 5 minutes in tap water after which they were dipped 10-12 times in acid EtOH solution (see section 2.1.3 for reagent composition). This was followed by staining the slides for 45 seconds in Eosin stain (see section 2.1.3 for reagent composition), washing twice for 10 seconds in absolute EtOH and twice for 10 seconds in xylene, and mounting in Entellan®.

H. hepaticus infected mice were scored for granulomas on Hematoxylin and Eosin (H & E) stained ileal sections by the pathologist Prof. Dr. Michael Muders (University Hospital Bonn, Bonn, Germany) as described previously.¹⁷² Histopathological scoring for the colitis experiments was performed on H & E stained colonic Swiss rolls in a blinded manner.³³⁹

2.2.5 Fluorescence *in situ* hybridization staining

Fluorescence *in situ* hybridization (FISH) staining was performed on large intestinal 'Swiss rolls' that were fixed overnight at 4°C in Carnoy's fixative (see section 2.1.3 for reagent composition). Following fixation, samples were dehydrated and embedded in paraffin. Four µm paraffin sections were cut using a microtome and sections were then dehydrated by first washing the slides thrice in xylene for 5 minutes, then twice in absolute ethanol for 3 minutes. Slides were air dried at 50°C for 25 minutes followed

by incubation for 1 hour in hybridization buffer (see section 2.1.3 for reagent composition) containing 25 ng of Cy3-labeled universal bacterial probe Bact338 (see section 2.1.2 for the nucleotide sequence), pre-warmed to 50°C. Thereafter, slides were washed in washing buffer pre-warmed to 50°C (see section 2.1.3 for reagent composition) for 5 minutes, rinsed with distilled water, dried at 50°C for 5 minutes and incubated with DAPI in PBS (see section 2.1.1 for DAPI concentration) for 15 minutes at RT. This was followed by rinsing with distilled water and embedding the slides in FluorSave™ Reagent.

2.2.6 RNA extraction and quantitative polymerase chain reaction

Tissues were washed in PBS, incubated overnight at 4°C in RNA*later* RNA Stabilization Reagent. The following day, RNA*later* was removed and tissues were stored at -80 °C until RNA extraction was performed. To perform RNA extraction, tissues were crushed quickly using a mortar and pestle in RLT lysis buffer from the RNeasy Mini Kit containing 2-mercaptoethanol (10 µl 2-mercaptoethanol in 1000 µl RLT buffer). The lysed samples were homogenized by passing through shredder columns and spinning at 14,000 rpm for 3 minutes at RT. Further steps of RNA isolation were carried out according to the manufacturer's instructions of the RNeasy Mini Kit. To perform quantitative polymerase chain reaction (qPCR), one µg of RNA was transcribed into cDNA using the High-Capacity cDNA Reverse Transcription Kit from as per the manufacturer's instructions. qPCR was carried out using Maxima SYBR Green/rox qPCR Master Mix (2x). The cycle threshold (Ct) values for all genes were acquired by the Stratagene Mx3005P qPCR System. The acquired Ct values for all genes were normalized to the Ct values of the β-actin gene. Furthermore, the relative expression was calculated using the $\Delta\Delta C_t$ method.³⁴⁰ Primers used in the qPCR are mentioned in section 2.1.2.

2.2.7 Bacterial killing assay

Crypts were isolated as described previously.^{341,342} Ten centimeters of the distal end of the mouse small intestine was cut out, opened longitudinally and washed by gently shaking in PBS. The intestine was cut into approximately 1 cm pieces and was vortexed at 1200 rpm/min in 5 ml of ice-cold PBS containing 30 mM EDTA for 5 min. This step allowed the villi and crypts to be released from the tissues into the liquid containing PBS with 30 mM EDTA. The liquid fraction containing PBS with 30 mM

EDTA was stored on ice and the tissue pieces were transferred into new tubes containing fresh ice-cold PBS with EDTA at the same concentration. The pieces were further vortexed under the same conditions as mentioned in the previous step and the procedure was repeated ten times, during which ten fractions were collected. These fractions were then individually centrifuged at 1300 rpm for 5 min, after which the supernatant was discarded and the pellet was re-suspended in 5 ml ice-cold PBS. The fractions with the most number of crypts and least amounts of villi were pooled for the experiment. The pooled crypts were then centrifuged at 1200 rpm for 5 min and re-suspended in 5 ml ice-cold PIPES buffer (see section 2.1.3 for the buffer composition), and the crypts were counted. Five thousand crypts were taken, spun down and re-suspended in 50 μ l of PIPES buffer, transferred to round bottom 96 well plate, and left unstimulated for 30 minutes whilst shaking at 37°C. Additionally, as a vehicle control, 50 μ l PIPES buffer without crypts were also added to the round bottom 96 well plate and left unstimulated for 30 minutes whilst shaking at 37°C. Following this incubation period, the plate was spun down at 1300 rpm for 5 min at 4°C and 30 μ l of supernatants from all the samples and vehicle were carefully transferred to tubes without disturbing the crypts and frozen at -80°C until used in the bacterial killing assay.

To test bacterial killing from crypts³⁴³, *Escherichia coli* (ATCC 35218) was cultured overnight at 37°C in TBE medium (see section 2.1.3 for broth preparation). The following day different volumes of the *E. coli* culture such as 5 μ l, 10 μ l, 20 μ l and 50 μ l were transferred into separate tubes containing 8 ml of fresh TBE medium. Two hours after incubation, the optical density was measured using a spectrophotometer and the tube with 0.2 OD was chosen for the next step. Thereafter, this culture was serially diluted (1:10, 1:100, 1:1000, 1:10000, 1:20000) in 2 % TBE, supplemented with 0.1 % BSA in sodium phosphate buffer (see section 2.1.3 for buffer composition). Further, 5 μ l of the frozen supernatants from the unstimulated crypts or 5 μ l of PIPES buffer alone (vehicle) was mixed with 20 μ l sodium phosphate buffer and incubated in 25 μ l of the 1:20000 dilution of the previously serially diluted *E. coli* culture for 3 hours at 37°C. Following incubation, 200 μ l sodium phosphate buffer was added to make up a total volume of 250 μ l and mixed thoroughly. Triplicates of 50 μ l of this mixture were plated on tryptic soy broth agar (see section 2.1.3 for agar composition) and incubated overnight at 37°C. The following day, colonies on the agar plate were enumerated. Since the number of bacteria varied in the individual experiments, the groups were

normalized by expressing bacterial cell killing as a percentage (\pm standard deviation) relative to the bacteria incubated 3 hours at 37 °C in PIPES buffer alone (vehicle).

2.2.8 Flow cytometry

The small intestine was taken from WT and *Xiap*^{-/-} mice and flushed with 10 ml ice-cold PBS using a 10 ml syringe. The intestine was cut open longitudinally and the villi along with the luminal contents were scraped off by gently sliding the corner of a cover slip along the inner surface of the small intestine. The intestine was then cut into small pieces (2-4 mm). The tissue pieces were transferred to a 50 ml tube containing 10 ml ice-cold PBS and pipetted up and down few times using a 10 ml pipet. Once the tissue pieces sank to the bottom of the tube, the supernatant was removed and 10 ml of fresh ice-cold PBS was added. The above step was repeated 10-20 times until the supernatant was almost clear. The tissues were then incubated with 2 mM EDTA in PBS and incubated on a rocking platform at 4°C for 30 minutes. Following incubation, the tissue pieces were allowed to settle down and the supernatant was discarded. To the tissues, 10 ml of 10 % FCS in PBS was added and pipetted up and down for three to five times. Once tissue pieces settled down, the supernatant was again discarded. The above step was repeated three more times but the supernatant was collected and pooled from these steps into a 50 ml tube after passing through a 70 μ m cell strainer. The pooled supernatants were spun down at 800 rpm for 5 minutes at 4°C and the pelleted crypts were washed once with 10 ml ice-cold PBS. The crypts were further pelleted by spinning at 800 rpm for 5 minutes at 4°C.

To check for the eGFP⁺ stem cells, small intestinal crypts from *Lgr5-EGFP-IRES-creER*^{T2} mice crossed into WT and *Xiap*^{-/-} mice were isolated as described above and dissociated in 3 ml TrypLE™ Express Enzyme reagent containing 2,000 U/ml DNase enzyme (Sigma) for 30 minutes at 37°C and passed through a 40 μ m cell strainer. The cells were pelleted by spinning at 1200 rpm for 5 minutes 4°C and re-suspended in 200 μ l flow cytometry buffer (section 2.1.3 for buffer composition). Thereafter, the dead cells were excluded using cell viability solution 7-Amino-actinomycin D and flow cytometry data were collected using BDTM LSR II Flow Cytometer. Samples were analyzed using FlowJo software.

2.2.9 16S rRNA sequencing for detection of bacteria in tissues

16S rRNA amplicon sequencing of small intestinal mucosa adherent bacteria was performed in the laboratory of Prof. John Baines (University Hospital Schleswig-Holstein, Kiel, Germany). The AllPrep DNA/RNA Mini Kit was used for performing RNA extraction from the tissues that were snap frozen in liquid nitrogen. The 27F and 338R primer pairs with flanking multiplex identifier (MID)-adaptors were used in the PCR for amplifying the V1–V2 regions of 16S rRNA gene.³⁴⁴ The MiSeq V3 sequencing kit was used for sequencing on the Illumina® MiSeq system and FLASH software was used for merging the paired-end FASTQ sequences.³⁴⁵ The merged reads were filtered such that over 90 % of nucleotides have a quality score of 30 or higher per read. The UCHIME utility of the USEARCH v6.0.307 tool was used to remove potential chimeras and samples were normalized to 20,000 random reads per sample.³⁴⁶ Sequences were classified into the new higher-order taxonomy by the Ribosomal Database Project (RDP) classifier, and the USEARCH v6.0.307 tool was used to cluster the species-level operational taxonomic units (OTUs).^{347,348} Perl scripts were used for plotting the data, and statistical analysis was performed using the Vegan92 package in R software.³⁴⁹

2.2.10 Dextran sulfate sodium-induced colitis

Mice were given 2.5 % DSS in autoclaved water for five days, followed by replacement with normal autoclaved water. For the acute colitis model, mice were sacrificed at day five following replacement with autoclaved water. In the chronic colitis model, mice were administered 2.5 % DSS for two or more discontinuous cycles between which they were given autoclaved water. The schematic representation of the experimental layout is outlined in **Fig. 2.2**.

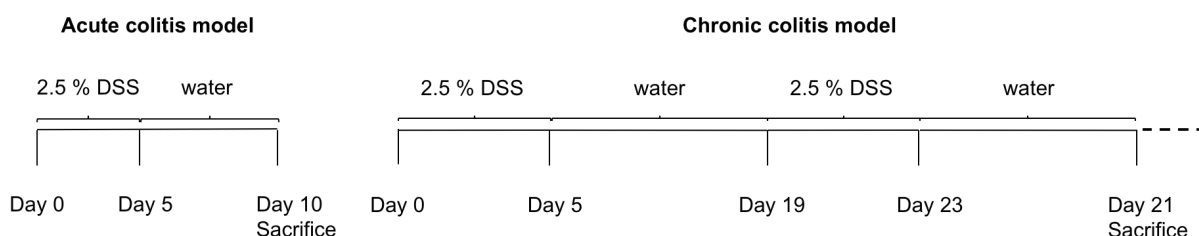


Figure 2.2 Acute and chronic infection models of DSS-induced colitis

Schematic representation of acute and chronic models of colitis.

2.2.11 Colon explant culture and enzyme-linked immunosorbent assay

To make colon explant cultures, a small piece of the mouse colon was weighed, washed several times in PBS and incubated for 24 hours at 37°C with 5 % CO₂ in 96 well round bottom plates containing 200 µL of RPMI 1640 medium supplemented with 10 % FCS (v/v), 2 mM L-glutamine and 1 % penicillin-streptomycin (v/v). After the incubation period, the plate was centrifuged at 1300 rpm for 5 minutes at 4°C, 100 µl of the supernatant was carefully removed without disturbing the pieces and transferred to a new 96 well plate and stored at -20°C until used for the enzyme-linked immunosorbent assay (ELISA). ELISA kits from BioLegend® for detecting secreted IL-6 and MCP-1 cytokines in the supernatants of colon explants were used as per manufacturer's instruction. The protein concentrations from the ELISA experiments were measured at 450 nm using a FlexStation 3 Multi-Mode Microplate Reader and data were presented as picogram per milliliter (pg/ml).

2.2.12 Image capture and analysis

All images were captured using ZEISS Axiovert 200M Microscope and analyzed using FIJI software.

2.2.13 Statistical analysis

The D'Agostino-Pearson omnibus normality test was used to determine the normality of the datasets. For datasets following Gaussian distribution, statistical significance was calculated using the parametric two-tailed Student's *t*-test. Further, for data following skewed distributions, the non-parametric Mann-Whitney *U* test was used. For the survival analysis, the log-rank test was used. All *P* values lower than 0.05 were considered statistically significant. Prism version 6 from GraphPad Software was used for performing the D'Agostino-Pearson omnibus normality test as well as calculating the *P* values.

3. Results

3.1 XIAP regulates Paneth cell homeostasis

Previous studies have demonstrated that CD patients harboring *XIAP* mutations show severe defects in NOD2 signaling.²¹⁶ Since patients with *NOD2* polymorphisms and mice with *Nod2* deficiency exhibit reduced expression of PC α -defensins^{176,226}, we investigated whether *Xiap*^{-/-} mice³³¹ also show similar alterations in α -defensin expression. While the ileum of *Xiap*^{-/-} mice, compared to that of wild-type (WT) mice, indeed exhibited decreased expression of the α -defensin *Defa5*, defects in the expression of PC genes were not limited to α -defensins but observed across the entire PC signature (**Fig. 3.1a**). Given the broad defect in the expression of PC-derived genes, we analyzed PCs by immunofluorescence using antibodies directed against the PC marker lysozyme C (LyzC). These experiments revealed an intact morphology of PCs in the small intestine of *Xiap*^{-/-} mice but reduced numbers of PCs compared to WT littermates (**Fig. 3.1b**). In contrast, other secretory cell types such as goblet cells (**Fig. 3.2a**) and enteroendocrine cells (**Fig. 3.2b**) were present in unaltered numbers in *Xiap*^{-/-} mice.

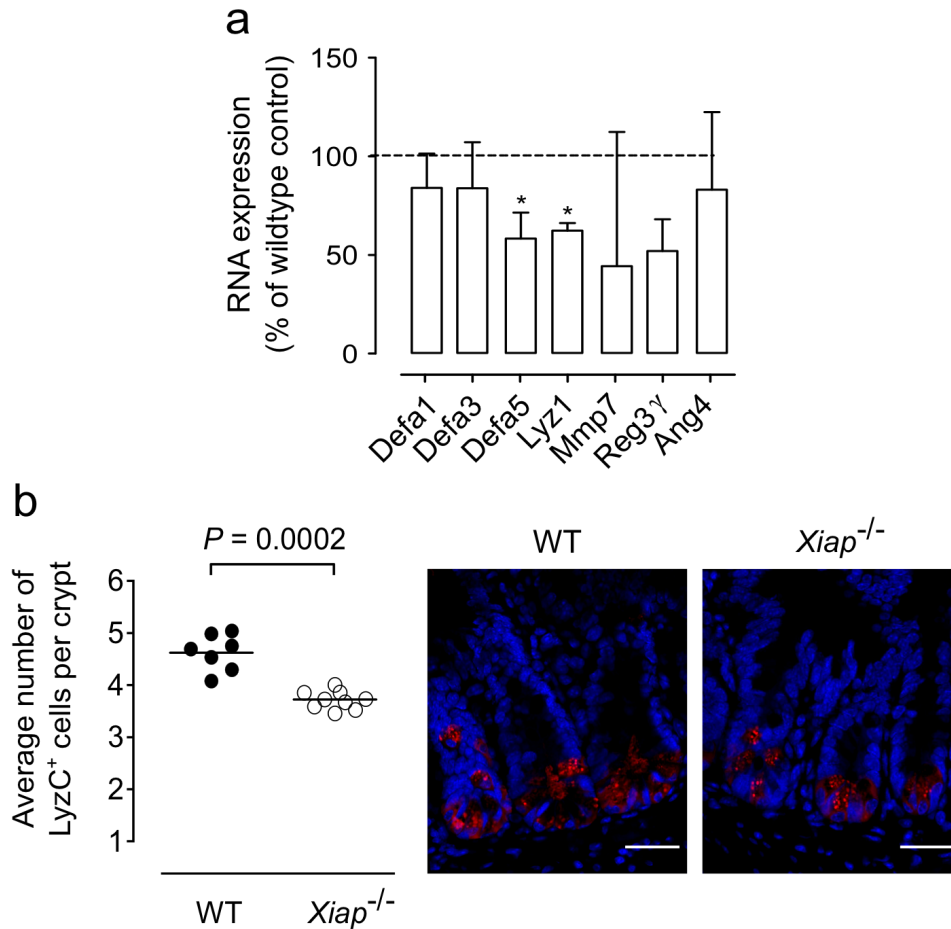


Figure 3.1 XIAP regulates PC homeostasis

(a) qPCR analysis of expression of different PC genes in the ileum of *Xiap*^{-/-} mice ($n = 5$) plotted as % of WT mice ($n = 8$). (b) Quantification of average numbers of lysozyme C positive (LyzC⁺) cells per crypt (left) and representative images for LyzC (red) and DAPI (blue) staining (right) in the ileum of WT ($n = 7$) and *Xiap*^{-/-} ($n = 9$) mice. Scale bar represents 100 μm . In (a) the bar plot indicates the mean \pm s.e.m for *Defa1*, *Defa3*, *Defa5* and *Lyz1*, and median for *Mmp7*, *Reg3 γ* and *Ang4*. In (b) dots represent individual mice and the bar indicates the mean. P values were calculated using the Student's t -test for (b) and *Defa1*, *Defa3*, *Defa5* and *Lyz1* in (a). For *Mmp7*, *Reg3 γ* and *Ang4*, P values were calculated using the Mann-Whitney U -test. In (a) * indicates $P < 0.05$.

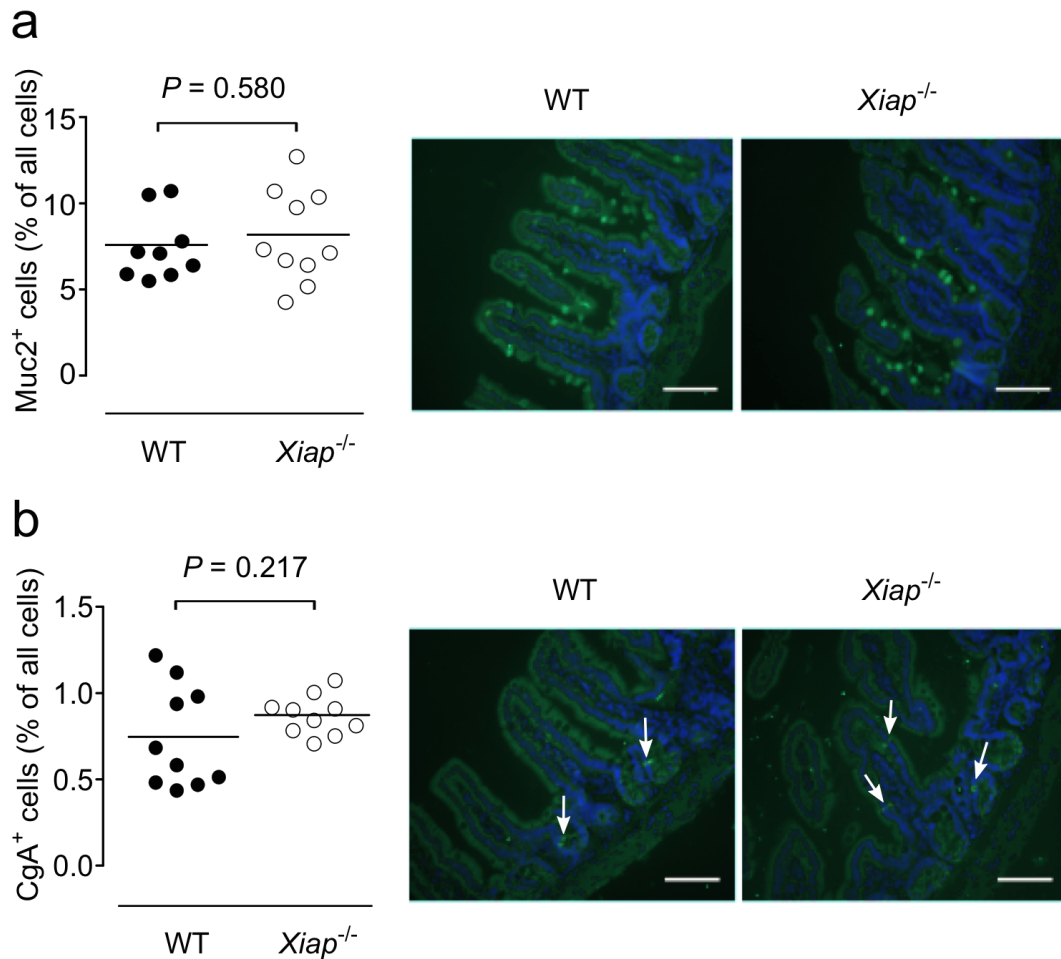


Figure 3.2 Unaltered numbers of goblet cells and enteroendocrine cells in *Xiap*^{-/-} mice

(a) Quantification of Mucin 2-positive (Muc2⁺) cells (left) and representative immunofluorescence images for Muc2 (green) and DAPI (blue) staining (right) in the ileum of WT ($n = 9$) and *Xiap*^{-/-} ($n = 10$) littermates. (b) Quantification of Chromogranin A-positive (CgA⁺) cells (left) and representative immunofluorescence images (right) for CgA (green) indicated by white arrows, and DAPI staining (blue) in the ileum of WT ($n = 10$) and *Xiap*^{-/-} ($n = 10$) littermates. Scale bar for all images represents 100 μm . In all graphs, dots represent individual mice and the bar indicates the mean. P values were calculated using the Student's t -test.

Since PCs secrete various factors that support the homeostasis of ISCs¹³⁰, we also directly investigated ISCs by crossing *Xiap*^{-/-} mice with *Lgr5-EGFP-IRES-CreER*^{T2} mice, which express *EGFP* under the control of *Lgr5* promoter.¹⁶ There were no differences in the number of stem cells in the ileum of *Xiap*^{-/-} mice when compared to WT littermates by immunofluorescence (**Fig. 3.3a**) or flow cytometry (**Fig. 3.3b**). Unaltered stem cell numbers *in vivo* in *Xiap*^{-/-} mice are in line with recent reports which demonstrated that PC-derived factors are critical for the support of ISCs in isolated

epithelial organoid cultures *in vitro* but dispensable for ISC maintenance *in vivo*.^{133,134,350,351} In conclusion, these results demonstrate that XIAP plays a central role in regulating the homeostasis of PCs but not of other secretory cells or ISCs in the gut.

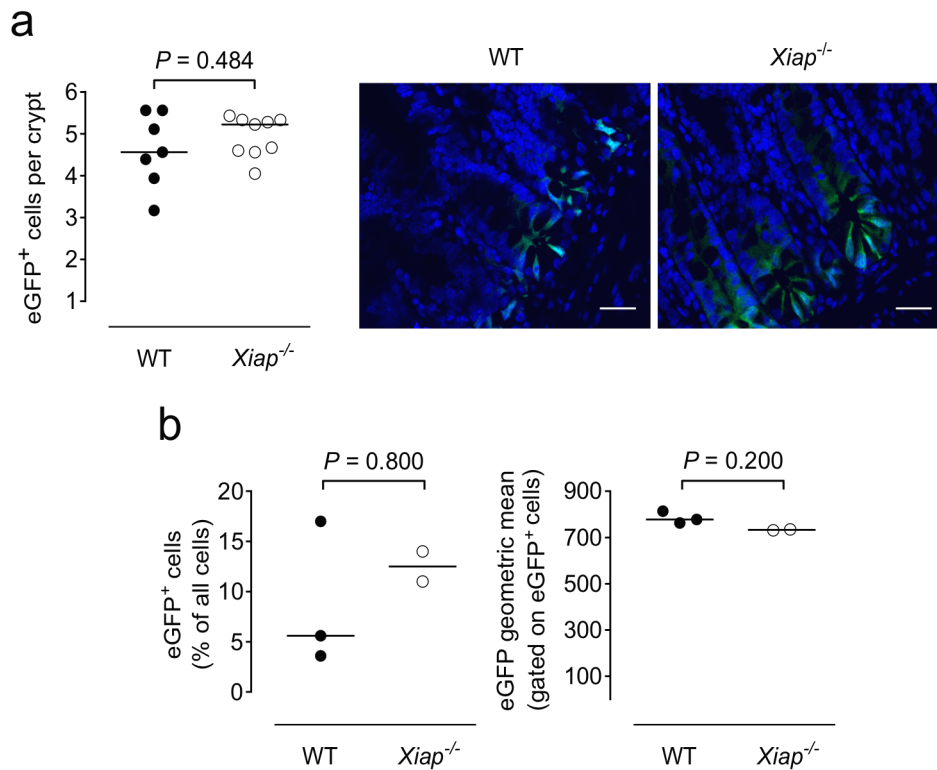


Figure 3.3 Unaltered stem cell numbers in $Xiap^{-/-}$ mice

(a) Quantification of Lgr5-eGFP⁺ cells per crypt (left) and representative immunofluorescence images (right) for Lgr5-eGFP (green) using an anti-GFP antibody and DAPI (blue) staining in the ileum of WT ($n = 7$) and $Xiap^{-/-}$ ($n = 9$) mice on the Lgr5-EGFP-IRES-CreER^{T2} background. (b) Flow cytometry analysis depicting relative numbers of eGFP⁺ cells (left) and the geometric mean (right) of GFP expression gated on live eGFP⁺ ISCs of WT ($n = 3$) and $Xiap^{-/-}$ ($n = 2$) mice on the Lgr5-EGFP-IRES-CreER^{T2} background. Scale bar for all images represents 100 μm . In all graphs, dots represent individual mice and the bar indicates the median. P values were calculated using the Mann-Whitney U -test.

3.2 Microbial-dependent TNF signaling mediates PC death in $Xiap^{-/-}$ mice

Based on previous findings which have demonstrated that XIAP directly acts on effector caspase such as caspase-3, -7 and -9 to inhibit cell apoptosis,^{259–261,299,300,352,353} we next addressed whether loss of PCs may occur due to increased cell apoptosis in the absence of XIAP. For these reasons, we investigated apoptosis of ileal PCs by immunofluorescence staining using antibodies directed against active cleaved caspase-3. We observed an increase in the number of cleaved caspase-3-positive PCs in $Xiap^{-/-}$ mice compared to WT littermates (**Fig. 3.4**), thus confirming that deletion of $Xiap$ is associated with apoptotic loss of PCs.

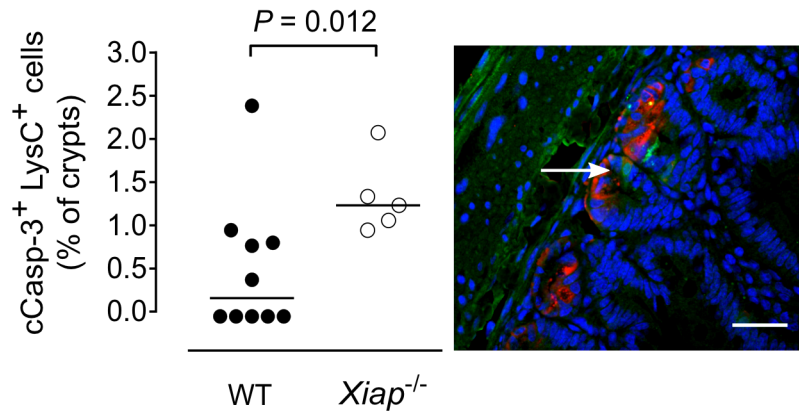


Figure 3.4 Increased PC apoptosis in in *Xiap*^{-/-} mice

Quantification of LyzC cleaved caspase 3 (cCasp-3) double-positive cells in the ileum (left) of WT ($n = 10$) and *Xiap*^{-/-} ($n = 5$) mice and representative immunofluorescence image (right) depicting LyzC (red), cCasp-3 (green) double-positive cells indicated by a white arrow along with DAPI (blue) staining in the ileum of *Xiap*^{-/-} mice. Scale bar indicates 100 μm . All dots represent individual mice and the bar indicates the median. P value was calculated using the Mann-Whitney U -test.

Since XIAP is known to inhibit TNFR1-dependent cell death signaling²⁷³, we next examined whether abolishing TNFR1 signaling prevents PC death in *Xiap*^{-/-} mice. For these reasons, we obtained mice with deletion of *Tnfr1* (*Tnfr1*^{-/-} mice)³³² and crossed them with WT and *Xiap*^{-/-} mice. Upon examination, the *Xiap*^{-/-}; *Tnfr1*^{-/-} mice depicted increased PC numbers when compared to *Xiap*^{WT}; *Tnfr1*^{-/-} mice (**Fig. 3.5a**). Accordingly, there was also increased expression of some of the PC-AMPs (**Fig. 3.5b**) in *Xiap*^{-/-}; *Tnfr1*^{-/-} mice when compared to the *Xiap*^{WT}; *Tnfr1*^{-/-} mice. Since XIAP also regulates RIPK3-dependent cell death by inhibiting the ripoptosome downstream of TNFR1 signaling,^{273,282,289} we next addressed whether PC death may be mediated through ripoptosome formation in the absence of XIAP. To this end, we generated *Xiap*^{-/-} and WT mice on a *Ripk3*-deficient background by crossing *Xiap*^{-/-} and WT mice with *Ripk3*^{-/-} mice.³³⁴ Indeed, we observed no differences in the average number of PCs per crypt (**Fig. 3.6a**) or expression of different PC-derived genes (**Fig. 3.6b**) between *Xiap*^{WT}; *Ripk3*^{-/-} and *Xiap*^{-/-}; *Ripk3*^{-/-} mice. Together, these results demonstrate that XIAP plays a critical role in mediating PC survival downstream of TNFR1 signaling.

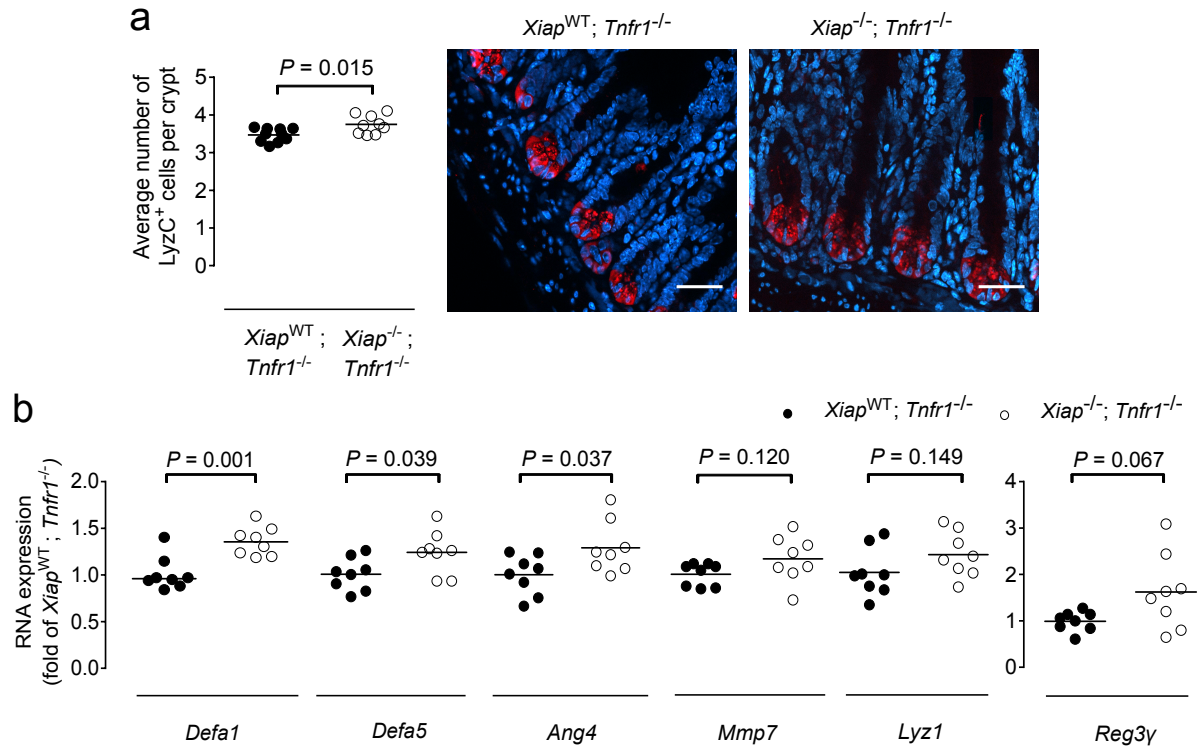


Figure 3.5 PC death in $Xiap^{-/-}$ mice is abrogated by the deletion of $Tnfr1$

(a) Quantification of numbers of LyzC⁺ cells per crypt (left) and representative images for LyzC (red) and DAPI (blue) staining (right) in the ileum of $Xiap^{WT}; Tnfr1^{-/-}$ ($n = 10$) and $Xiap^{-/-}; Tnfr1^{-/-}$ ($n = 9$) mice. (b) qPCR analysis of expression of different PC genes in the ileum of $Xiap^{WT}; Tnfr1^{-/-}$ ($n = 8$) and $Xiap^{-/-}; Tnfr1^{-/-}$ mice ($n = 8$). Scale bar indicates 100 μ m. In all graphs, dots represent individual mice and the bar indicates the mean. P values were calculated using the Student's t -test.

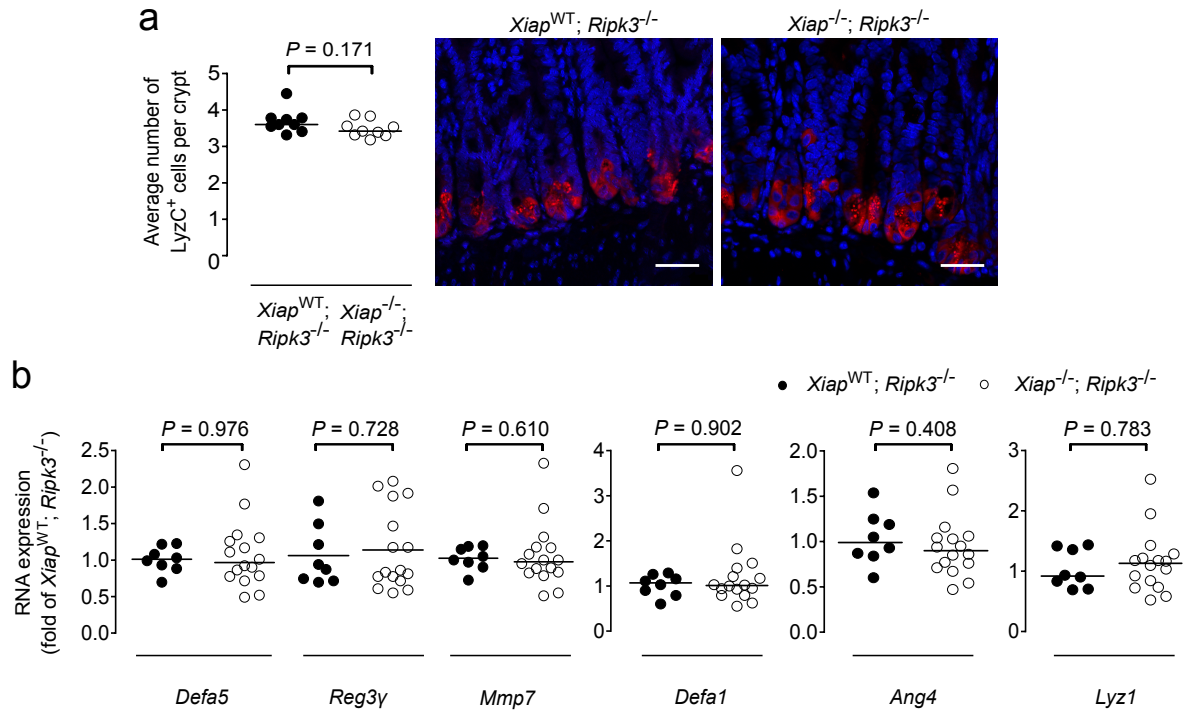


Figure 3.6 PC defects in $Xiap^{-/-}$ mice are mediated by RIPK3 signaling pathway

(a) Quantification of average numbers of LyzC⁺ cells per crypt (left) and representative images for LyzC (red) and DAPI (blue) staining (right) in the ileum of $Xiap^{WT}; Ripk3^{-/-}$ ($n = 9$) and $Xiap^{-/-}; Ripk3^{-/-}$ ($n = 9$) mice. Scale bar represents 100 μ m. (b) qPCR analysis of expression of different PC genes in the ileum of $Xiap^{WT}; Ripk3^{-/-}$ ($n = 8$) and $Xiap^{-/-}; Ripk3^{-/-}$ ($n = 16$) mice. In all graphs, dots represent individual mice and bar indicates either mean (for *Reg3γ* in b) or median (for a and rest of the indicated genes except *Reg3γ* in b). P values were calculated using the Student's t -test (for *Reg3γ* in b) or Mann-Whitney U -test (for a and rest of the indicated genes except *Reg3γ* in b).

Since XIAP regulates cell death downstream of TNFR1 in response to TLR stimulation,^{273,275,354} we next assessed if PC death in mice lacking XIAP is driven by the commensal microbiota. Therefore, we investigated PCs in germ-free $Xiap^{-/-}$ (GF $Xiap^{-/-}$) mice and germ-free WT (GF WT) mice. We observed a mild reduction in the number of PCs per crypt in all germ-free compared to SPF mice (data not shown). Importantly, however, GF $Xiap^{-/-}$ and WT mice, in contrast to their SPF counterparts, did not exhibit XIAP-dependent differences in the number of PCs (**Fig. 3.7a**) or the expression of PC-derived genes (**Fig. 3.7b**). Thus, PC death in mice lacking XIAP is driven by the commensal microbiota.

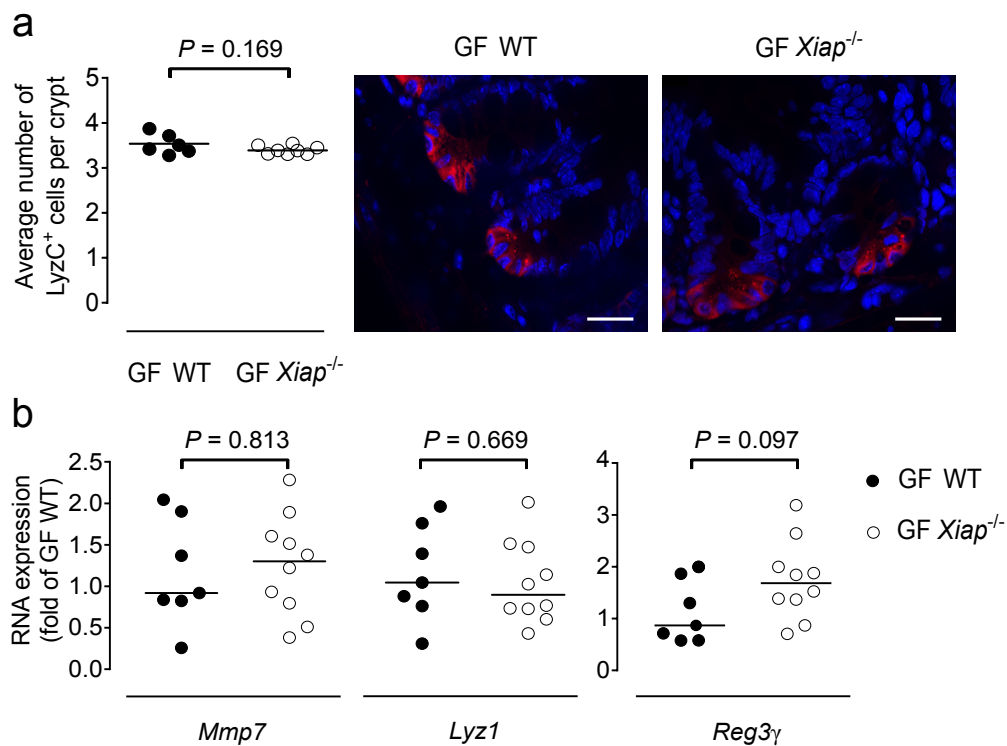


Figure 3.7 PC death in *Xiap*^{-/-} mice is mediated by the commensal microbiota

(a) Quantification of LyzC⁺ cells per crypt (left) and representative images for LyzC (red) and DAPI (blue) staining (right) in the ileum of GF WT ($n = 6$) and GF *Xiap*^{-/-} ($n = 8$) mice. Scale bar represents 100 μm . (b) qPCR analysis of expression of different PC-AMP genes in the ileum of GF WT ($n = 7$) and GF *Xiap*^{-/-} ($n = 10$) mice. In all graphs, dots represent individual mice. The bar indicates mean (a) or median (b). P values were calculated using the Student's t -test (a) or Mann-Whitney U -test (b).

3.3 XIAP is required for control of the commensal intestinal microbiota

PCs produce various AMPs critical for control of the microbiota.¹² Accordingly, mice that carry defects in the processing and activation of antimicrobial α -defensins as a result of deletion of *Mmp7*, exhibit dysbiosis.⁷⁴ We therefore examined whether loss of PCs in *Xiap*^{-/-} mice is associated with alterations in microbial control. To this end, we first compared the bactericidal activity of crypt content derived from *Xiap*^{-/-} and WT mice *in vitro*.¹⁰⁹ We isolated small intestinal crypts from *Xiap*^{-/-} and WT mice, left the crypts unstimulated for 30 minutes whilst shaking at 37°C, incubated crypt secretions from the *Xiap*^{-/-} and WT mice with *Escherichia coli* and assessed *E. coli* survival after co-incubation with crypt secretions overnight at 37°C. We observed that when compared to crypt secretions from WT mice, those of *Xiap*^{-/-} mice showed increased survival of *E. coli* (**Fig. 3.8a**). We therefore wondered whether bacterial control is also impaired *in vivo* and quantified mucosa-adherent bacteria in the ileum and colon by

16S rDNA PCR using total bacteria (*Eub338*) primers (see table 2.2 for primer sequences). We noted an increase in ileal mucosa-adherent bacteria (**Fig. 3.8b**) and a similar but non-significant trend in the colon (**Fig. 3.8c**) of *Xiap*^{-/-} mice when compared to WT mice. FISH staining using the Cy3-labeled DNA probe Bact338 (that detects all bacteria, see table 2.2 for probe sequence) further revealed that bacteria colonized the intestinal crypts of *Xiap*^{-/-} but not WT mice (**Fig. 3.8d**), in line with a defect in antimicrobial peptide secretion and impaired bacterial compartmentalization or stratification.

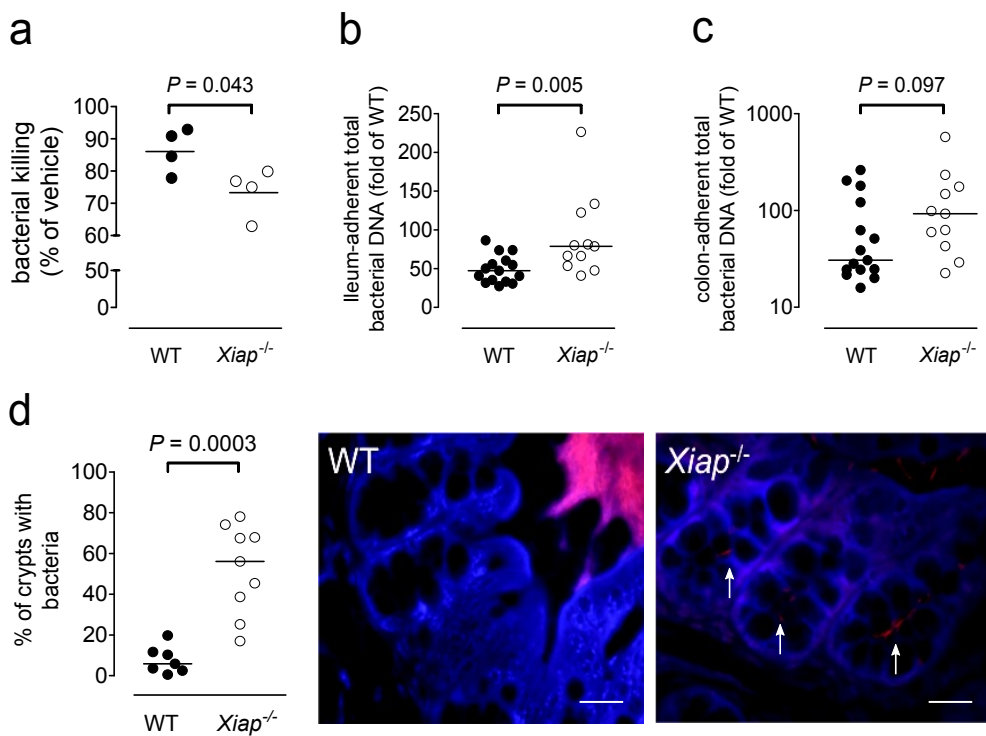


Figure 3.8 XIAP-dependent regulation of microbial abundance in the gut

(a) Bacterial killing assay using unstimulated crypt supernatants from WT ($n = 4$) and *Xiap*^{-/-} ($n = 4$) mice, co-incubated with *E.coli*. The data represents bacterial cell killing expressed as percentage (\pm standard deviation) relative to the bacteria incubated 3 hours at 37 °C in PIPES buffer alone (vehicle) in each group. (b,c) qPCR of bacterial DNA in the ileum-adherent (b) and colon-adherent (c) microbiota (using *Eub338* primers, see table 2.2) in WT ($n = 15$) and *Xiap*^{-/-} ($n = 11$) mice. (d) Quantification of bacteria in crypts, averaged from 10 high-power fields (plotted as % of colonized crypts) in the colon of WT ($n = 7$) and *Xiap*^{-/-} ($n = 9$) mice (left). Representative FISH staining in the colon of WT and *Xiap*^{-/-} mice for total bacteria using Cy3-labeled DNA probe Bact338 (pink) and DAPI (blue) are shown on the right. White arrows indicate bacteria at the bottom of crypts in *Xiap*^{-/-} mice. Scale bar represents 100 μ m. In all graphs, dots represent individual mice and the bar indicates either mean (a) or median (b-d). *P* values were calculated using the Student's *t*-test (a) or Mann-Whitney *U*-test (b-d).

PC also profoundly influence the microbial composition in the gut as highlighted by studies performed on *Mmp7*^{-/-} mice that lack mature α -defensins and present with altered microbial communities in the small intestine.⁷⁴ We therefore investigated whether loss of XIAP and resulting defects in PC-AMP expression lead to an altered composition of mucosa-adherent microbial populations in the intestine of *Xiap*^{-/-} mice. 16S rRNA sequencing revealed changes in microbial communities in *Xiap*^{-/-} compared to WT mice (**Fig. 3.9a**). Moreover, the ileum of *Xiap*^{-/-} mice exhibited increased abundance of Bacteroidetes and Deltaproteobacteria phyla, as well as reduced abundance of Firmicutes phylum compared to WT mice (**Fig. 3.9b**). This included, in accordance with distal effects of PC-AMPs in the colon⁵⁸, an increased abundance of *Bilophila wadsworthia* in the colon of *Xiap*^{-/-} mice, a Deltaproteobacterium and pathobiont previously shown to be associated with intestinal inflammation in *I10*^{-/-} mice (**Fig. 3.9c**).¹⁶⁹ In conclusion, *Xiap*^{-/-} mice exhibit an altered compartmentalization and composition of the commensal microbiota.

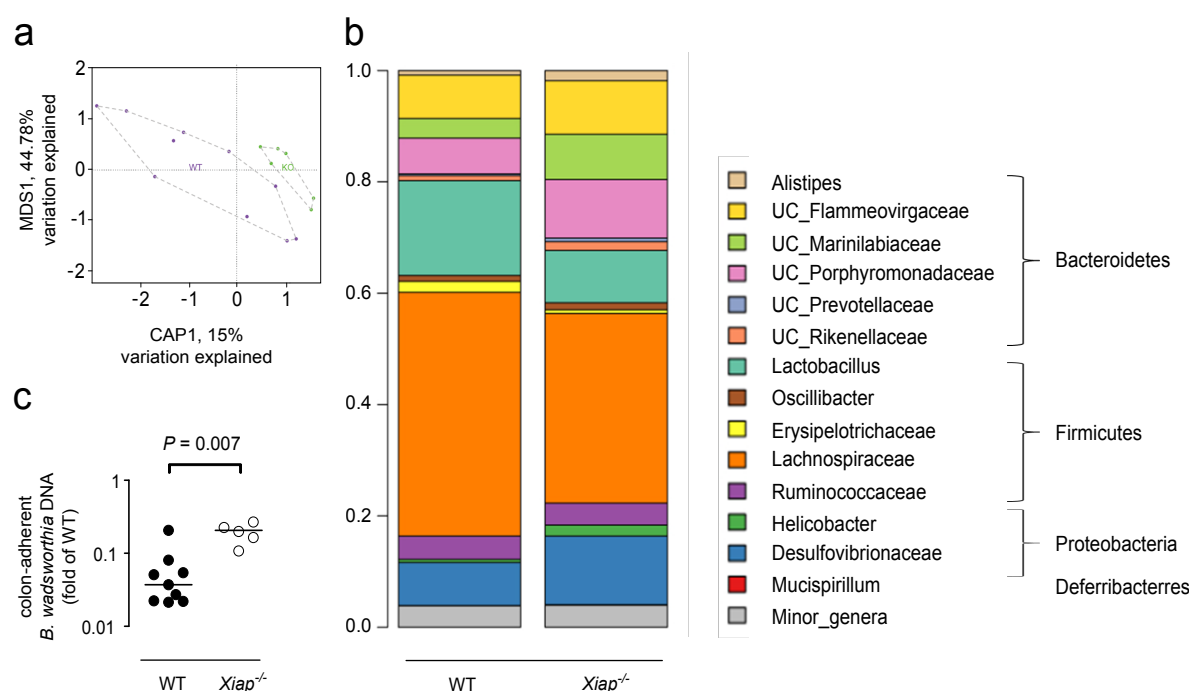


Figure 3.9 XIAP-dependent regulation of intestinal microbial composition

(a) Constrained analysis of principle coordinates ('capscale'; CAP) based on Bray-Curtis distances for WT ($n = 10$) and *Xiap*^{-/-} ($n = 6$) mice. CAP1 separates ileal tissue-associated microbial communities between WT mice (purple) and *Xiap*^{-/-} mice (green). MDS1 represents first non-constrained axis after controlling the effect of tissues. $P < 0.05$ in analysis of dissimilarity, 'adonis'. (b) Bar plot depicting relative abundance of microbial genera and their respective phylum in the ileum of WT ($n > 10$) and *Xiap*^{-/-} ($n > 10$) mice. (c) qPCR analysis of expression of colon-adherent *B. wadsworthia* DNA in WT ($n = 9$) and *Xiap*^{-/-} ($n = 5$) mice. In graph (c), dots represent individual mice and bars indicates the median. P values were calculated using the Mann-Whitney U -test.

3.4 Absence of spontaneous intestinal inflammation in *Xiap*^{-/-} mice

Since CD patients with *XIAP* mutations develop intestinal inflammation with a penetrance of 5-30%, we asked whether *Xiap*^{-/-} mice also display intestinal inflammation. As observed histologically, there was no inflammation in the small intestine (**Fig. 3.10**) and the colon (**Fig. 3.11**) of the *Xiap*^{-/-} mice when compared to the WT mice.

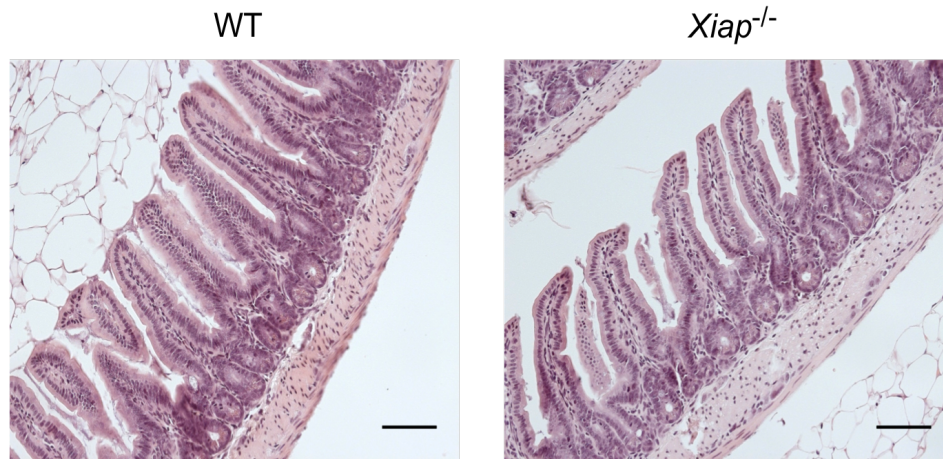


Figure 3.10 Absence of spontaneous inflammation in the ileum of *Xiap*^{-/-} mice

H&E stained sections of the ileum of WT and *Xiap*^{-/-} mice (20x magnification). Scale bars represent 100 µm.

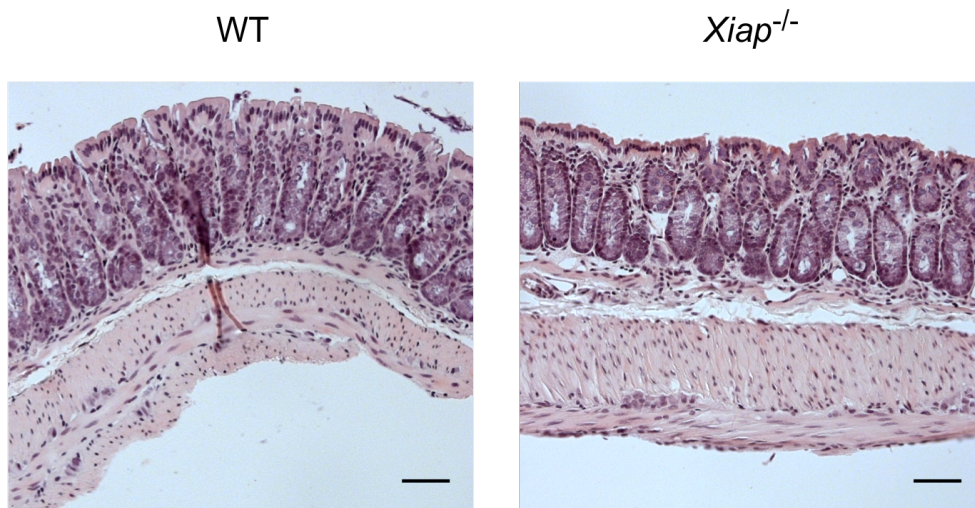


Figure 3.11 Absence of spontaneous inflammation in the colon of *Xiap*^{-/-} mice

H&E stained sections of the colon of WT and *Xiap*^{-/-} mice (20x magnification). Scale bars represent 100 µm.

We also investigated the expression of different cytokines in the ileum of *Xiap*^{-/-} and WT mice by qPCR. Under the SPF housing conditions of our animal facility, we observed no changes in the expression of cytokines between WT and *Xiap*^{-/-} mice in the small intestine (**Fig. 3.12**). Therefore, PC defects and subsequent dysbiosis observed in *Xiap*^{-/-} mice is not sufficient to elicit spontaneous intestinal inflammation. The absence of intestinal inflammation in *Xiap*^{-/-} mice is thereby in line with incomplete penetrance of CD in patients who carry loss-of-function mutations in *XIAP* and

suggests a requirement for additional environmental and potentially microbial factors to induce intestinal inflammation in a XIAP-deficient context.²⁰⁶

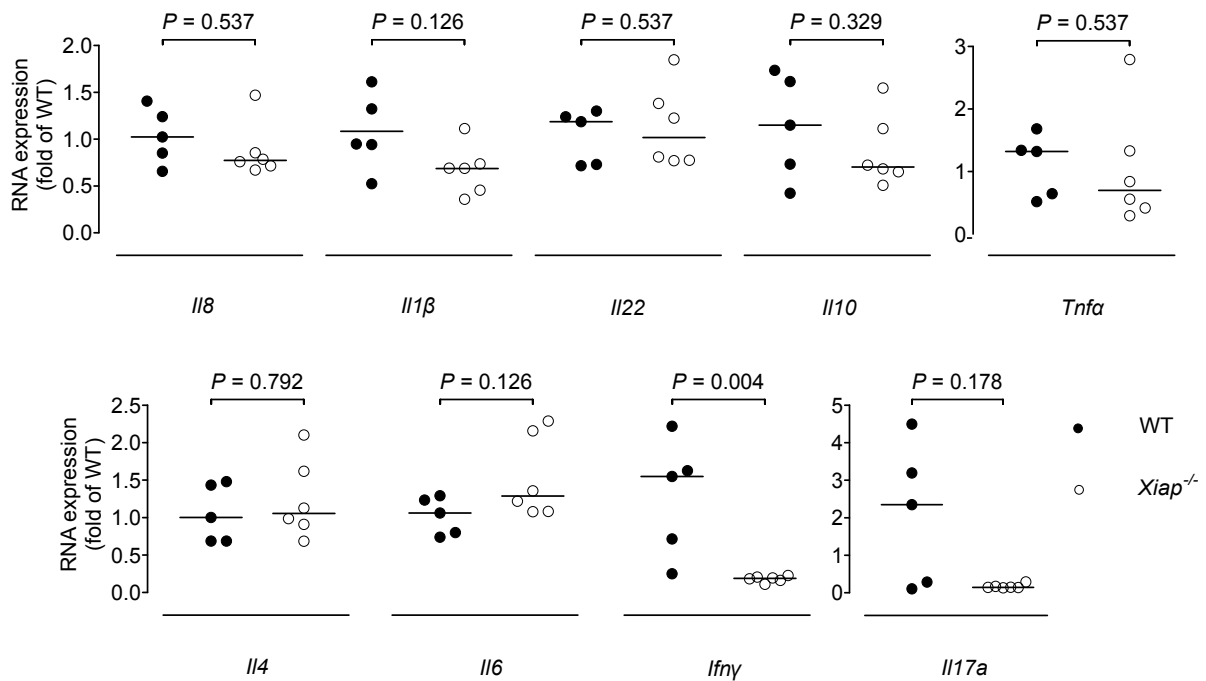


Figure 3.12 No evidence of small intestinal inflammation in $Xiap^{-/-}$ mice

qPCR analysis of the expression of the indicated genes in the ileum of WT ($n = 5$) and $Xiap^{-/-}$ ($n = 6$) mice. In all graphs, dots represent individual mice and bars indicate the median. P values were calculated using the Mann-Whitney U -test.

3.5 Deficiency in $Xiap$ is associated with susceptibility to microbiota-induced intestinal inflammation

The observation that patients with $XIAP$ mutations show incomplete CD penetrance suggests that environmental factors play pivotal roles in inducing inflammation in genetically susceptible hosts.^{215–218,220} Since XLP-2, a disease that is also associated with $XIAP$ mutations, is often induced by Epstein Barr virus infection, we hypothesized that intestinal inflammation may similarly be elicited by microbial triggers. Previous studies have demonstrated that $Nod2^{-/-}$ mice but not WT mice develop granulomatous ileitis upon infection with the opportunistic bacterium *H. hepaticus*.¹⁷² We therefore examined whether $XIAP$ deficiency is similarly associated with susceptibility to *H. hepaticus*. To this end, we infected WT (represented as *H.h* WT) and $Xiap^{-/-}$ (represented as *H.h* $Xiap^{-/-}$) mice, both of which were free of *H. hepaticus* at baseline, with *H. hepaticus* and investigated mice at early (2 weeks) and subsequent (12 weeks) time points after infection (p.i) (**Fig. 2.1**). At both time points, *H. hepaticus*-infected $Xiap^{-/-}$ mice showed increased numbers of macroscopically visible Peyer's

patches compared to WT mice (**Fig. 3.13a**). Since *Xiap*^{-/-} mice exhibit a loss of PCs, we next investigated whether *Xiap*^{-/-} mice can efficiently control *H. hepaticus* colonization in the intestine. Interestingly, two weeks after infection, *Xiap*^{-/-} mice showed increased amounts of ileum-adherent *H. hepaticus* when compared to the WT mice (**Fig. 3.13b**). Investigation of chronic stages of infection demonstrated that *Xiap*^{-/-} mice had an increased size of Peyer's patches in the small intestine (**Fig. 3.13c**). Most importantly, *Xiap*^{-/-} but not WT mice showed non-necrotizing granuloma in the lamina propria of the ileum (**Fig. 3.13d**), a hallmark of intestinal inflammation observed in patients with CD. As such, the loss of PCs and PC-derived AMPs in *Xiap*^{-/-} mice is associated with defects in the control of the pathobiont *H. hepaticus* leading to granulomatous ileitis in these mice. Together, these results demonstrate how a genetic defect in the host provides the basis for impaired host-microbial interactions and susceptibility to microbiota-induced intestinal inflammation.

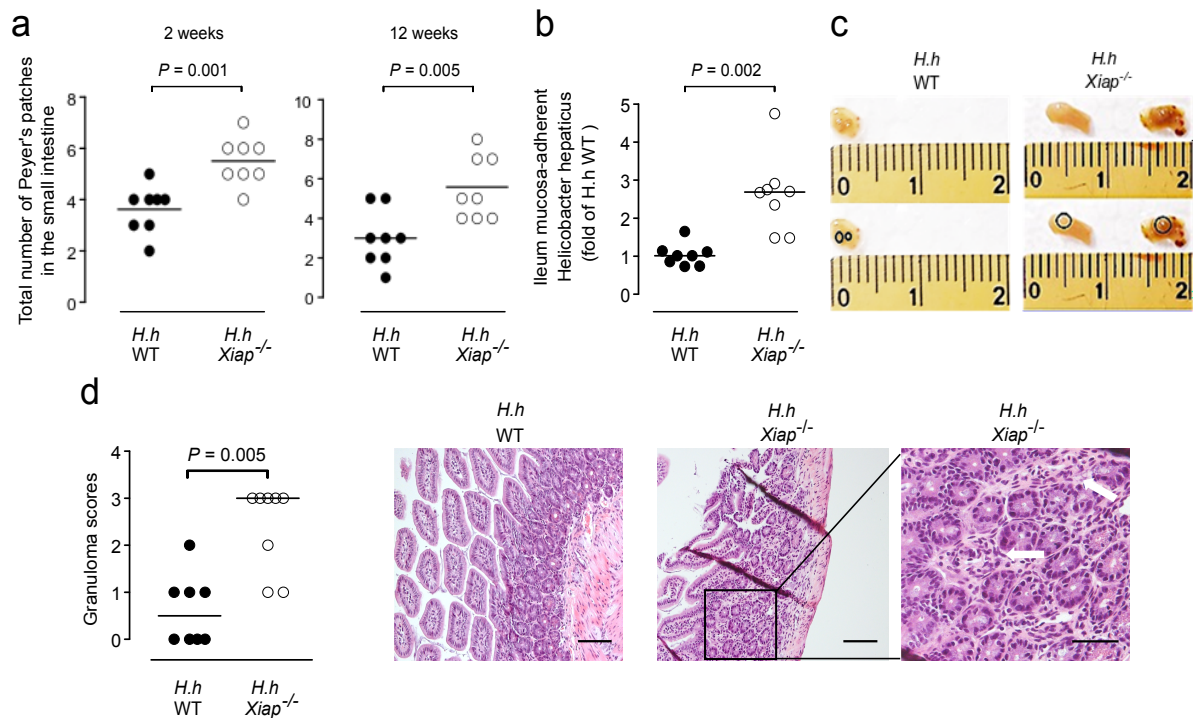


Figure 3.13 Granulomatous ileitis in *Xiap*^{-/-} mice but not WT mice exposed to *H. hepaticus*

(a) Quantification of macroscopically visible Peyer's patches in WT ($n = 8$) and *Xiap*^{-/-} ($n = 8$) mice, 2 weeks (left) and 12 weeks (right) after infection with *H. hepaticus*. (b) qPCR analysis of ileum-adherent *H. hepaticus* DNA in WT ($n = 8$) and *Xiap*^{-/-} ($n = 8$) mice, 2 weeks p.i. (c) Image showing the size of Peyer's patches, indicated using black circles, in WT (left) and *Xiap*^{-/-} (right) mice analyzed 12 weeks p.i. (d) Granuloma scores (left) in the ileum of WT ($n = 8$) and *Xiap*^{-/-} ($n = 8$) mice 12 weeks p.i. Representative H&E stained sections are shown of ileum of WT (left – 20x magnification) and *Xiap*^{-/-} mice (20x magnification (center) and 40x magnification (right)). White arrows indicate non-necrotizing granulomas. Scale bars represent 100 μ m. In all graphs, dots represent individual mice. Bar indicate the mean (a) or median (b and d). P values were calculated using the Student's t -test (a) or the Mann-Whitney U -test (b and d).

3.6 Increased susceptibility to chemically-induced colitis in *Xiap*^{-/-} mice

Previous studies have demonstrated that mice with deletion of *Nod2* or *Mmp7* that have PC defects, develop no spontaneous inflammation under SPF conditions but show increased susceptibility to inflammation when compared to the WT mice upon environmental disturbances, induced by the treatment of DSS.^{355,356} DSS is a sulfated polysaccharide that binds to medium-chain-length fatty acids present in the colon to form nanometer-sized vesicles that damage colonocytes.³⁵⁷ This process allows for disruption of the epithelial barrier in the colon which leads to the dissemination of microbes and their products into the host to initiate excessive immune responses.

DSS-induced colitis is associated with weight loss, rectal bleeding, diarrhea, colonic shortening and mortality.³⁵⁸ Since *Xiap*^{-/-} mice bear PC defects similar to *Nod2*^{-/-} mice and *Mmp7*^{-/-} mice, we hypothesized that XIAP deficiency may also be associated with increased susceptibility to DSS-induced colitis. To test this hypothesis, we administered 2.5% DSS (acute and chronic DSS model, see **Fig. 2.2**) to WT and *Xiap*^{-/-} mice. *Xiap*^{-/-} mice, compared to WT mice showed increased susceptibility to colitis as indicated by increased weight loss (**Fig. 3.14a**), higher colonic mucosal levels of pro-inflammatory cytokines such as Il-6 (**Fig. 3.14b**), monocyte chemoattractant protein 1 (Mcp-1) (**3.14c**), and *Il1β* (**Fig. 3.14d**) and reduced colon lengths (**Fig. 3.14e**). Histopathological examination revealed that *Xiap*^{-/-} mice had severe transmural inflammation, distorted crypt structures and an increased loss of goblet cells indicating increased histopathological damage when compared to the WT mice (**Fig. 3.14f**). Furthermore, there was a tendency towards reduced survival in *Xiap*^{-/-} mice (**Fig. 3.14g**). In addition, *Xiap*^{-/-} mice showed increased dissemination of bacteria to mesenteric lymph nodes compared to WT mice (**Fig. 3.14h**).

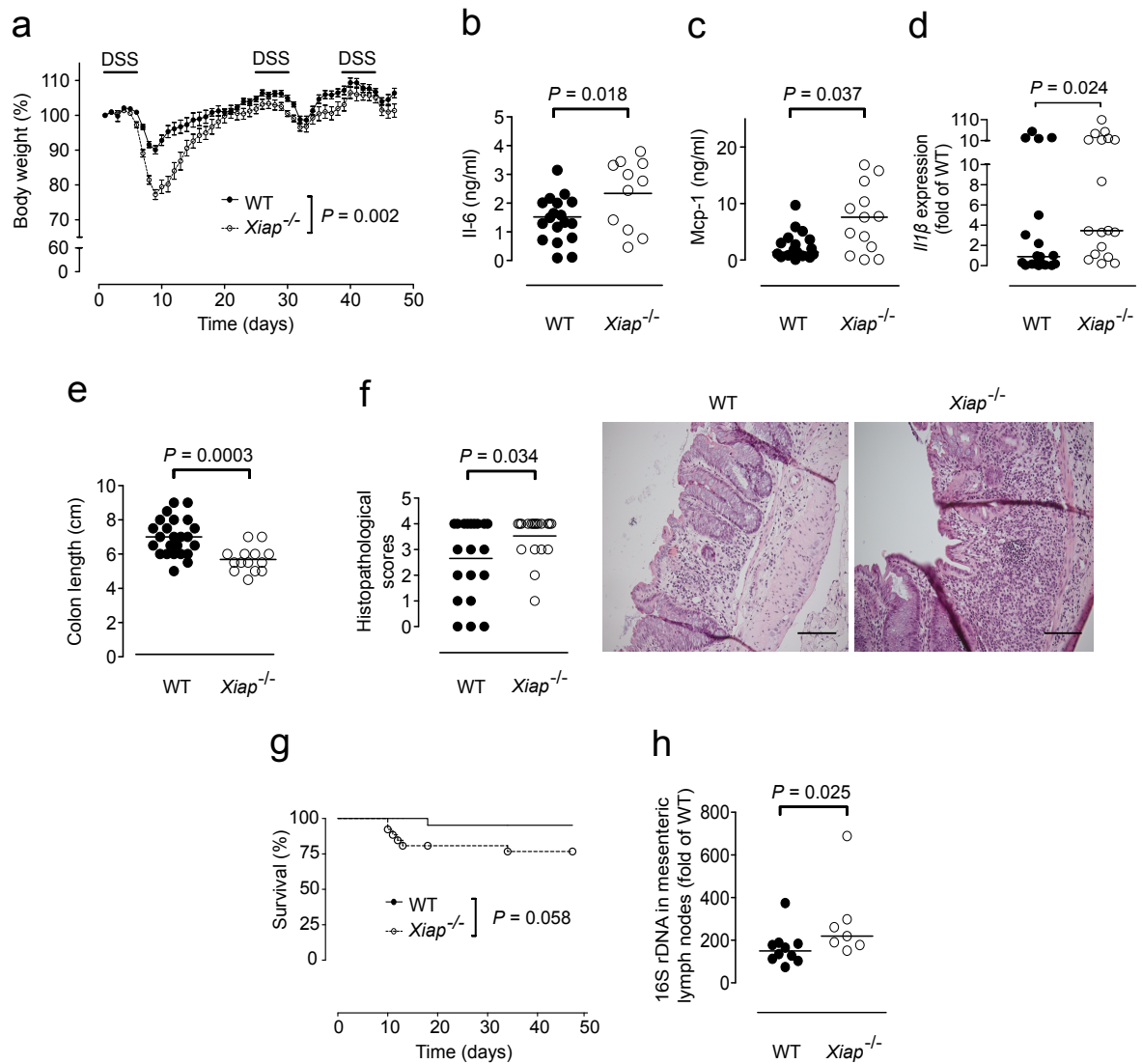


Figure 3.14 Increased susceptibility to DSS-induced colitis in *Xiap*^{-/-} mice

Acute DSS colitis model (panel f) and chronic DSS colitis model (panels a-e, g and h) (a) Body weight curves of WT ($n = 24$) and *Xiap*^{-/-} ($n = 14$) mice presented as mean \pm s.e.m, % of initial weights (day 0). (b) IL-6 secretion and (c) MCP-1 secretion from supernatants of colon explant cultures of WT ($n = 18$) and *Xiap*^{-/-} ($n = 11$) mice as evaluated by ELISA. (d) qPCR analysis of *I11 β* expression in the colon of WT ($n = 19$) and *Xiap*^{-/-} ($n = 18$) mice. (e) Colon length of WT ($n = 24$) and *Xiap*^{-/-} ($n = 14$) mice in centimeters (cm). (f) Histopathological scores of colonic inflammation in WT ($n = 20$) and *Xiap*^{-/-} ($n = 19$) mice after 5 days of treatment with 2.5% DSS, followed by 5 days of water (left) and representative H&E stained images of colon (right). Scale bar represents 100 μ m (g) Kaplan-Meier analysis of the survival (death from DSS treatment) in WT ($n = 24$) and *Xiap*^{-/-} ($n = 14$) mice. (h) qPCR analysis of expression of bacterial 16S rDNA in the mesenteric lymph nodes of WT ($n = 10$) and *Xiap*^{-/-} ($n = 7$) mice. In all graphs, dots represent individual mice. The bar indicates either the mean (b, e and f) or median (a, c, d and h). The P values were calculated using the Student's t -test (b, e and f), Mann-Whitney U -test (a, c, d and h) or log-rank test (g).

3.6.1 Increased colitis susceptibility in *Xiap*^{-/-} mice is maintained in the absence of the adaptive immune system

The increased susceptibility to colitis in *Xiap*^{-/-} mice was observed during acute stages of colitis (Fig 3.14a), which are largely independent of adaptive immunity³⁵⁹, thus suggesting that differences in innate immunity are responsible for increased disease susceptibility. To further address this question, we investigated WT and *Xiap*^{-/-} mice on *Rag1* deficient background, in the absence of mature adaptive immune T and B cells, by crossing WT and *Xiap*^{-/-} mice with *Rag1*^{-/-} mice.³³⁴ Upon DSS administration, *Xiap*^{-/-}; *Rag1*^{-/-} mice showed increased histopathological inflammation (Fig. 3.15a), cytokine expression (Fig. 3.15b), and colonic shortening (Fig. 3.15c) compared to *Xiap*^{WT}; *Rag1*^{-/-} mice. These results confirm that increased susceptibility to intestinal inflammation in *Xiap*^{-/-} mice is driven by innate immunity.

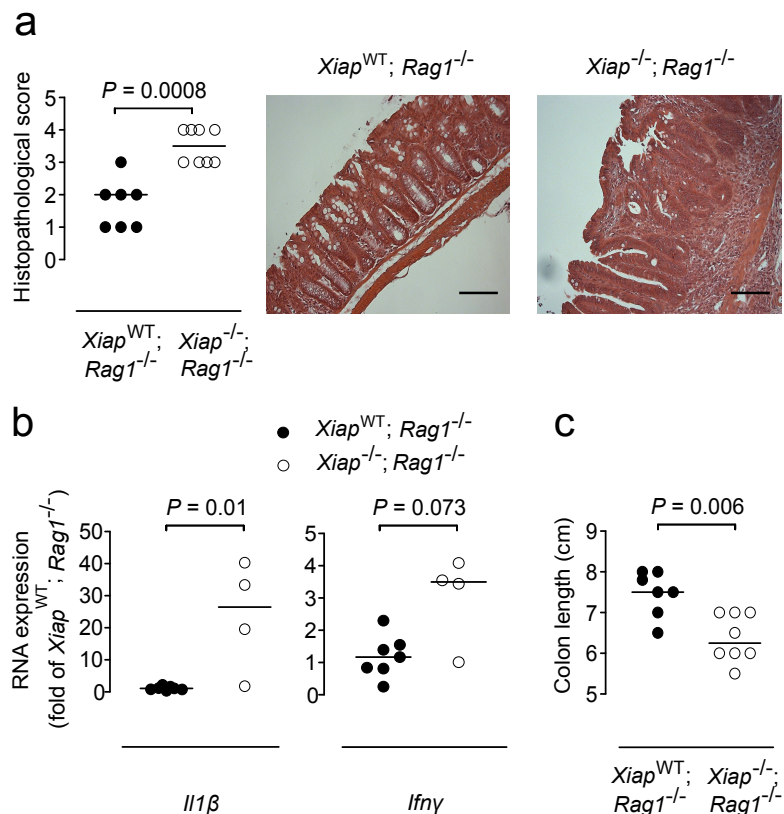


Figure 3.15 XIAP-dependent susceptibility to DSS-induced colitis is mediated by the innate immune system

Chronic colitis model (a-c). (a) Histopathological scores (left) of colonic inflammation in *Xiap*^{WT}; *Rag1*^{-/-} ($n = 7$) and *Xiap*^{-/-}; *Rag1*^{-/-} ($n = 8$) mice, and representative H&E-stained images of colon (right). Scale bar represents 100 μ m. (b) qPCR analysis of expression of the indicated genes in the colon of *Xiap*^{WT}; *Rag1*^{-/-} ($n = 7$) and *Xiap*^{-/-}; *Rag1*^{-/-} ($n = 4$) mice. (c) Colon length of *Xiap*^{WT}; *Rag1*^{-/-} ($n = 7$) and *Xiap*^{-/-}; *Rag1*^{-/-} ($n = 8$) mice measured in cm. In all graphs, dots represent individual mice and the bar indicates the median. The P values were calculated using the Mann-Whitney U -test.

3.7 Intestinal epithelial- or myeloid-specific deletion of *Xiap* is not sufficient to elicit PC death or susceptibility to intestinal inflammation

To understand the cellular origin of PC defects and intestinal inflammation observed in the absence of XIAP, we crossed conditional ready mice which carry loxP-flanked alleles of *Xiap* (*Xiap^{fl/fl}* mice)³³⁵ with mice expressing *Cre* recombinase under control of different promoters to generate cell-specific deletion of *Xiap* in individual cellular compartments. Because XIAP is important for PC survival (**Fig. 3.1b**), we generated and investigated mice with loss of *Xiap* in IECs by crossing *Xiap^{fl/fl}* mice with villin-*Cre* mice³³⁶ (*villin-Cre; Xiap^{fl/fl}*, hereafter referred to as *Xiap^{ΔIEC}*) or loss of *Xiap* in PCs by crossing *Xiap^{fl/fl}* mice with *Defa6-Cre* mice²³⁸ (*Defa6-Cre; Xiap^{fl/fl}* hereafter referred to as *Xiap^{ΔPC}*) and compared them with their *Cre* negative littermates (*Xiap^{WT}*). Firstly, deletion of the *Xiap* gene was verified in crypt IECs isolated from *Xiap^{ΔIEC}* mice and *Xiap^{WT}* mice by qPCR (**Fig. 3.16a**). Next, upon investigation of PC numbers in the conditional knockouts by immunofluorescence, no differences were detected between *Xiap^{ΔIEC}* and *Xiap^{WT}* (**Fig. 3.16b**) and between *Xiap^{ΔPC}* and *Xiap^{WT}* mice (**Fig. 3.16c**). Since the absence of XIAP in myeloid cells has previously been shown to lead to increased inflammasome-dependent IL-1 β secretion and subsequent cell death, we hypothesized that loss of XIAP in myeloid cells may indirectly promote PC loss through increased IL-1 β secretion and activation of the inflammasome pathway.^{273,354} For these reasons we generated mice which have a myeloid-specific deletion of *Xiap* using *Xiap^{fl/fl}* mice and mice expressing *Cre* recombinase under the control of the Lysozyme M (*Lyz2*) promoter³³⁷ (*LysM-Cre; Xiap^{fl/fl}* hereafter referred to as *Xiap^{ΔMYE}*). However, no differences were detected in the number of PCs between *Xiap^{ΔMYE}* and their *Xiap^{WT}* littermates (**Fig. 3.16d**).

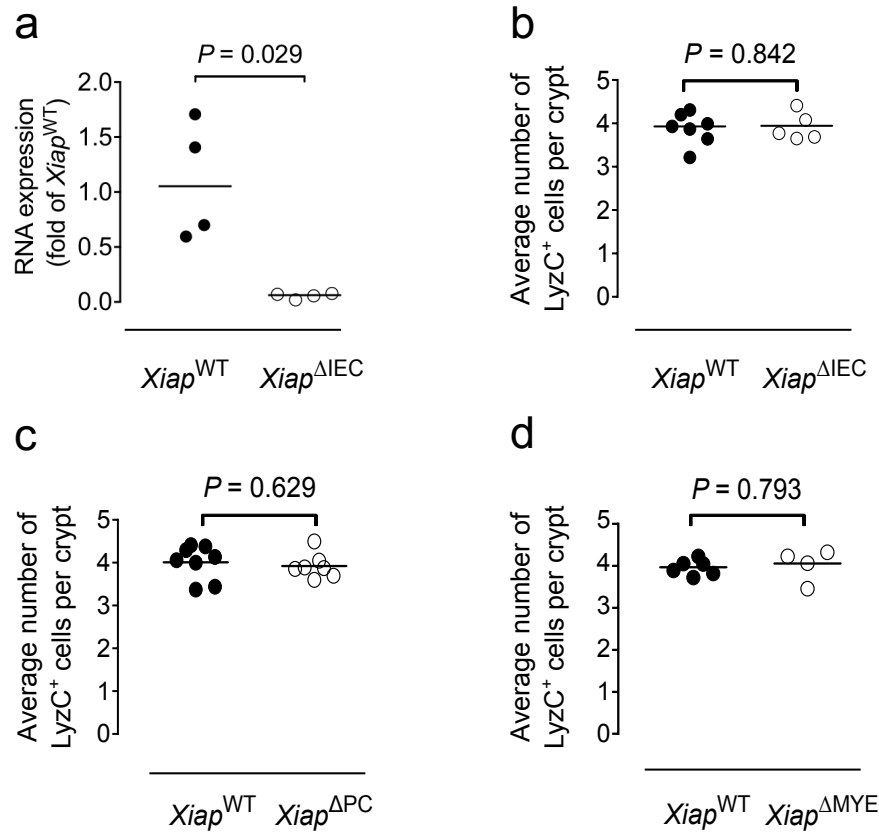


Figure 3.16 Absence of PC loss in mice with PC-, IEC- and myeloid cell-specific deletion of *Xiap*

(a) qPCR analysis of expression of *Xiap* in crypt IECs of $Xiap^{WT}$ ($n = 4$) and $Xiap^{\Delta IEC}$ ($n = 4$) littermates. (b) Quantification of average numbers of $LyzC^+$ cells per crypt in the ileum of $Xiap^{WT}$ ($n = 7$) and $Xiap^{\Delta IEC}$ ($n = 5$) littermates. (c) Quantification of average numbers of $LyzC^+$ cells per crypt in the ileum of $Xiap^{WT}$ ($n = 8$) and $Xiap^{\Delta PC}$ ($n = 7$) littermates. (d) Quantification of average numbers of $LyzC^+$ cells per crypt in the ileum of $Xiap^{WT}$ ($n = 6$) and $Xiap^{\Delta MYE}$ ($n = 4$) littermates. In all graphs, dots represent individual mice. The bar indicates either the median (a) or mean (b-d). The P values were calculated using either the Mann-Whitney U -test (a) or the Student's t -test (b-d).

We next addressed the cellular origin of susceptibility to intestinal inflammation by studying mice with conditional *Xiap* deletion in the DSS model of colitis. Upon DSS administration, no differences in the severity of colitis were detected in $Xiap^{\Delta IEC}$ (**Fig. 3.17**), $Xiap^{\Delta PC}$ mice (**Fig. 3.18**) or $Xiap^{\Delta MYE}$ mice (**Fig. 3.19**) when compared to their respective $Xiap^{WT}$ littermates.

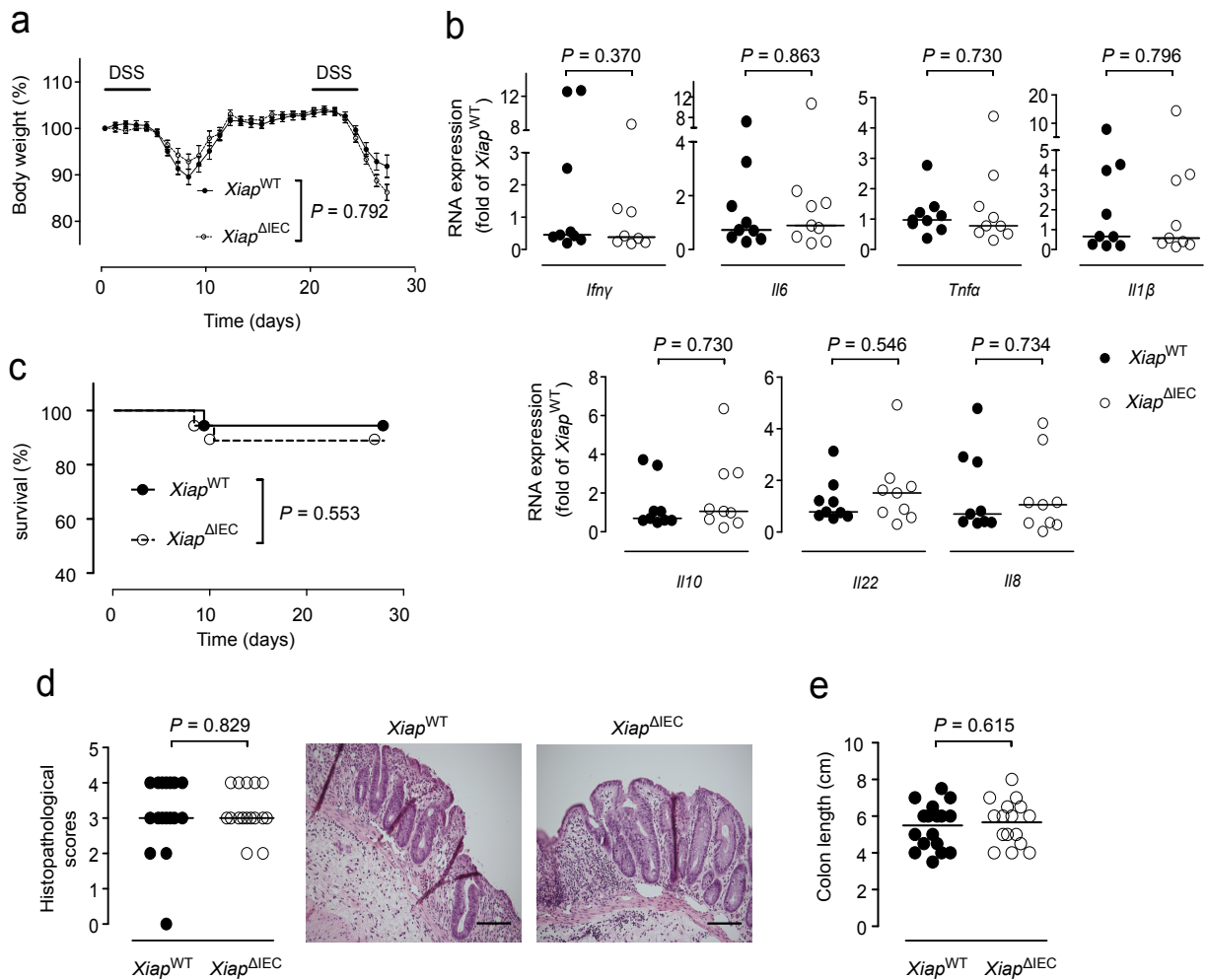


Figure 3.17 No increase in susceptibility to DSS colitis in $Xiap^{\Delta IEC}$ mice

Chronic colitis model (a-e). (a) Body weight curves of $Xiap^{WT}$ ($n = 18$) and $Xiap^{\Delta IEC}$ ($n = 18$) mice presented as mean \pm s.e.m, % of initial weight (day 0). (b) qPCR analysis of expression of indicated genes in the colon of $Xiap^{WT}$ ($n = 9$) and $Xiap^{\Delta IEC}$ ($n = 9$) mice. (c) Kaplan-Meier analysis of the survival (death from DSS treatment) of $Xiap^{WT}$ ($n = 18$) and $Xiap^{\Delta IEC}$ ($n = 18$) mice. (d) Histopathological scores (left) of colonic inflammation in $Xiap^{WT}$ ($n = 17$) and $Xiap^{\Delta IEC}$ ($n = 16$) mice and representative H&E-stained images of colon (right). Scale bar represents 100 μ m. (e) Colon length of $Xiap^{WT}$ ($n = 17$) and $Xiap^{\Delta IEC}$ ($n = 16$) mice measured in cm. In all graphs, dots represent individual mice. The bar indicates either the mean (e) or median (a, b and d). P values were calculated using the Student's t -test (e) or Mann-Whitney U -test (a, b and d) or log-rank test (c).

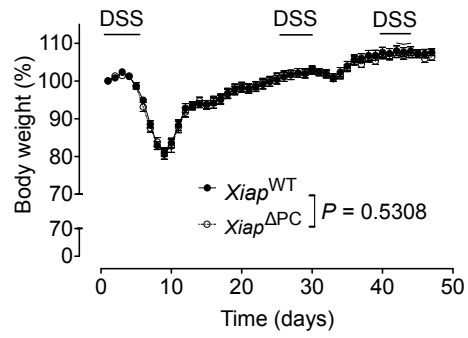


Figure 3.18 No increase in susceptibility to DSS colitis in *Xiap*^{ΔPC} mice

Chronic colitis model, body weight curves of *Xiap*^{WT} ($n = 19$) and *Xiap*^{ΔPC} ($n = 17$) mice presented as mean \pm s.e.m, % of initial weights (day 0).

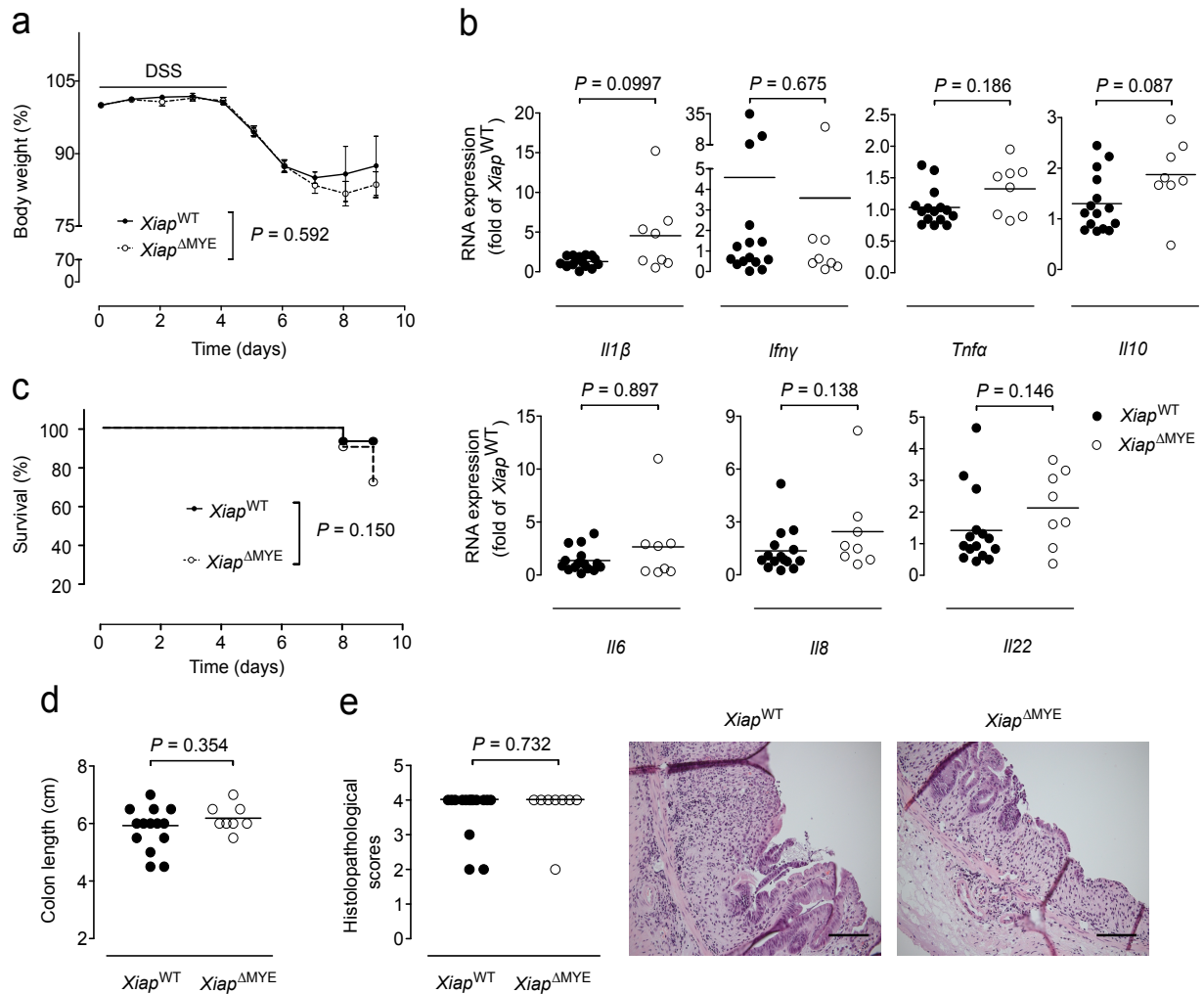


Figure 3.19 No increase in susceptibility to DSS colitis in $Xiap^{\Delta MYE}$ mice

Acute colitis model (a-e). (a) Body weight curves of $Xiap^{WT}$ ($n = 16$) and $Xiap^{\Delta MYE}$ ($n = 11$) mice presented as the mean \pm s.e.m, % of initial weights (day 0). (b) qPCR analysis of expression of the indicated genes in the colon of $Xiap^{WT}$ ($n = 15$) and $Xiap^{\Delta MYE}$ ($n = 8$) mice. (c) Kaplan-Meier analysis of the survival (death from DSS treatment) in $Xiap^{WT}$ ($n = 16$) and $Xiap^{\Delta MYE}$ ($n = 11$) mice. (d) Colon length of $Xiap^{WT}$ ($n = 15$) and $Xiap^{\Delta MYE}$ ($n = 8$) mice in cm. (e) Histopathological scores (left) of colonic inflammation in $Xiap^{WT}$ ($n = 16$) and $Xiap^{\Delta MYE}$ ($n = 11$) mice and representative H&E-stained images of colon (right). Scale bar represents 100 μ m. In all graphs, dots represent individual mice. The bar indicates either the mean (d) or median (a, b and e). P values were calculated using the Student's t -test (d) or Mann-Whitney U -test (a, b, and e) or log-rank test (c).

In conclusion, individual deletion of $Xiap$ in IECs, PCs or myeloid cells is not associated with apoptotic loss of PCs and susceptibility to DSS colitis suggesting synergistic actions of $Xiap$ loss in different cellular compartments in promoting the phenotype of $Xiap^{-/-}$ mice.

4. Discussion and outlook

The investigation of rare Mendelian forms of IBD has provided critical insight into the pathogenesis of intestinal inflammation. The Zeissig group and others recently described that *XIAP* mutations are associated with early-onset CD and demonstrated that up to four percent of males with early-onset CD carry mutations in *XIAP*.^{215,216,218,220,311} With the aim of understanding the mechanisms through which loss of XIAP provides susceptibility to CD, we performed studies on mice that have constitutive and conditional deletions of *Xiap*. These studies have demonstrated a novel role of XIAP in the survival of PCs. Moreover, we have described how in the absence of XIAP, loss of PCs and subsequent improper control of the microbiota in the gut, may promote intestinal inflammation in response to environmental triggers (**Fig. 4.1**).

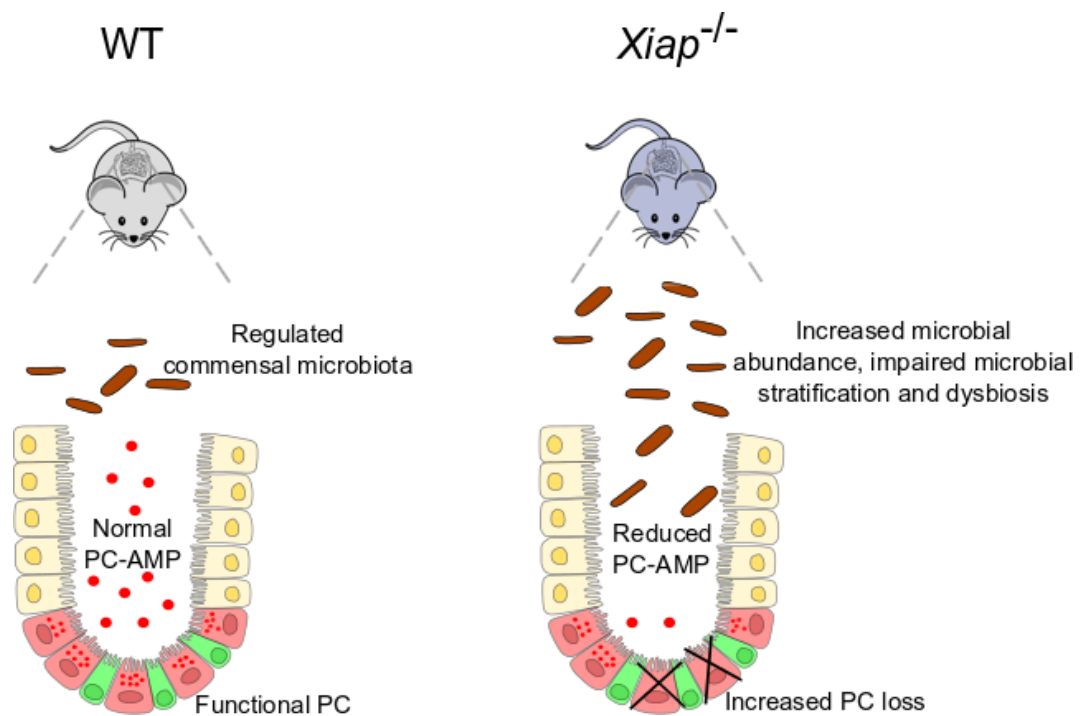


Figure 4.1 Model of XIAP-dependent regulation of PC homeostasis and the commensal microbiota

Intestinal homeostasis in WT mice (left) with functional PCs and normal levels of PC-AMPs that allows for regulation of the commensal microbiota in the intestine. XIAP deficiency (right) leads to increased PC loss and defective production of PC-AMPs that causes increased microbial abundance, impaired microbial stratification and dysbiosis in the gut – defects that can promote intestinal inflammation in response to microbial and environmental triggers.

Previous studies performed by Zeissig *et al.*, demonstrated that *XIAP* mutations are associated with severely impaired NOD1/2 signaling.²¹⁶ More specifically, PBMCs from a subset of patients with *XIAP* mutations were unable to bind to RIPK2 (downstream signal transducer of the NOD1/2 pathway) and had reduced expression and activation of NF- κ B. These defects were observed in response to the NOD1 and NOD2 ligands Tri-DAP and MDP respectively but not to other TLR ligands, which led to diminished secretion of IL-8 from the PBMCs, confirming that *XIAP* mutations selectively impair NOD1/2 signaling.²¹⁶ Keeping in mind that loss of XIAP leads to dysfunctional NOD2 signaling^{216,324}, and that patients with *NOD2* polymorphisms and mice with *Nod2* deletion show defective expression of PC α -defensins^{176,226}, we investigated the expression of genes associated with the PC signature in the *Xiap*^{-/-} mice. We found that the *Xiap*^{-/-} mice showed broad defects in the expression of PC genes, which were not specific to α -defensins. This raised the question of general defects in PCs in *Xiap*^{-/-} mice. Indeed, PC numbers were found to be reduced in the ileum of the *Xiap*^{-/-} mice when compared to WT mice. The observation that *Xiap*^{-/-} mice have defects in the production of PC-AMP in the ileum is of much interest since PC defects are a hallmark of CD. As such, morphological changes in PCs and PC dysfunction have been consistently described in CD^{109,178,227,236}, with some studies describing a reduction of PC numbers in CD patients.^{360,361} However, whether PC loss is a primary or secondary event in IBD is unclear. Studies have shown that PCs loss may occur as a consequence of intestinal inflammation. For example, studies by Simms *et al.*, showed that tissue damages in CD patients lead to PC loss.³⁶¹ Similarly, mice that have a deletion of the TNF adenosine-uracil (AU)-rich elements (ARE) show TNF-driven spontaneous chronic inflammation in the small intestine that leads to PC loss and dysfunction.^{362,363} On the other hand, IEC- or PC-specific deletion of *Xbp1* in mice is associated with PC loss due to ER stress in these cells that causes spontaneous intestinal inflammation suggesting that primary PC loss itself can promote intestinal inflammation.^{236,238} Here we show that Mendelian defects associated with IBD can give rise to a primary loss of PCs and susceptibility to microbiota- or environmentally-induced intestinal inflammation. As such, our studies support the concept of PC defects as the origin of intestinal inflammation in a subset of patients with CD.²³⁸

Individuals with *XIAP* mutations as well as those harboring *NOD2* polymorphisms show incomplete penetrance of CD, which suggests that other genetic or environmental

factors are required to elicit intestinal inflammation.²⁰⁶ The penetrance of CD in patients with *NOD2* polymorphisms (1%), however, is considerably lower than that observed in individuals harboring *XIAP* mutations (5-30%).²⁰⁶ Moreover, *NOD2* polymorphisms completely abrogate NOD2 signaling³⁶⁴, which suggests that *XIAP* mutations also affect pathways independent of NOD2 signaling that are critical for intestinal homeostasis. In line with the role of XIAP to act on effector caspases to inhibit apoptosis^{253,259,261,299}, we asked whether the loss of PCs was due to increased caspase-mediated apoptosis in the absence of XIAP. Indeed, we found increased numbers of cleaved caspase-3 positive PCs, indicating elevated PC apoptosis in *Xiap*^{-/-} mice compared to WT mice. XIAP inhibits caspase-dependent cell death downstream of TNFR1 signaling, a process that is dependent on RIPK3.^{273,274,289,365} Interestingly, we also observed that upon deletion of *Tnfr1* or *Ripk3*, the PC defect in *Xiap*^{-/-} mice is absent, leading us to conclude that XIAP-dependent regulation of PCs is indeed dependent on RIPK3, downstream to TNFR1 signaling. While these results are in accordance with the finding that XIAP deficiency is associated with ripoptosome formation and that RIPK3 controls both apoptotic and necroptotic forms of cell death, it is still unclear whether necroptosis contributes to PC loss in *Xiap*^{-/-} mice. However, investigating *Xiap*^{-/-} mice in the absence of the necrosome-associated molecule MLKL may provide insights as to whether the PCs undergo necroptosis.²⁸⁵ Moreover, we have also shown that the PC defects in *Xiap*^{-/-} mice are absent under GF conditions further highlighting the central role of the commensal microbiota in mediating PC death. Since XIAP inhibits TNF production downstream of TLR stimulation^{273,275,354}, it is likely that XIAP deficiency leads to increased microbial-induced production of TNF which induces TNF-TNFR1 cell death signaling, that drives the PC loss *in vivo*. As such, XIAP deficiency is associated with a self-reinforcing pathway of PC loss, impaired microbial control and further microbiota-dependent stimulation of PC death.

Through the provision of chemical barriers in the gut, PC-AMPs tightly regulate microbial abundance in the intestine. The importance of PC-AMPs in regulating microbial abundance has been demonstrated in mice with deletion of *Nod2* which present with defective expression of PC α -defensins and increased microbial load in the ileum when compared to WT mice.¹⁰⁹ Similarly, we have observed that *Xiap*^{-/-} mice that have defective expression of PC-derived genes, present with increased abundance of tissue-adherent bacteria in the ileum. Moreover, PC-AMPs regulate the

microbial composition in the gut and accordingly, mice that have a deletion of *Mmp7*, which lack mature α -defensins, present with dysbiosis.⁷⁴ Likewise, *Xiap*^{-/-} mice also exhibit dysbiosis with higher abundance of Bacteroidetes and Deltaproteobacteria when compared to WT mice. Interestingly, members belonging to the Bacteroidetes phylum such as *Bacteroides vulgatus*, *Bacteroides thetaiotaomicron* and *Bacteroides uniformis*, as well as the Deltaproteobacteria phylum such as *Enterobacteriaceae*, and *Helicobacter* spp., are capable of initiating intestinal inflammation in genetically susceptible hosts.^{155,156,366–368} In line with the long-range effects of PC-AMPs in the colon⁵⁸, the colon of *Xiap*^{-/-} mice has increased abundance of *B. wadsworthia*, a Deltaproteobacterium capable of inducing intestinal inflammation in *Il10*^{-/-} mice.^{169–171} Furthermore, *Xiap*^{-/-} mice also have reduced abundance of the Firmicutes phylum which represents microbes that are associated with protective roles in intestinal inflammation.^{157,158} Thus, XIAP deficiency leads to improper control of commensal abundance and microbial composition in the gut. Furthermore, *Xiap*^{-/-} mice also show altered microbial stratification in the gut with dense bacterial colonization of crypts that is not observed in WT mice. This observation is in line with the role of PC-AMP in the segregation of bacteria in the gut. Mice that have a deletion of the antimicrobial lectin *Reg3 γ* and therefore have increased mucosa-associated microbiota, also display impaired microbial stratification in the gut.¹⁰⁰ Despite the PC loss and subsequent microbial dysbiosis and stratification, the genetic deletion of *Xiap* in mice does not elicit spontaneous intestinal inflammation in the context of an SPF microbiota. This finding is similar to several other mouse models such as *Nod2*^{-/-} and *Mmp7*^{-/-} mice that have defects in PCs but display no spontaneous intestinal inflammation.^{73,74,109,172} Thus, while spontaneous inflammation is absent, dysbiosis and impaired stratification due to dysfunctional PCs provides susceptibility to pathobionts and microbiota-induced intestinal inflammation.

CD patients carrying *XIAP* mutations can develop XLP2, partially in response to microbial triggers such as Epstein-Barr virus.^{212,213} While both CD and XLP2 display incomplete penetrance in patients with *XIAP* mutations, the involvement of microbial triggers in XLP2 indicates that such triggers may also play vital roles in eliciting CD in patients with *XIAP* mutations. We therefore investigated whether exposure to opportunistic microbes can elicit intestinal inflammation in mice with *Xiap* deficiency. Indeed, we could show that *Xiap*^{-/-} mice display susceptibility to the opportunistic

microbe *H. hepaticus*. The inability to clear *H. hepaticus* at acute stages of infection likely arises due to the PC-defects in the *Xiap*^{-/-} mice. Moreover, the failure to eliminate *H. hepaticus* eventually contributes to the development of non-necrotizing granulomas in the ileum of *Xiap*^{-/-} mice at chronic stages of infection.¹³⁶ Non-necrotizing granulomas are a hallmark of CD, suggesting a potential relevance of our findings in mice to the pathogenesis of intestinal inflammation in human CD. Moreover, these observations are in line with other IBD-associated mouse models which also require such microbial triggers to initiate inflammation. For example, MNV infection of *Atg16l1*^{HM} mice, leads to changes in PC morphology and gene expression. Furthermore, exposure of MNV-positive *Atg16l1*^{HM} mice to DSS is associated with pathology in the ileum resembling CD that is not observed in WT mice or MNV-negative *Atg16l1*^{HM} mice.¹⁷⁹ Likewise, *Nod2*^{-/-} mice which carry defects in PC α -defensins develop granulomatous ileitis when infected with the opportunistic microbe *H.hepaticus*.¹⁷² Thus, loss of XIAP also serves as a model that supports the finding that PC dysfunction in genetically susceptible hosts can cause susceptibility to microbiota-induced intestinal inflammation.

Since patients with *XIAP* mutations may also present with inflammation in the colon, we examined the responses of *Xiap*^{-/-} mice to the colitis-inducing agent DSS. While DSS colitis is a colonic inflammation model, previous studies have indeed demonstrated antimicrobial activity of PC α -defensins in the large intestine of mice.^{57,58} Additionally, we have described how defects in PC-AMPs cause perturbations in the microbiota as well as altered microbial stratification in the large intestine of *Xiap*^{-/-} mice. Further, several mouse models such as *Nod2*^{-/-} mice, *Mmp7*^{-/-} mice or IEC-specific deletion of *Xbp1* in mice that are associated with dysfunctional PCs, present with increased susceptibility to DSS-induced colitis when compared to their WT counterparts.^{179,355,369} Upon DSS treatment, *Xiap*^{-/-} mice also showed increased susceptibility to colitis that was accompanied by upregulated secretion of various cytokines including IL-6. IL-6 is a multi-functional pro-inflammatory cytokine which upon binding to the IL-6 receptor complex, activates signal transducer and activator of transcription 3, a transcription factor known to have central effector roles in IBD.³⁷⁰ Studies on colitis models in WT mice revealed that anti-IL-6 treatment reduced the expression of cytokines such as *Tnfa* and *Ifny*, and blocked the recruitment of leukocytes thereby abrogating colitis.³⁷¹ Intriguingly, high levels of IL-6 are present in

lesions of pediatric patients with IBD, which may be critical in the context of XIAP, given that patients with *XIAP* mutations most often present with pediatric-onset CD.³⁷² Furthermore, upregulation of the chemokine MCP-1 was also observed in the inflamed mucosa of *Xiap*^{-/-} mice, in line with increased MCP-1 levels observed in IBD patients and in accordance with the observation that deletion of *Mcp1* in mice is associated with decreased susceptibility to colitis.^{373,374} Lastly, DSS treatment also upregulated the expression of *Il1β* in the colon of *Xiap*^{-/-} mice, in accordance with the role of XIAP in regulating inflammasome activation and the production of IL-1β in response to TLR stimulation.^{273,275,354} Thus, these findings suggest that XIAP deficiency is associated with increased sensitivity to DSS-induced colitis which is accompanied by increased expression of pro-inflammatory cytokines and chemokines.

Interestingly, tissue-specific loss of *Xiap* in PCs, the intestinal epithelium or the myeloid compartment was not associated with PC loss or increased susceptibility to DSS-induced intestinal inflammation, which was observed upon the systemic loss of *Xiap*. This suggests that XIAP deficiency is likely required in several cellular compartments of the gut to synergistically promote PC death and susceptibility to intestinal inflammation. A possible hypothesis for these observations is that XIAP deficiency in the myeloid system likely promotes an increased inflammatory tone associated with inflammasome activation²⁷³, which then acts on PCs that, in the additional loss of XIAP in PCs (or IECs), respond with increased PC death. Mice with individual deletion of *Xiap* in PCs/IECs or the myeloid compartment do not show these defects because, neither mice with IEC-specific deletion of *Xiap* have increased IL-1β production, nor mice with myeloid-specific *Xiap* deletion are susceptible to PC death. As such, humans with *XIAP* mutations carry germline mutations and thus, similar to *Xiap*^{-/-} mice, exhibit constitutive XIAP deficiency.^{216,218–220,375} The *Xiap*^{-/-} mice therefore best reflect the human situation. In line with the absence of intestinal inflammation in the conditional knockout mice, restoration of *XIAP* expression in one compartment (myeloid compartment) by allogenic hematopoietic stem cell transplantation is sufficient to abrogate intestinal inflammation in CD patients with *XIAP* mutations.^{213,216,376,217–219,222,223,311,312,321} Thus, PC death and susceptibility to intestinal inflammation in the context of XIAP deficiency require loss of XIAP in several cellular compartments of the gut.

5. Conclusion

The data presented in this thesis demonstrate an unanticipated, critical role of XIAP in PC homeostasis. In the absence of XIAP, as modeled in *Xiap*^{-/-} mice, PCs undergo apoptotic cell death in response to microbial signaling and TNF release. PC loss in turn is associated with decreased secretion of PC-AMPs, which leads to impaired microbial stratification/compartmentalization and dysbiosis. Most importantly, deficiency in XIAP and associated PC defects promote susceptibility to environmental-induced intestinal inflammation. Together, this work demonstrates how genetic defects in the host can disrupt host-microbial interactions through alterations in PC biology and can promote intestinal inflammation in response to microbial triggers. These results provide novel insights into the mechanisms that contribute to the development of IBD in patients with *XIAP* mutations and raise the question of whether targeting of the microbiota could be efficacious for the prevention and/or treatment of intestinal inflammation in these individuals.

Summary

Intestinal homeostasis requires dynamic crosstalk between the host and the commensal microbiota. These interactions are not just crucial for maintaining homeostasis but also play an important role in mounting protective immunity to invading pathogens. Moreover, disruption of this physiological cross-talk may contribute to chronic intestinal damage as observed in inflammatory bowel disease (IBD).

IBD, a group of disorders characterized by chronic intestinal inflammation, is believed to arise in genetically susceptible hosts through dysregulated host-environmental responses. Genome-wide association studies have documented common polymorphisms in over 200 genetic loci which regulate the risk to develop IBD. While common genetic variants are associated with low to moderate disease risk and have thus provided limited insight into disease pathogenesis, exome sequencing studies recently revealed rare genetic variants that give rise to mono- and oligogenic forms of IBD. These Mendelian forms of IBD have provided substantial new insight into the mechanisms underlying chronic intestinal inflammation and damage in IBD and revealed new targets for the treatment of IBD.

We and others recently described a monogenic form of IBD caused by mutations in the gene encoding X chromosome-linked inhibitor of apoptosis protein (XIAP) and have described *XIAP* mutations in approximately 4% of male children with early-onset Crohn's disease (CD). While the only curative treatment regime currently available for CD patients with *XIAP* mutations is allogeneic hematopoietic stem cell transplantation, significant mortality associated with the outcome of this procedure calls for alternative therapies. Investigation of alternative therapies requires a better understanding of the CD pathogenesis in patients with *XIAP* mutations.

To provide insight into the pathways that link *XIAP* mutations to IBD, we investigated the role of XIAP in intestinal homeostasis and inflammation through the study of mice with constitutive and cell-specific deletion of *Xiap*. In these studies, we discovered a novel function of XIAP in the regulation of survival of antimicrobial peptide producing cells called Paneth cells. Specifically, we could demonstrate that the commensal microbiota elicits tumor necrosis factor (TNF) production under constitutive conditions,

which promotes Paneth cell death and XIAP serves as a critical inhibitor of this pathway. In the absence of XIAP, microbiota-induced TNF release leads to apoptotic loss of Paneth cells, which is associated with decreased Paneth cell-antimicrobial peptides production, impaired control of the intestinal microbiota and dysbiosis as well as altered bacterial stratification. These alterations are insufficient to elicit spontaneous intestinal inflammation in the presence of a pathogen-free microbiota but provide susceptibility to microbial and chemical triggers of intestinal inflammation. As such, exposure to the bacterial pathobiont *Helicobacter hepaticus* leads to the development of granulomatous ileitis in the *Xiap*^{-/-} but not in wild type mice. Non-necrotizing granulomas are a hallmark of CD, suggesting a potential relevance of our findings in mice to the pathogenesis of human CD. Moreover, administration of dextran sulfate sodium was also associated with increased severity of colitis in *Xiap*^{-/-} mice when compared to the wild type mice.

Together, these findings demonstrate how genetic defects associated with CD can provide susceptibility to environmentally-induced chronic intestinal inflammation. Furthermore, these results raise the question of whether targeting of the microbiota can be efficacious in the treatment and prevention of intestinal inflammation in patients harboring mutations in *XIAP*.

Zusammenfassung

Die intestinale Homöostase erfordert eine dynamische Interaktion zwischen dem Wirt und der Mikrobiota. Diese Wechselwirkungen sind nicht nur entscheidend für den Erhalt der intestinalen Homöostase sondern spielen auch eine wichtige Rolle im Aufbau der protektiven Immunität gegenüber eindringenden Pathogenen. Störungen der physiologischen Interaktionen zwischen Wirt und Mikrobiota hingegen können zu intestinaler Schädigung, wie in chronisch-entzündlichen Darmerkrankungen (CED) beobachtet, beitragen.

CED sind eine Gruppe von Erkrankungen, die charakterisiert sind durch die Entwicklung chronischer intestinaler Entzündung. Das Risiko an CED zu erkranken ist zumindest partiell genetisch determiniert und genomweite Assoziationsstudien konnten CED-Risiko-Polymorphismen in mehr als 200 genetischen Loci dokumentieren. Während diese auch in der gesunden Population häufigen genetischen Varianten nur mit einem geringen bis moderaten Erkrankungsrisiko verbunden sind und somit nur bedingt Einsicht in die Pathogenese der Erkrankung lieferten, konnten in den letzten Jahren eine Vielzahl seltener genetischer Defekte beschrieben werden, die in mono- oder oligogener Weise zur Entstehung einer CED führen. Diese Mendelschen CED-Formen lieferten entscheidende neue Einblicke in die Mechanismen die der chronischen intestinalen Entzündung bei CED zu Grunde liegen und deckten neue potentielle Zielstrukturen für die individualisierte Behandlung von CED auf.

Unsere Arbeitsgruppe sowie mehrere andere Arbeitsgruppen konnten vor wenigen Jahren eine neue monogene CED-Form beschreiben, die durch Mutationen im X-chromosomalen Inhibitor der Apoptose (Englisch: X-linked inhibitor of apoptosis, XIAP) verursacht wird. Wir konnten dabei zeigen, dass XIAP-Mutationen eine der häufigsten monogenen Formen der CED darstellen und in bis zu 4 % der männlichen Kinder mit CED zu finden sind. Monogene CED-Formen, auch die mit XIAP-Mutationen assoziierten, zeigen häufig schwere und therapierefraktäre Verläufe. Die einzige kausale Therapieoption für Patienten mit CED auf dem Boden von XIAP-Mutationen stellt die allogene Stammzelltransplantation dar. Da diese Therapie jedoch mit einer signifikanten Sterblichkeit einhergeht ist, werden alternative Therapien dringend

benötigt. Notwendig hierfür ist ein besseres Verständnis der Pathogenese der CED in Patienten mit XIAP-Mutationen.

Um Einblick in die Mechanismen der Entwicklung intestinaler Entzündung in Patienten mit *XIAP* Mutationen zu erhalten, untersuchten wir Mäuse mit konstitutiver oder zellspezifischer Deletion von *Xiap*. *Xiap*^{-/-} Mäuse wiesen einen selektiven Verlust von Paneth-Zellen auf, einer Gruppe von epithelialen Zellen, die am Boden intestinaler Krypten lokalisiert sind und durch Sekretion antimikrobieller Peptide die intestinale Mikrobiota regulieren. Weiterführende Studien konnten zeigen, dass der Verlust des Zelltod-Inhibitors XIAP zu einer gesteigerten Apoptose von Paneth-Zellen führt, wobei mikrobielle Signale in Tumornekrosefaktor (TNF)-abhängiger Weise den Zelltod von Paneth-Zellen stimulierten. Der Verlust von Paneth-Zellen in *Xiap*^{-/-} Mäusen war verbunden mit einer reduzierten Sekretion von AMPs, was zu einer gestörten Kompartimentalisierung der Mikrobiota und Veränderungen in der Komposition der intestinalen Mikrobiota führte. Während diese Veränderungen in einer Pathogen-freien Tierhaltung nicht mit spontaner intestinaler Entzündung in *Xiap*^{-/-} Mäusen assoziiert waren, führte die Exposition mit dem Pathobionten *Helicobacter hepaticus* in *Xiap*^{-/-} Mäusen, aber nicht in WT-Mäusen, zu einer granulomatösen Ileitis und somit zu Crohn-typischen histologischen Läsionen. Auch zeigten *Xiap*^{-/-} Mäuse eine gesteigerte Suszeptibilität gegenüber einer chemisch induzierten Colitis.

Zusammenfassend zeigen diese Daten, wie genetische Defekte im Wirt und die damit verbundene Störung von Wirt-Mikrobiota-Interaktionen zu mikrobiell induzierter intestinaler Entzündung führen können. Diese Daten sind von zentraler Relevanz für das Verständnis der Pathogenese von CED.

6. References

1. Palmer C, Bik EM, DiGiulio DB, Relman DA, Brown PO. Development of the human infant intestinal microbiota. *PLoS Biol.* 2007;5(7):1556-1573.
2. Cerutti A, Rescigno M. The Biology of Intestinal Immunoglobulin A Responses. *Immunity.* 2008;28(6):740-750.
3. Eckburg PB, Bik EM, Bernstein CN, et al. Diversity of the human intestinal microbial flora. *Science.* 2005;308(June):1635-1638.
4. Bäckhed F, Ley RE, Sonnenburg JL, Peterson DA, Gordon JI. Host-bacterial mutualism in the human intestine. *Science.* 2005;307(5717):1915-1920.
5. Schamberger GP, Diez-Gonzalez F. Selection of recently isolated colicinogenic *Escherichia coli* strains inhibitory to *Escherichia coli* O157:H7. *J Food Prot.* 2002;65(9):1381-1387.
6. Fukuda S, Toh H, Hase K, et al. Bifidobacteria can protect from enteropathogenic infection through production of acetate. *Nature.* 2011;469(7331):543-549.
7. Momose Y, Hirayama K, Itoh K. Competition for proline between indigenous *Escherichia coli* and *E. coli* O157:H7 in gnotobiotic mice associated with infant intestinal microbiota and its contribution to the colonization resistance against *E. coli* O157:H7. *Antonie van Leeuwenhoek, Int J Gen Mol Microbiol.* 2008;94(2):165-171.
8. Chu H, Mazmanian SK. Innate immune recognition of the microbiota promotes host-microbial symbiosis. *Nat Immunol.* 2013;14(7):668-675.
9. Round JL, Lee SM, Li J, et al. The Toll-Like Receptor 2 Pathway Establishes Colonization by a Commensal of the Human Microbiota. *Science.* 2011;332(6032):974-977.
10. Takeuchi O, Akira S. Pattern Recognition Receptors and Inflammation. *Cell.* 2010;140(6):805-820.
11. Maloy KJ, Powrie F. Intestinal homeostasis and its breakdown in inflammatory bowel disease. *Nature.* 2011;474(7351):298-306.
12. Bevins CL, Salzman NH. Paneth cells, antimicrobial peptides and maintenance of intestinal homeostasis. *Nat Rev Microbiol.* 2011;9(5):356-368.
13. Rakoff-Nahoum S, Pglino J, Eslami-Varzaneh F, Edberg S, Medzhitov R. Recognition of comensal microflora by toll-like receptors is required for intestinal homeostasis. *Cell.* 2004;118:229-241.
14. Barker N. Adult intestinal stem cells: critical drivers of epithelial homeostasis and regeneration. *Nat Rev Mol Cell Biol.* 2013;15(1):19-33.

15. Cheng H, Leblond CP. Origin, differentiation and renewal of the four main epithelial cell types in the mouse small intestine V. Unitarian theory of the origin of the four epithelial cell types. *Am J Anat.* 1974;141(4):537-561.
16. Barker N, van Es JH, Kuipers J, et al. Identification of stem cells in small intestine and colon by marker gene Lgr5. *Nature.* 2007;449(7165):1003-1007.
17. Troughton WD, Trier JS. Paneth and goblet cell renewal in mouse duodenal crypts. *J Cell Biol.* 1969;41(1):251-268.
18. Stappenbeck TS1, Wong MH, Saam JR, Mysorekar IU, Gordon JI. Notes from some crypt watchers: regulation of renewal in the mouse intestinal epithelium. *Curr Opin Cell Biol.* 1998 Dec;10(6):702-9.
19. Muñoz J, Stange DE, Schepers AG, et al. The Lgr5 intestinal stem cell signature: robust expression of proposed quiescent '+4' cell markers. *EMBO J.* 2012;31(14):3079-3091.
20. Potten CS, Kovacs L, Hamilton E. Continuous labelling studies on mouse skin and intestine. *Cell Tissue Kinet.* 1974;7(3):271-283.
21. Peterson LW, Artis D. Intestinal epithelial cells: regulators of barrier function and immune homeostasis. *Nat Rev Immunol.* 2014;14(3):141-153.
22. Maury J, Nicoletti C, Guzzo-Chambraud L, Maroux S. The Filamentous Brush Border Glycocalyx, a Mucin-like Marker of Enterocyte Hyper-Polarization. *Eur J Biochem.* 1995;228(2):323-331.
23. Mooseker MS. Organization, chemistry, and assembly of the cytoskeletal apparatus of the intestinal brush border. *Annu Rev Cell Biol.* 1985;1:209-41.
24. Abreu MT. Toll-like receptor signalling in the intestinal epithelium : how bacterial recognition shapes intestinal function. *Nat Rev Immunol.* 2010;10(2):131-144.
25. Frey A, Giannasca KT, Weltzin R, et al., Role of the glycocalyx in regulating access of microparticles to apical plasma membranes of intestinal epithelial cells: implications for microbial attachment and oral vaccine targeting. *J Exp Med.* 1996 Sep 1;184(3):1045-59.
26. Noah TK, Donahue B, Shroyer NF. Intestinal development and differentiation. *Exp Cell Res.* 2011;317(19):2702-2710.
27. McCauley HA, Guasch G. Three cheers for the goblet cell: Maintaining homeostasis in mucosal epithelia. *Trends Mol Med.* 2015;21(8):492-503.
28. Round AN, Rigby NM, Garcia De La Torre A, Maclerzanka A, Mills ENC, MacKie AR. Lamellar structures of MUC2-rich mucin: A potential role in governing the barrier

and lubricating functions of intestinal mucus. *Biomacromolecules*. 2012;13(10):3253-3261.

29. Johansson ME V, Phillipson M, Petersson J, Velcich A, Holm L, Hansson GC. The inner of the two Muc2 mucin-dependent mucus layers in colon is devoid of bacteria. *Proc Natl Acad Sci U S A*. 2008 Sep 30;105(39):15064-9.

30. Atuma C, Strugala V, Allen A, Holm L. The adherent gastrointestinal mucus gel layer: thickness and physical state in vivo. *Am J Physiol Gastrointest Liver Physiol*. 2001 May;280(5):G922-9.

31. Salzman NH, Underwood MA, Bevins CL. Paneth cells, defensins, and the commensal microbiota: A hypothesis on intimate interplay at the intestinal mucosa. *Semin Immunol*. 2007;19:70-83.

32. Selleri S, Palazzo M, Deola S, et al. Induction of pro-inflammatory programs in enteroendocrine cells by the Toll-like receptor agonists flagellin and bacterial LPS. *Int Immunol*. 2008;20(8):961-970.

33. Besedovsky HO, del Rey A. Immune-neuro-endocrine interactions: facts and hypotheses. *Endocr Rev*. 1996;17(1):64-102.

34. Gribble FM, Reimann F. Enteroendocrine Cells: Chemosensors in the Intestinal Epithelium. *Annu Rev Physiol*. 2016.

35. Sjolund K, Sanden G, Hakanson R, Sundler F. Endocrine Cells in Human Intestine: An Immunocytochemical Study. *Gastroenterology*. 1983;1120-1130.

36. Gerbe F, Legraverend C, Jay P. The intestinal epithelium tuft cells: specification and function. *Cell Mol Life Sci*. 2012:2907-2917.

37. Gerbe F, Sidot E, Smyth DJ, et al. Intestinal epithelial tuft cells initiate type 2 mucosal immunity to helminth parasites. *Nature*. 2016;529(7585):226-230.

38. Howitt MR, Lavoie S, Michaud M, et al. Tuft cells, taste-chemosensory cells, orchestrate parasite type 2 immunity in the gut. *Science*. 2016;351(6279):1436-1441.

39. Lorenz RG, Newberry RD. Isolated Lymphoid Follicles Can Function as Sites for Induction of Mucosal Immune Responses. *Ann N Y Acad Sci*. 2004;57:44-57.

40. Kanaya T, Hase K, Takahashi D, et al. The Ets transcription factor Spi-B is essential for the differentiation of intestinal microfold cells. *Nat Immunol*. 2012;13(8).

41. Rosenblatt J, Raff MC, Cramer LP. An epithelial cell destined for apoptosis signals its neighbors to extrude it by an actin- and myosin-dependent mechanism. *Curr Biol*. 2001;11(23):1847-1857.

42. Marchiando AM, Shen L, Graham WV, et al. The epithelial barrier is maintained by

- in vivo tight junction expansion during pathologic intestinal epithelial shedding. *Gastroenterology*. 2011;140(4):1208-1218.
43. Schwalbe G. Beiträge zur Kenntniss der Driisen in den Darm- wandungen, in's Besondere der Brunner'schen. Driisen. *Arc. Mikrosk. Anat.* 8: 92-114.
 44. Paneth, J. Ueber die secernirenden Zellen des Dünndarm-Epithels. *Arc. Mikrosk. Anat.* 31, 113–191 (1887).
 45. Deckx RJ, Vantrappen GR, Parein MM. Localization of lysozyme activity in a Paneth cell granule fraction. *BBA - Enzymol.* 1967;139(1):204-207.
 46. Jones DE, Bevins CL. Paneth cells of the human small intestine express an antimicrobial peptide gene. *J Biol Chem.* 1992;267(32):23216-23225.
 47. Porter EM, Bevins CL, Ghosh D, Ganz T. The multifaceted Paneth cell. *Cell Mol Life Sci.* 2002;59:156-170.
 48. Mallow EB, Harris A, Salzman N, et al. Human enteric defensins. Gene structure and developmental expression. *J Biol Chem.* 1996;271(8):4038-4045.
 49. Bry L, Falk PER, Huttnert K, Gordon JI, Midtvedt T. Paneth cell differentiation in the developing intestine of normal and transgenic mice. *Proc Natl Acad Sci USA.* 1994;91(October):10335-10339.
 50. Smith VC, Genta RM. Role of Helicobacter pylori gastritis in gastric atrophy, intestinal metaplasia, and gastric neoplasia. *Microsc Res Tech.* 2000;48(6):313-320.
 51. Cunliffe R, Rose F, Keyte J, Abberley L, Chan W, and Mahida Y. Human defensin 5 is stored in precursor form in normal Paneth cells and is expressed by some villous epithelial cells and by metaplastic Paneth cells in the colon in inflammatory bowel disease. *Gut.* 2001:176-185.
 52. Klockars M, Reitamo S, Reitamo JJ, Möller C. Immunohistochemical identification of lysozyme in intestinal lesions in ulcerative colitis and Crohn's disease. *Gut.* 1977;18(5):377-381.
 53. Haapamaki MM, Gronroos JM, Nurmi H, et al. Gene expression of group II phospholipase A2 in intestine in ulcerative colitis. *Gut.* 1997 Jan;40(1):95-101.
 54. Elphick DA, Mahida YR. Paneth cells: their role in innate immunity and inflammatory disease. *Gut.* 2005 Dec; 54(12): 1802–1809.
 55. Muniz LR, Knosp C, Yeretssian G. Intestinal antimicrobial peptides during homeostasis, infection, and disease. *Front Immunol.* 2012;3(Oct):1-13.
 56. Wells JM, Brummer RJ, Derrien M, et al. Homeostasis of the gut barrier and potential biomarkers. *Am J Physiol - Gastrointest Liver Physiol.* 2017;312(3):G171-

G193.

57. Mastroianni JR, Ouellette AJ. α -Defensins in enteric innate immunity. Functional paneth cell α -defensins in mouse colonic lumen. *J Biol Chem*. 2009;284(41):27848-27856.
58. Mastroianni JR, Costales JK, Zaksheske J, Selsted ME, Salzman NH, Ouellette AJ. Alternative luminal activation mechanisms for paneth cell α -defensins. *J Biol Chem*. 2012;287(14):11205-11212.
59. Mukherjee S, Hooper L V. Antimicrobial Defense of the Intestine. *Immunity*. 2015;42(1):28-39.
60. Ayabe T, Satchell DP, Wilson CL, Parks WC, Selsted ME, Ouellette AJ. Secretion of microbicidal alpha-defensins by intestinal Paneth cells in response to bacteria. *Nat Immunol*. 2000;1(2):113-118.
61. Satoh Y, Habara Y, Ono K, Kanno T. Carbamylcholine- and catecholamine-induced intracellular calcium dynamics of epithelial cells in mouse ileal crypts. *Gastroenterology*. 1995 May;108(5):1345-56.
62. Ayabe T, Wulff H, Darmoul D, Cahalan MD, George Chandy K, Ouellette AJ. Modulation of mouse paneth cell α -defensin secretion by mIKCa1, a Ca²⁺-activated, intermediate conductance potassium channel. *J Biol Chem*. 2002;277(5):3793-3800.
63. Trezise AE, Romano PR, Gill DR, et al. The multidrug resistance and cystic fibrosis genes have complementary patterns of epithelial expression. *EMBO J*. 1992;11(12):4291-4303.
64. De Lisle RC. Altered transit and bacterial overgrowth in the cystic fibrosis mouse small intestine. *AJP Gastrointest Liver Physiol*. 2007;293(1):G104-G111.
65. Liu J, Walker NM, Cook MT, Ootani A, Clarke LL. Functional Cftr in crypt epithelium of organotypic enteroid cultures from murine small intestine. *Am J Physiol Physiol*. 2012;302(10):C1492-C1503.
66. Ganz T. Defensins: antimicrobial peptides of innate immunity. *Nat Rev Immunol*. 2003;3(9):710-720.
67. Ganz T, Lehrer RI. Defensins. *Pharmac Ther*. 1995;66(94):191-205.
68. Huttner KM, Selsted ME, Ouellette AJ. Structure and Diversity of the Murine Cryptdin Gene Family. *Genomics*. 1994;19(3):448-453.
69. Linzmeier R, Michaelson D, Liu L, Ganz T. The structure of neutrophil defensin genes. *FEBS Lett*. 1993;321(2-3):267-273.
70. Ouellette AJ, Miller SI, Henschen AH, Selsted ME. Purification and primary

- structure of murine cryptdin-1, a Paneth cell defensin. *FEBS Lett.* 1992;304(2-3):146-148.
71. Ouellette AJ, Hsieh MM, Nosek MT, et al. Mouse Paneth cell defensins: Primary structures and antibacterial activities of numerous cryptdin isoforms. *Infect Immun.* 1994;62(11):5040-5047.
72. Shanahan MT, Tanabe H, Ouellette AJ. Strain-specific polymorphisms in paneth cell α -defensins of C57BL/6 mice and evidence of vestigial myeloid α -defensin pseudogenes. *Infect Immun.* 2011;79(1):459-573.
73. Wilson CL. Regulation of Intestinal α -Defensin Activation by the Metalloproteinase Matrilysin in Innate Host Defense. *Science.* 1999;286(5437):113-117.
74. Salzman NH, Hung K, Haribhai D, et al. Enteric defensins are essential regulators of intestinal microbial ecology. *Nat Immunol.* 2010;11(1):76-83.
75. Ghosh D, Porter E, Shen B, et al. Paneth cell trypsin is the processing enzyme for human defensin-5. *Nat Immunol.* 2002;3(6):583-590.
76. Kagan BL, Selsted ME, Ganz T, Lehrer RI. Antimicrobial defensin peptides form voltage-dependent ion-permeable channels in planar lipid bilayer membranes. *Proc Natl Acad Sci USA.* 1990;87(January):210–214.
77. Madison MN, Kleshchenko YY, Nde PN, Simmons KJ, Lima MF, Villalta F. Human defensin α -1 causes *Trypanosoma cruzi* membrane pore formation and induces DNA fragmentation, which leads to trypanosome destruction. *Infect Immun.* 2007;75(10):4780-4791.
78. Chu H, Pazgier M, Jung G, et al. Human-Defensin 6 Promotes Mucosal Innate Immunity Through Self-Assembled Peptide Nanonets. *Science.* 2012;337(6093):477-481.
79. Ericksen B, Wu Z, Lu W, Lehrer RI. Antibacterial activity and specificity of the six human alpha defensins. *Antimicrob Agents Chemother.* 2005;49(1):8-15.
80. Porter EM, Van Dam E, Valore E V., Ganz T. Broad-spectrum antimicrobial activity of human intestinal defensin 5. *Infect Immun.* 1997;65(6):2396-2401.
81. Smith JG, Nemerow GR. Mechanism of Adenovirus Neutralization by Human α -Defensins. *Cell Host Microbe.* 2008;3(1):11-19.
82. Zins SR, Nelson CDS, Maginnis MS, Banerjee R, O'Hara BA, Atwood WJ. The Human Alpha Defensin HD5 Neutralizes JC Polyomavirus Infection by Reducing Endoplasmic Reticulum Traffic and Stabilizing the Viral Capsid. *J Virol.* 2014;88(2):948-960.

83. Pütsep K, Axelsson LG, Boman A, et al. Germ-free and colonized mice generate the same products from enteric prodefensins. *J Biol Chem*. 2000;275(51):40478-40482.
84. Andersson ML, Karlsson-Sjöberg JMT, Pütsep KL. CRS-peptides: unique defense peptides of mouse Paneth cells. *Mucosal Immunol*. 2012;5(4):367-376.
85. Turner J, Cho Y, Dinh N, Waring AJ, Lehrer RI. Activities of LL-37, a cathelin-associated antimicrobial peptide of human neutrophils. *Antimicrob Agents Chemother*. 1998 Sep;42(9):2206-14.
86. Tomasinsig L, Zanetti M. The cathelicidins - structure, function and evolution. *Curr Protein Pept Sci*. 2005;6(1):23-34.
87. Hase K, Eckmann L, Leopard JD, Varki N, Kagnoff MF. Cell Differentiation Is a Key Determinant of Cathelicidin LL-37 / Human Cationic Antimicrobial Protein 18 Expression by Human Colon Epithelium. *Infect Immun*. 2002;70(2):953-963.
88. Gallo RL, Kim KJ, Bernfield M, Kozak CA, et al. Identification of CRAMP, a cathelin-related antimicrobial peptide expressed in the embryonic and adult mouse. *J Biol Chem*. 1997;272(20):13088-13093.
89. Schaubert J, Svanholm C, Termén S, et al. Expression of the cathelicidin LL-37 is modulated by short chain fatty acids in colonocytes: relevance of signalling pathways. *Gut*. 2003;52(5):735-741.
90. Sochacki KA, Barns KJ, Bucki R, Weisshaar JC. Real-time attack on single Escherichia coli cells by the human antimicrobial peptide LL-37. *Proc Natl Acad Sci USA*. 2011;108(16):E77-81.
91. López-García B, Lee PHA, Yamasaki K, Gallo RL. Anti-fungal activity of cathelicidins and their potential role in Candida albicans skin infection. *J Invest Dermatol*. 2005;125(1):108-115.
92. Kościuczuk EM, Lisowski P, Jarczak J, et al. Cathelicidins: family of antimicrobial peptides. A review. *Mol Biol Rep*. 2012;39(12):10957-10970.
93. Singh D, Qi R, Jordan JL, Mateo LS, Kao CC. The human antimicrobial peptide LL-37, but not the mouse ortholog, mCRAMP, can stimulate signaling by poly(I:C) through a FPRL1-dependent pathway. *J Biol Chem*. 2013;288(12):8258-8268.
94. Cash HL, Whitham C V, Behrendt CL, Hooper L V. Symbiotic bacteria direct expression of an intestinal bactericidal lectin. *Science*. 2006;313(5790):1126-1130.
95. Hervieu V, Christa L, Gouysse G, et al. HIP/PAP, a member of the reg family, is expressed in glucagon-producing enteropancreatic endocrine cells and tumors. *Hum*

Pathol. 2006;37(8):1066-1075.

96. Mukherjee S, Zheng H, Derebe MG, et al. Antibacterial membrane attack by a pore-forming intestinal C-type lectin. *Nature.* 2014;505(7481):103-107.

97. Brandl K, Plitas G, Schnabl B, DeMatteo RP, Pamer EG. MyD88-mediated signals induce the bactericidal lectin RegIII γ and protect mice against intestinal *Listeria monocytogenes* infection. *J Exp Med.* 2007;204(8):1891-1900.

98. Medveczky P, Szmola R, Sahin-Tóth M. Proteolytic activation of human pancreatitis associated protein is required for peptidoglycan binding and bacterial aggregation. *J Biochem.* 2009;420(2):335-343.

99. Mukherjee S, Partch CL, Lehotzky RE, et al. Regulation of C-type lectin antimicrobial activity by a flexible N-terminal prosegment. *J Biol Chem.* 2009;284(8):4881-4888.

100. Vaishnava S, Yamamoto M, Severson KM, et al. The Antibacterial Lectin RegIII γ . *Science.* 2011;334(October):255-258.

101. Loonen LMP, Stolte EH, Jaklofsky MTJ, et al. REG3 γ -deficient mice have altered mucus distribution and increased mucosal inflammatory responses to the microbiota and enteric pathogens in the ileum. *Mucosal Immunol.* 2014;7(4):939-947.

102. Nevalainen TJ, Graham GG, Scott KF. Antibacterial actions of secreted phospholipases A2. Review. *Biochim Biophys Acta - Mol Cell Biol Lipids.* 2008;1781(1-2):1-9.

103. Harwig SSL, Tan L, Qu XD, Cho Y, Eisenhauer PB, Lehrer RI. Bactericidal properties of murine intestinal phospholipase A2. *J Clin Invest.* 1995;95(2):603-610.

104. Qu XD, Kent Lloyd KC, Walsh JH, Lehrer RI. Secretion of type II phospholipase A2 and cryptdin by rat small intestinal Paneth cells. *Infect Immun.* 1996;64(12):5161-5165.

105. Peeters T, Vantrappen G. The Paneth cell: a source of intestinal lysozyme. *Gut.* 1975;16(7):553-558.

106. Erlandsen SL, Parsons JA, Taylor TD. Ultrastructural immunocytochemical localization of lysozyme in the Paneth cells of man. *J Histochem Cytochem.* 1974 Jun;22(6):401-13.

107. Ganz T. Antimicrobial polypeptides. *J Leukoc Biol.* 2004;75(1):34-38.

108. Hooper LV, Stappenbeck TS, Hong CV, Gordon JI. Angiogenins: a new class of microbicidal proteins involved in innate immunity. *Nat Immunol.* 2003;4(3):269-273.

109. Petnicki-Ocwieja T, Hrcir T, Liu Y-J, et al. Nod2 is required for the regulation of

- commensal microbiota in the intestine: Commentary. *Proc Natl Acad Sci USA*. 2009 Sep 15;106(37):15813-8.
110. Persson EK, Scott CL, Mowat AM, Agace WW. Dendritic cell subsets in the intestinal lamina propria: Ontogeny and function. *Eur J Immunol*. 2013;43(12):3098-3107.
111. Sun C-M, Hall JA, Blank RB, et al. Small intestine lamina propria dendritic cells promote de novo generation of Foxp3 T reg cells via retinoic acid. *J Exp Med*. 2007;204(8):1775-1785.
112. Niess JH, Brand S, Gu X, et al., CX3CR1-Mediated Dendritic Cell Access to the Intestinal Lumen and Bacterial Clearance. *Science*. 2005; Jan 14;307(5707):254-8.
113. Macpherson AJ, Uhr T. Induction of Protective IgA by Dendritic Cells Carrying Commensal Bacteria. *Science*. 2008;1662(2004):1-8.
114. Vaishnava S, Behrendt CL, Ismail AS, Eckmann L, Hooper L V. Paneth cells directly sense gut commensals and maintain homeostasis at the intestinal host-microbial interface. *Proc Natl Acad Sci USA*. 2008;105(52):20858-20863.
115. vanov II, Atarashi K, Manel N, et al. Induction of Intestinal Th17 Cells by Segmented Filamentous Bacteria. *Cell*. 2009;139(3):485-498.
116. Farkas AM, Panea C, Goto Y, et al. Induction of Th17 cells by segmented filamentous bacteria in the murine intestine. *J Immunol Methods*. 2015;421:104-111.
117. Stzepourginski I, Nigro G, Jacob J-M, et al. CD34⁺ mesenchymal cells are a major component of the intestinal stem cells niche at homeostasis and after injury. *Proc Natl Acad Sci*. 2017;114(4):E506-E513.
118. Smith RJ, Rao-Bhatia A, Kim T-H. Signaling and epigenetic mechanisms of intestinal stem cells and progenitors: insight into crypt homeostasis, plasticity, and niches. *Wiley Interdiscip Rev Dev Biol*. 2017;1(Figure 1):e281.
119. Pinto D, Gregorieff A, Begthel H, Clevers H. Canonical Wnt signals are essential for homeostasis of the intestinal epithelium. *Genes Dev*. 2003 Jul 15;17(14):1709-13.
120. Gregorieff A, Clevers H. Wnt signaling in the intestinal epithelium : from endoderm to cancer Wnt signaling in the intestinal epithelium : from endoderm to cancer. *Genes Dev*. 2005:877-890.
121. Crosnier C, Stamataki D, Lewis J. Organizing cell renewal in the intestine: Stem cells, signals and combinatorial control. *Nat Rev Genet*. 2006;7(5):349-359.
122. Van Es JH, Jay P, Gregorieff A, et al. Wnt signalling induces maturation of Paneth cells in intestinal crypts. *Nat Cell Biol*. 2005;7(4):381-386.

123. Stanger BZ, Datar R, Murtaugh LC, Melton DA. Direct regulation of intestinal fate by Notch. *Proc Natl Acad Sci USA*. 2005;102(35):12443-12448.
124. Van Es JH, Van Gijn ME, Riccio O, et al. Notch/ γ -secretase inhibition turns proliferative cells in intestinal crypts and adenomas into goblet cells. *Nature*. 2005;435(7044):959-963.
125. Fre S, Huyghe M, Mourikis P, Robine S, Louvard D, Artavanis-Tsakonas S. Notch signals control the fate of immature progenitor cells in the intestine. *Nature*. 2005;435(7044):964-968.
126. Crosnier C. Delta-Notch signalling controls commitment to a secretory fate in the zebrafish intestine. *Development*. 2005;132(5):1093-1104.
127. Suzuki A, Sekiya S, Gunshima E, Fujii S, Taniguchi H. EGF signaling activates proliferation and blocks apoptosis of mouse and human intestinal stem/progenitor cells in long-term monolayer cell culture. *Lab Invest*. 2010;90(10):1425-1436.
128. Biteau B, Jasper H. EGF signaling regulates the proliferation of intestinal stem cells in *Drosophila*. *Development*. 2011;138(6):1045-1055.
129. Van Es JH, de Geest N, van de Born M, Clevers H, Hassan BA. Intestinal stem cells lacking the Math1 tumour suppressor are refractory to Notch inhibitors. *Nat Commun*. 2010;1(2):1-5.
130. Sato T, Van Es JH, Snippert HJ, et al. Paneth cells constitute the niche for Lgr5 stem cells in intestinal crypts. *Nature*. 2011;469(7330):415-418.
131. Yang Q, Bermingham NA, Finegold MJ. Requirement of Math1 for Secretory Cell Lineage Commitment in the Mouse Intestine. *Science*. 2001;294(December):2155-2159.
132. Durand A, Donahue B, Peignon G, et al. Functional intestinal stem cells after Paneth cell ablation induced by the loss of transcription factor Math1 (*Atoh1*). *Proc Natl Acad Sci USA*. 2012;109(23):8965-8970.
133. Farin HF, Van Es JH, Clevers H. Redundant sources of Wnt regulate intestinal stem cells and promote formation of paneth cells. *Gastroenterology*. 2012;143(6):1518-1529.e7.
134. Kabiri Z, Greicius G, Madan B, et al. Stroma provides an intestinal stem cell niche in the absence of epithelial Wnts. *Development*. 2014;141(11):2206-2215.
135. Podolsky DK. Inflammatory bowel disease. *N Engl J Med*. 2002 Aug 8;347(6):417-29.
136. Xavier RJ, Podolsky DK. Unravelling the pathogenesis of inflammatory bowel

- disease. *Nature*. 2007;448(7152):427-434.
137. Burisch J, Jess T, Martinato M, Lakatos PL. The burden of inflammatory bowel disease in Europe. *J Crohn's Colitis*. 2013;7(4):322-337.
138. Colombel J, Mahadevan U. Inflammatory Bowel Disease 2017: Innovations and Changing Paradigms. *Gastroenterology*. 2017;152(2):309-312.
139. West EM. The Changing Landscape of Inflammatory Bowel Disease: *Gastroenterology*. 2016;150(1):24-26.
140. Johnston RD, Logan RFA. What is the peak age for onset of IBD? *Inflamm Bowel Dis*. 2008;14(October 2008):S4-S5.
141. Neurath MF. Current and emerging therapeutic targets for IBD. *Nat Rev Gastroenterol Hepatol*. 2017 May;14(5):269-278.
142. Kaser A, Zeissig S, Blumberg RS. Inflammatory Bowel Disease. *Annu Rev Immunol*. 2010;28:573-621.
143. Jostins L, Ripke S, Weersma RK, et al. Host-microbe interactions have shaped the genetic architecture of inflammatory bowel disease. *Nature*. 2012;491(7422):119-124.
144. Spencer SD, Di Marco F, Hooley J, et al., The orphan receptor CRF2-4 is an essential subunit of the interleukin 10 receptor. *J Exp Med* 1998;187:571-8.
145. Madsen KL, Doyle JS, Tavernini MM, Jewell LD, Rennie RP, Fedorak RN. Antibiotic Therapy Attenuates Colitis in Interleukin 10 Gene-Deficient Mice. *Gastroenterology*. 2000 Jun;118(6):1094-105.
146. Sellon RK, Tonkonogy S, Schultz M, et al. Resident Enteric Bacteria Are Necessary for Development of Spontaneous Colitis and Immune System Activation in Interleukin-10-Deficient Mice. *Infect Immun*. 1998;66(11):5224-5231.
147. Zeissig S, Blumberg RS. Life at the beginning: perturbation of the microbiota by antibiotics in early life and its role in health and disease. *Nat Immunol*. 2014 Apr;15(4):307-10.
148. Dethlefsen L, Relman DA. Incomplete recovery and individualized responses of the human distal gut microbiota to repeated antibiotic perturbation. *Proc Natl Acad Sci USA*. 2011;(Suppl 1):4554-4561.
149. Jakobsson HE, Jernberg C, Andersson AF, Sjölund-Karlsson M, Jansson JK, Engstrand L. Short-term antibiotic treatment has differing long-term impacts on the human throat and gut microbiome. *PLoS One*. 2010 Mar 24;5(3):e9836.
150. Willing BP, Russell SL, Finlay BB. Shifting the balance: Antibiotic effects on host-

- microbiota mutualism. *Nat Rev Microbiol*. 2011;9(4):233-243.
151. Shaw SY, Blanchard JF, Bernstein CN. Association between the use of antibiotics in the first year of life and pediatric inflammatory bowel disease. *Am J Gastroenterol*. 2010;105(12):2687-2692.
152. Virta L, Auvinen A, Helenius H, Huovinen P, Kolho KL. Association of repeated exposure to antibiotics with the development of pediatric crohn's disease - A nationwide, register-based Finnish case-control study. *Am J Epidemiol*. 2012;175(8):775-784.
153. An D, Oh SF, Olszak T, et al. Sphingolipids from a symbiotic microbe regulate homeostasis of host intestinal natural killer T cells. *Cell*. 2014;156(1-2):123-133.
154. Bloom SM, Bijanki VN, Nava GM, et al. Commensal Bacteroides species induce colitis in host-genotype-specific fashion in a mouse model of inflammatory bowel disease. *Cell Host Microbe*. 2011;9(5):390-403.
155. Garrett WS, Lord GM, Punit S, et al. Communicable Ulcerative Colitis Induced by T-bet Deficiency in the Innate Immune System. *Cell*. 2007;131(1):33-45.
156. Garrett WS, Gallini CA, Yatsunencko T, et al. Enterobacteriaceae Act in concert with the gut microbiota to induce spontaneous and maternally transmitted colitis. *Cell Host Microbe*. 2010;8(3):292-300.
157. Sokol H, Pigneur B, Watterlot L, et al. Faecalibacterium prausnitzii is an anti-inflammatory commensal bacterium identified by gut microbiota analysis of Crohn disease patients. *Proc Natl Acad Sci USA*. 2008;105(43):16731-16736.
158. Atarashi K, Tanoue T, Shima T, et al. Induction of colonic regulatory T cells by indigenous *Clostridium* species. *Science*. 2011;331(6015):337-341.
159. Geuking MB, Cahenzli J, Lawson MAE, et al. Intestinal Bacterial Colonization Induces Mutualistic Regulatory T Cell Responses. *Immunity*. 2011;34(5):794-806.
160. Sohn M, Harding MJ, Park J, et al. Correction for Choi et al., Cell-permeable Foxp3 protein alleviates autoimmune disease associated with inflammatory bowel disease and allergic airway inflammation. *Proc Natl Acad Sci USA*. 2010;107(50):21943-21943.
161. Andoh A, Imaeda H, Aomatsu T, et al. Comparison of the fecal microbiota profiles between ulcerative colitis and Crohn's disease using terminal restriction fragment length polymorphism analysis. *J Gastroenterol*. 2011;46(4):479-486.
162. Vrakas S, Mountzouris KC, Michalopoulos G, et al. Intestinal bacteria composition and translocation of bacteria in inflammatory bowel disease. *PLoS One*. 2017;12(1):1-

11.

163. Matsuoka K, Kanai T. The gut microbiota and inflammatory bowel disease. *Semin Immunopathol.* 2015;37(1):47-55.

164. Lucke K, Miehle S, Jacobs E, Schuppler M. Prevalence of Bacteroides and Prevotella spp. in ulcerative colitis. *J Med Microbiol.* 2006;55(5):617-624.

165. Kaakoush NO, Day AS, Huinao KD, et al. Microbial dysbiosis in pediatric patients with Crohn's disease. *J Clin Microbiol.* 2012;50(10):3258-3266.

166. Manichanh C, Rigottier-Gois L, Bonnaud E, et al. Reduced diversity of faecal microbiota in Crohn's disease revealed by a metagenomic approach. *Gut.* 2006;55(2):205-211.

167. Hill DA, Hoffmann C, Abt MC, et al. Metagenomic analyses reveal antibiotic-induced temporal and spatial changes in intestinal microbiota with associated alterations in immune cell homeostasis. *Mucosal Immunol.* 2010;3(2):148-158.

168. Seksik P, Rigottier-Gois L, Gramet G, et al. Alterations of the dominant faecal bacterial groups in patients with Crohn's disease of the colon. (Inflammation and Inflammatory Bowel Disease). *Gut.* 2003;52(2):237(6).

169. Devkota S, Wang Y, Musch MW, et al. Dietary-fat-induced taurocholic acid promotes pathobiont expansion and colitis in Il10^{-/-} mice. *Nature.* 2012;487(7405):104-108.

170. Feng Z, Long W, Hao B, et al. A human stool-derived Bilophila wadsworthia strain caused systemic inflammation in specific-pathogen-free mice. *Gut Pathog.* 2017;9(1):1-10.

171. Devkota S, Change EB. Interactions between diet, bile acid metabolism, gut microbiota, and Inflammatory Bowel Diseases. *Dig Dis.* 2015;33(3):351-356.

172. Amlan Biswas, Yuen-Joyce Liu, Liming Hao, Atsushi Mizoguchi, Nita H. Salzman CLB, Kobayashi KS. Induction and rescue of Nod2-dependent Th1-driven granulomatous inflammation of the ileum. *Proc Natl Acad Sci USA.* 2010;107(33):14739-14744.

173. Kullberg MC, Ward JM, Gorelick PL, et al. Helicobacter hepaticus triggers colitis in specific-pathogen-free interleukin-10 (IL-10)-deficient mice through an IL-12-and gamma interferon- dependent mechanism. *Infect Immun.* 1998;66(11):5157-5166.

174. Lupp C, Robertson ML, Wickham ME, et al. Host-Mediated Inflammation Disrupts the Intestinal Microbiota and Promotes the Overgrowth of Enterobacteriaceae. *Cell Host Microbe.* 2007;2(2):119-129.

175. Elinav E, Strowig T, Kau AL, et al. NLRP6 Inflammasome Regulates Colonic Microbial Ecology and Risk for Colitis. *Cell*. 2011;145(5):745-757.
176. Kobayashi KS, Chamaillard M, Ogura Y, et al. Nod2-dependent regulation of innate and adaptive immunity in the intestinal tract. *Science*. 2005;307(5710):731-734.
177. Büchler G, Wos-Oxley ML, Smoczek A, et al. Strain-specific colitis susceptibility in IL10-deficient mice depends on complex gut microbiota-host interactions. *Inflamm Bowel Dis*. 2012;18(5):943-954.
178. Cadwell K, Liu JY, Brown SL, et al. A key role for autophagy and the autophagy gene Atg16l1 in mouse and human intestinal Paneth cells. *Nature*. 2008;456(7219):259-263.
179. Cadwell K, Patel KK, Maloney NS, et al. Virus-Plus-Susceptibility Gene Interaction Determines Crohn's Disease Gene Atg16L1 Phenotypes in Intestine. *Cell*. 2010;141(7):1135-1145.
180. Kullberg MC, Rothfuchs AG, Caspar P, et al. Helicobacter hepaticus -Induced Colitis in Interleukin-10-Deficient Mice : Cytokine Requirements for the Induction and Maintenance of Intestinal Inflammation. *Infect Immun*. 2001;69(7):4232-4241.
181. Whary MT, Danon SJ, Feng Y, et al. Rapid onset of ulcerative typhlocolitis in B6.129P2-IL10tm1Cgn (IL-10^{-/-}) mice infected with Helicobacter trogontum is associated with decreased colonization by altered Schaedler's flora. *Infect Immun*. 2006;74(12):6615-6623.
182. Darfeuille-Michaud A, Neut C, Barnich N, et al. Presence of adherent Escherichia coli strains in ileal mucosa of patients with Crohn's disease. *Gastroenterology*. 1998;115(6):1405-1413.
183. Barnich N, Glasser A, Darcha C, et al. CEACAM6 acts as a receptor for adherent-invasive E. coli, supporting ileal mucosa colonization in Crohn disease. *J Clin Invest*. 2007;117(6) :1566-74.
184. Halme L, Paavola-Sakki P, Turunen U, Lappalainen M, Färkkilä M, Kontula K. Family and twin studies in inflammatory bowel disease. *World J Gastroenterol*. 2006;12(23):3668-3672.
185. Uhlig HH, Muise AM. Clinical Genomics in Inflammatory Bowel Disease. *Trends Genet*. 2017 Sep;33(9):629-641.
186. Lange KM De, Moutsianas L, Lee JC, et al. Genome-wide association study implicates immune activation of multiple integrin genes in inflammatory bowel disease. *Nat Genet*. 2017 Feb;49(2):256-261.

187. Hampe J, Franke A, Rosenstiel P, et al. A genome-wide association scan of nonsynonymous SNPs identifies a susceptibility variant for Crohn disease in ATG16L1. *Nat Genet.* 2007 Feb;39(2):207-11.
188. Hugot J, Chamaillard M, Zouali H, Lesage S, Ce J, Macry J. Association of NOD2 leucine-rich repeat variants with susceptibility to Crohn ' s disease. *Nature.* 2001 May 31;411(6837):599-603.
189. Ogura Y, Bonen DK, Inohara N, et al. A frameshift mutation in NOD2 associated with susceptibility to Crohn ' s disease. *Nature.* 2001 May 31;411(6837):603-6.
190. Duerr RH, Taylor KD, Brant SR, et al. A Genome-Wide Association Study Identifies IL23R as an Inflammatory Bowel Disease Gene. *Science.* 2006 Dec 1;314(5804):1461-3.
191. Manolio TA, Collins FS, Cox NJ, et al. Finding the missing heritability of complex diseases. *Nature.* 2009;461(7265):747-753.
192. Kotlarz D, Beier R, Murugan D, et al. Loss of interleukin-10 signaling and infantile inflammatory bowel disease: Implications for diagnosis and therapy. *Gastroenterology.* 2012;143(2):347-355.
193. Glocker E-O, Kotlarz D, Boztug K, et al. Inflammatory bowel disease and mutations affecting the interleukin-10 receptor. *N Engl J Med.* 2009;361(21):2033-2045.
194. Kühn R, Löhler J, Rennick D, Rajewsky K, Müller W. Interleukin-10-deficient mice develop chronic enterocolitis. *Cell.* 1993;75(2):263-274.
195. Okou DT, Mondal K, Faubion WA, et al. Exome sequencing identifies a novel FOXP3 mutation in a 2-generation family with inflammatory bowel disease. *J Pediatr Gastroenterol Nutr.* 2014;58(5):561-568.
196. Zeissig S, Petersen B-S, Tomczak M, et al. Early-onset Crohn's disease and autoimmunity associated with a variant in CTLA-4. *Gut.* 2014:1-9.
197. Berasain C, Perugorria MJ, Latasa MU, et al. The Epidermal Growth Factor Receptor: A Link Between Inflammation and Liver Cancer. *Exp Biol Med.* 2009;234(7):713-725.
198. Peschon JJ, Slack JL, Reddy P, Stocking KL, Sunnarborg SW et al. An essential role for ectodomain shedding in mammalian development. *Science.* 1998 Nov 13;282(5392):1281-4.
199. Blaydon DC, Biancheri P, Di W-L, et al. Inflammatory skin and bowel disease linked to ADAM17 deletion. *N Engl J Med.* 2011;365(16):1502-1508.

200. Chalaris A, Adam N, Sina C, et al. Critical role of the disintegrin metalloprotease ADAM17 for intestinal inflammation and regeneration in mice. *J Exp Med*. 2010;207(8):1617-1624.
201. Cheng LE, Kanwar B, Tcheurekdjian H, et al. Persistent systemic inflammation and atypical enterocolitis in patients with NEMO syndrome. *Clin Immunol*. 2009;132(1):124-131.
202. Nenci A, Becker C, Wullaert A, et al. Epithelial NEMO links innate immunity to chronic intestinal inflammation. *Nature*. 2007;446(7135):557-561.
203. Muise AM, Xu W, Guo CH, et al. NADPH oxidase complex and IBD candidate gene studies: Identification of a rare variant in NCF2 that results in reduced binding to RAC2. *Gut*. 2012;61(7):1028-1035.
204. Schappi MG. Colitis in chronic granulomatous disease. *Arch Dis Child*. 2001;84(2):147-151.
205. Matute JD, Arias AA, Wright NAM, et al. A new genetic subgroup of chronic granulomatous disease with autosomal recessive mutations in p40 phox and selective defects in neutrophil NADPH oxidase activity. *Blood*. 2009;114(15):3309-3315.
206. Uhlig HH. Monogenic diseases associated with intestinal inflammation: implications for the understanding of inflammatory bowel disease. *Gut*. 2013;62(12):1795-1805.
207. Glocker EE-O, Kotlarz D, Boztug K, et al. Inflammatory bowel disease and mutations affecting the interleukin-10 receptor. *N Engl J Med*. 2009;361(21):2033-2045.
208. Glocker EO, Frede N, Perro M, et al. Infant colitis-its in the genes. *Lancet*. 2010;376(9748):1272.
209. Hauck F, Koletzko S, Walz C, et al. Diagnostic and treatment options for severe IBD in female X-CGD carriers with non-random X-inactivation. *J Crohn's Colitis*. 2016;10(1):112-115.
210. Åhlin A, Fugeläng J, de Boer M, Ringden O, Fasth A, Winiarski J. Chronic granulomatous disease - haematopoietic stem cell transplantation versus conventional treatment. *Acta Paediatr*. 2013 Nov;102(11):1087-94.
211. Seger RA, Gungor T, Belohradsky BH, et al. Treatment of chronic granulomatous disease with myeloablative conditioning and an unmodified hemopoietic allograft: A survey of the European experience, 1985-2000. *Blood*. 2002;100(13):4344-4350.
212. Rigaud S, Fondanèche M-C, Lambert N, et al. XIAP deficiency in humans causes

- an X-linked lymphoproliferative syndrome. *Nature*. 2006;444(7115):110-114.
213. Filipovich AH, Zhang K, Snow AL, Marsh RA. X-linked lymphoproliferative syndromes: Brothers or distant cousins? *Blood*. 2010;116(18):3398-3408.
214. Schmid JP, Canioni D, Moshous D, et al. Clinical similarities and differences of patients with X-linked lymphoproliferative syndrome type 1 (XLP-1 / SAP deficiency) versus type 2 (XLP-2 / XIAP deficiency). *Blood*. 2010;117(5):1-3.
215. Worthey EA, Mayer AN, Syverson GD, et al. Making a definitive diagnosis: Successful clinical application of whole exome sequencing in a child with intractable inflammatory bowel disease. *Genet Med*. 2011;13(3):255-262.
216. Zeissig Y, Petersen B-S, Milutinovic S, et al. XIAP variants in male Crohn's disease. *Gut*. 2014:1-11.
217. Speckmann C, Lehmborg K, Albert MH, et al. X-linked inhibitor of apoptosis (XIAP) deficiency: The spectrum of presenting manifestations beyond hemophagocytic lymphohistiocytosis. *Clin Immunol*. 2013;149(1):133-141.
218. Girardelli M, Arrigo S, Barabino A, et al. The diagnostic challenge of very early-onset enterocolitis in an infant with XIAP deficiency. *BMC Pediatr*. 2015;15(1):208.
219. Kim SC. Monozygotic Twin Cases of XIAP Deficiency Syndrome. *J Pediatr Gastroenterol Nutr*. 2017:1.
220. Kelsen JR, Dawany N, Martinez A, et al. A de novo whole gene deletion of XIAP detected by exome sequencing analysis in very early onset inflammatory bowel disease: a case report. *BMC Gastroenterol*. 2015;15(1):160.
221. Suzuki T, Sasahara Y, Kikuchi A, et al. Targeted Sequencing and Immunological Analysis Reveal the Involvement of Primary Immunodeficiency Genes in Pediatric IBD: a Japanese Multicenter Study. *J Clin Immunol*. 2017;37(1):67-79.
222. Speckmann C, Ehl S. XIAP deficiency is a mendelian cause of late-onset IBD. *Gut*. 2014;63(6):1031-1032.
223. Aguilar C, Lenoir C, Lambert N, et al. Characterization of Crohn disease in X-linked inhibitor of apoptosis-deficient male patients and female symptomatic carriers. *J Allergy Clin Immunol*. 2014;134(5):1131-1141.e9.
224. Dziadzio M, Ammann S, Canning C, et al. Symptomatic Males and Female Carriers in a Large Caucasian Kindred with XIAP Deficiency. *J Clin Immunol*. 2015 Jul;35(5):439-44.
225. Lala S, Ogura Y, Osborne C, et al. Crohn's disease and the NOD2 gene: A role for paneth cells. *Gastroenterology*. 2003;125(1):47-57.

226. Wehkamp J, Harder J, Weichenthal M, et al. NOD2 (CARD15) mutations in Crohn's disease are associated with diminished mucosal alpha-defensin expression. *Gut*. 2004;53(11):1658-1664.
227. Wehkamp J, Wang G, Kübler I, et al. The Paneth cell alpha-defensin deficiency of ileal Crohn's disease is linked to Wnt/Tcf-4. *J Immunol*. 2007;179(5):3109-3118.
228. Bevins CL, Stange EF, Wehkamp J. Decreased Paneth cell defensin expression in ileal Crohn's disease is independent of inflammation, but linked to the NOD2 1007fs genotype Authors' reply. *Gut*. 2009 Jun;58(6):882-3; discussion 883-4.
229. Logan CY, Nusse R. The Wnt Signaling Pathway in Development and Disease. *Annu Rev Cell Dev Biol*. 2004;20(1):781-810.
230. Koslowski MJ, Kübler I, Chamillard M, et al. Genetic variants of Wnt transcription factor TCF-4 (TCF7L2) putative promoter region are associated with small intestinal Crohn's disease. *PLoS One*. 2009;4(2):e4496.
231. Simms LA, Doecke JD, Roberts RL, et al. KCNN4 gene variant is associated with ileal Crohn's Disease in the Australian and New Zealand population. *Am J Gastroenterol*. 2010;105(10):2209-2217.
232. Di L, Srivastava S, Zhdanova O, et al. Inhibition of the K⁺ channel KCa3.1 ameliorates T cell-mediated colitis. *Proc Natl Acad Sci USA*. 2010;107(4):1541-1546.
233. Parkes M, Barrett JC, Prescott NJ, et al. Sequence variants in the autophagy gene IRGM and multiple other replicating loci contribute to Crohn's disease susceptibility. *Nat Genet*. 2007;39(7):830-832.
234. Glas J, Seiderer J, Bues S, et al. IRGM Variants and Susceptibility to Inflammatory Bowel Disease in the German Population. *PLoS One*. 2013;8(1):e54338.
235. Liu B, Gulati AS, Cantillana V, et al. Irgm1-deficient mice exhibit Paneth cell abnormalities and increased susceptibility to acute intestinal inflammation. *AJP Gastrointest Liver Physiol*. 2013;305(8):G573-G584.
236. Kaser A, Lee A, Franke A, et al. XBP1 Links ER Stress to Intestinal Inflammation and Confers Genetic Risk for Human Inflammatory Bowel Disease. *Cell*. 2008;134:743-756.
237. Shaffer AL, Shapiro-Shelef M, Iwakoshi NN, et al. XBP1, downstream of Blimp-1, expands the secretory apparatus and other organelles, and increases protein synthesis in plasma cell differentiation. *Immunity*. 2004;21(1):81-93.
238. Adolph TE, Tomczak MF, Niederreiter L, et al. Paneth cells as a site of origin for intestinal inflammation. *Nature*. 2013;503(7475):272-276.

239. Nakanishi Y, Reina-Campos M, Nakanishi N, et al. Control of Paneth Cell Fate, Intestinal Inflammation, and Tumorigenesis by PKC λ /I. *Cell Rep*. 2016;16(12):3297-3310.
240. Walsh CM. Grand challenges in cell death and survival: apoptosis vs. necroptosis. *Front Cell Dev Biol*. 2014 Feb 20;2:3.
241. Martin SJ, Henry CM. Distinguishing between apoptosis, necrosis, necroptosis and other cell death modalities. *Methods*. 2013;61(2):87-89.
242. Eckelman BP, Salvesen GS, Scott FL. Human inhibitor of apoptosis proteins: why XIAP is the black sheep of the family. *EMBO Rep*. 2006;7(10):988-994.
243. Crook NE, Clem RJ, Miller LK. An apoptosis-inhibiting baculovirus gene with a zinc finger-like motif. *J Virol*. 1993;67(4):2168-2174.
244. Birnbaum MJ, Clem RJ, Miller LK. An apoptosis-inhibiting gene from a nuclear polyhedrosis virus encoding a polypeptide with Cys/His sequence motifs. *J Virol*. 1994;68(4):2521-2528.
245. Duckett CS, Nava VE, Gedrich RW, et al. A conserved family of cellular genes related to the baculovirus iap gene and encoding apoptosis inhibitors. *EMBO J*. 1996;15(11):2685-2694.
246. Uren AG, Pakusch M, Hawkins CJ, Puls KL, Vaux DL. Cloning and expression of apoptosis inhibitory protein homologs that function to inhibit apoptosis and/or bind tumor necrosis factor receptor-associated factors. *Proc Natl Acad Sci USA*. 1996;93(10):4974-4978.
247. Kobayashi K, Hatano M, Otaki M, Ogasawara T, Tokuhisa T. Expression of a murine homologue of the inhibitor of apoptosis protein is related to cell proliferation. *Proc Natl Acad Sci USA*. 1999 Feb 16;96(4):1457-62.
248. Deveraux QL, Takahashi R, Salvesen GS, Reed JC. X-linked IAP is a direct inhibitor of cell-death proteases. *Nature*. 1997;388(July):300-304.
249. Oberoi-Khanuja TK, Murali A, Rajalingam K. IAPs on the move: role of inhibitors of apoptosis proteins in cell migration. *Cell Death Dis*. 2013;4(9):e784.
250. Pedersen J, LaCasse EC, Seidelin JB, Coskun M, Nielsen OH. Inhibitors of apoptosis (IAPs) regulate intestinal immunity and inflammatory bowel disease (IBD) inflammation. *Trends Mol Med*. 2014;20(11):652-665.
251. Sharma S, Kaufmann T, Biswas S. Impact of inhibitor of apoptosis proteins on immune modulation and inflammation. *Immunol Cell Biol*. 2017;95(3):236-243.
252. Hinds MG, Norton RS, Vaux DL, Day CL. Solution structure of a baculoviral

- inhibitor of apoptosis (IAP) repeat. *Letters*. 1999 Jul;6(7):648-51.
253. Sun C, Cai M, Gunasekera AH, et al. NMR structure and mutagenesis of the inhibitor-of-apoptosis protein XIAP. *Nature*. 1999;401(October):818-822.
254. Sun C, Cai M, Meadows RP, et al. NMR Structure and Mutagenesis of the Third Bir Domain of the Inhibitor of Apoptosis Protein XIAP. *J Biol Chem*. 2000;275(43):33777-33781.
255. Srinivasula SM, Ashwell JD. IAPs: What's in a Name? *Mol Cell*. 2008;30(2):123-135.
256. Reffey SB, Wurthner JU, Parks WT, Roberts AB, Duckett CS. X-linked Inhibitor of Apoptosis Protein Functions as a Cofactor in Transforming Growth Factor- beta Signaling. *J Biol Chem*. 2001;276(28):26542-26549.
257. Yamaguchi K, Nagai S, Ninomiya-tsuji J, et al. XIAP , a cellular member of the inhibitor of apoptosis protein family , links the receptors to TAB1 – TAK1 in the BMP signaling pathway. *EMBO J*. 1999 Jan 4;18(1):179-87.
258. Lin SC, Huang Y, Lo YC, Lu M, Wu H. Crystal Structure of the BIR1 Domain of XIAP in Two Crystal Forms. *J Mol Biol*. 2007;372(4):847-854.
259. Scott FL, Denault J, Riedl SJ, Shin H, Renatus M, Salvesen GS. XIAP inhibits caspase-3 and -7 using two binding sites : evolutionarily conserved mechanism of IAPs. *EMBO J*. 2005;24(3):645-655.
260. Chai J, Shiozaki E, Srinivasa M, et al. Structural Basis of Caspase-7 Inhibition by XIAP. *Cell*. 2001;104:769-780.
261. Riedl SJ, Renatus M, Schwarzenbacher R, et al. Structural Basis for the Inhibition of Caspase-3 by XIAP. *Cell*. 2001;104:791-800.
262. Sharma S, Kaufmann T, Biswas S. Impact of inhibitor of apoptosis proteins on immune modulation and in fl ammation. *Immunol Cell Biol*. 2017 Mar;95(3):236-243.
263. Gyrd-Hansen M, Darding M, Miasari M, et al. IAPs contain an evolutionarily conserved ubiquitin-binding domain that regulates NF-kappaB as well as cell survival and oncogenesis. *Nat Cell Biol*. 2008;10(11):1309-1317.
264. Pickart CM, Eddins MJ. Ubiquitin : structures , functions , mechanisms. *Biochim Biophys Acta*. 2004 Nov 29;1695(1-3):55-72.
265. Weissman AM. Themes and variations on ubiquitylation. *Nat Rev Mol Cell Biol*. 2001 Mar;2(3):169-78.
266. Suryadinata R, Roesley SNA, Yang G, Šarčević B. Mechanisms of generating polyubiquitin chains of different topology. *Cells*. 2014;3(3):674-689.

267. Lorick KL, Jensen JP, Fang S, Ong AM, Hatakeyama S, Weissman AM. RING fingers mediate ubiquitin-conjugating enzyme (E2) -dependent ubiquitination. *Proc Natl Acad Sci USA*. 1999 Sep 28;96(20):11364-9.
268. Vince JE, Wong WW, Khan N, et al. IAP Antagonists Target cIAP1 to Induce TNF α -Dependent Apoptosis. *Cell*. 2010:682-693.
269. Vince JE, Chau D, Callus B, et al. TWEAK-FN14 signaling induces lysosomal degradation of a cIAP1 – TRAF2 complex to sensitize tumor cells to TNF. *J Cell Biol*. 2008 Jul 14;182(1):171-84.
270. Bertrand MJM, Lippens S, Staes A, et al. cIAP1/2 Are Direct E3 Ligases Conjugating Diverse Types of Ubiquitin Chains to Receptor Interacting Proteins Kinases 1 to 4 (RIP1-4). *PLoS One*. 2011;6(9):e22356.
271. Gyrd-Hansen M, Meier P. IAPs: from caspase inhibitors to modulators of NF- κ B, inflammation and cancer. *Nat Rev Cancer*. 2010;10(8):561-574.
272. Hayden MS, Ghosh S. Shared Principles in NF- κ B Signaling. *Cell*. 2008 Feb 8;132(3):344-62.
273. Yabal M, Müller N, Adler H, et al. XIAP Restricts TNF- and RIP3-Dependent Cell Death and Inflammasome Activation. *Cell Rep*. 2014;7(6):1796-1808.
274. Wong WWL, Vince JE, Lalaoui N, et al. cIAPs and XIAP regulate myelopoiesis through cytokine production in an RIPK1- And RIPK3-dependent manner. *Blood*. 2014;123(16):2562-2572.
275. Lawlor KE, Khan N, Mildenhall A, et al. RIPK3 promotes cell death and NLRP3 inflammasome activation in the absence of MLKL. *Nat Commun*. 2015 Feb 18;6:6282.
276. Micheau O, Tschopp J. Induction of TNF receptor I-mediated apoptosis via two sequential signaling complexes. *Cell*. 2003;114(2):181-190.
277. Ting AT, Bertrand MJM. More to Life than NF- κ B in TNFR1 Signaling. *Trends Immunol*. 2016;37(8):535-545.
278. Wang L, Du F, Wang X. TNF- α Induces Two Distinct Caspase-8 Activation Pathways. *Cell*. 2008;133(4):693-703.
279. Brumatti G, Ma C, Lalaoui N, et al. The caspase-8 inhibitor emricasan combines with the SMAC mimetic birinapant to induce necroptosis and treat acute myeloid leukemia. *Sci Transl Med*. 2016;8(339):339ra69-339ra69.
280. Ashkenazi A. Targeting death and decoy receptors of the tumour-necrosis factor superfamily. *Nat Rev Cancer*. 2002;2(6):420-430.
281. Silke J, Rickard JA, Gerlic M. The diverse role of RIP kinases in necroptosis and

inflammation. *Nat Immunol.* 2015;16(7):689-697.

282. Tenev T, Bianchi K, Darding M, et al. The Ripoptosome, a Signaling Platform that Assembles in Response to Genotoxic Stress and Loss of IAPs. *Mol Cell.* 2011;43(3):432-448.

283. Donnell MAO, Perez-jimenez E, Oberst A, et al. Caspase 8 inhibits programmed necrosis by processing CYLD. *Nat Cell Biol.* 2011;13(12):1437-1442.

284. Murphy JM, Czabotar PE, Hildebrand JM, et al. Article The Pseudokinase MLKL Mediates Necroptosis via a Molecular Switch Mechanism. *Immunity.* 2013;39(3):443-453.

285. Wu J, Huang Z, Ren J, et al. Mkl1 knockout mice demonstrate the indispensable role of Mkl1 in necroptosis. *Cell Res.* 2013;23(8):994-1006.

286. Bertrand MJ, Milutinovic S, Dickson KM, et al. cIAP1 and cIAP2 Facilitate Cancer Cell Survival by Functioning as E3 Ligases that Promote RIP1 Ubiquitination. *Mol Cell.* 2008 Jun 20;30(6):689-700.

287. Gentle IE, Moelter I, Lechler N, et al. Inhibitor of apoptosis proteins (IAPs) are required for effective T cell expansion/survival during anti-viral immunity in mice. *Blood.* 2013;123(5):659-669.

288. Feoktistova M, Geserick P, Kellert B, et al. cIAPs Block Ripoptosome Formation, a RIP1/Caspase-8 Containing Intracellular Cell Death Complex Differentially Regulated by cFLIP Isoforms. *Mol Cell.* 2011;43(3):449-463.

289. Lawlor KE, Feltham R, Yabal M, et al. XIAP Loss Triggers RIPK3- and Caspase-8-Driven IL-1 β Activation and Cell Death as a Consequence of TLR-MyD88-Induced cIAP1-TRAF2 Degradation. *Cell Rep.* 2017;20(3):668-682.

290. Wicki S, Gurzeler U, Wei-Lynn Wong W, Jost PJ, Bachmann D, Kaufmann T. Loss of XIAP facilitates switch to TNF α -induced necroptosis in mouse neutrophils. *Cell Death Dis.* 2016;7(10):e2422.

291. Boatright KM, Renatus M, Scott FL, et al. A unified model for apical caspase activation. *Mol Cell.* 2003;11(2):529-541.

292. Ashkenazi A, Dixit V. Death receptors: signaling and modulation. *Science.* 1998;281(August):1305-1308.

293. Fischer U, Jänicke RU, Schulze-Osthoff K. Many cuts to ruin: a comprehensive update of caspase substrates. *Cell Death Differ.* 2003;10(1):76-100.

294. Fuentes-Prior P, Salvesen GS. The protein structures that shape caspase activity, specificity, activation and inhibition. *Biochem J.* 2004;384(Pt 2):201-232.

295. Jänicke RU, Sprengart ML, Wati MR, Porter AG. Caspase-3 is required for DNA fragmentation and morphological changes associated with apoptosis. *J Biol Chem.* 1998;273(16):9357-9360.
296. Wolf BB, Schuler M, Echeverri F, Green DR. Caspase-3 is the primary activator of apoptotic DNA fragmentation via DNA fragmentation factor-45/inhibitor of caspase-activated DNase inactivation. *J Biol Chem.* 1999;274(43):30651-30656.
297. Walsh JG, Cullen SP, Sheridan C, Luthi AU, Gerner C, Martin SJ. Executioner caspase-3 and caspase-7 are functionally distinct proteases. *Proc Natl Acad Sci USA.* 2008;105(35):12815-12819.
298. Lamkanfi M, Kanneganti TD. Caspase-7: A protease involved in apoptosis and inflammation. *Int J Biochem Cell Biol.* 2010;42(1):21-24.
299. Silke J, Ekert PG, Day CL, et al. Direct inhibition of caspase 3 is dispensable for the anti-apoptotic activity of XIAP. *EMBO J.* 2001 Jun 15; 20(12): 3114–3123.
300. Shiozaki EN, Chai J, Rigotti DJ, et al. Mechanism of XIAP-Mediated Inhibition of Caspase-9. *Mol Cell.* 2003;11:519-527.
301. Huang Y, Park YC, Rich RL, Segal D, Myszka DG, Wu H. Structural Basis of Caspase Inhibition by XIAP : Differential Roles of the Linker versus the BIR Domain. *Cell.* 2001;104:781-790.
302. Liu Z, Sun C, Olejniczak ET, et al. Structural basis for binding of Smac/DIABLO to the XIAP BIR3 domain. *Nature.* 2000;408(6815):1004-1008.
303. Yang Y, Fang S, Jensen JP, Weissman AM. Ubiquitin Protein Ligase Activity of IAPs and Their Degradation in Proteasomes in Response to Apoptotic Stimuli. *Science.* 2000;288(May):874-878.
304. Schile AJ, García-fernández M, Steller H. Regulation of apoptosis by XIAP ubiquitin-ligase activity. *Genes Dev.* 2008 Aug 15;22(16):2256-66.
305. Günther C, Martini E, Wittkopf N, et al. Caspase-8 regulates TNF- α -induced epithelial necroptosis and terminal ileitis. *Nature.* 2011 Sep 14;477(7364):335-9.
306. Kang T, Yang S, Toth B, Kovalenko A, Wallach D. Article Caspase-8 Blocks Kinase RIPK3-Mediated Activation of the NLRP3 Inflammasome. *Immunity.* 2013;38(1):27-40.
307. Van de Veerdonk FL, Netea MG, Dinarello CA, Joosten LAB. Inflammasome activation and IL-1 β and IL-18 processing during infection. *Trends Immunol.* 2011;32(3):110-116.
308. Guo H, Callaway JB, Ting JP-Y. Inflammasomes: mechanism of action, role in

- disease, and therapeutics. *Nat Med*. 2015;21(7):677-687.
309. Wada T, Kanegane H, Ohta K, et al. Sustained elevation of serum interleukin-18 and its association with hemophagocytic lymphohistiocytosis in XIAP deficiency. *Cytokine*. 2014;65(1):74-78.
310. Lopez-Granados E, Stacey M, Kienzler AK, et al. A mutation in X-linked inhibitor of apoptosis (G466X) leads to memory inflation of Epstein-Barr virus-specific T cells. *Clin Exp Immunol*. 2014;178(3):470-482.
311. Aguilar C, Latour S. X-linked Inhibitor of Apoptosis Protein Deficiency: More than an X-linked Lymphoproliferative Syndrome. *J Clin Immunol*. 2015;35(4):331-338.
312. Ono S, Okano T, Hoshino A, et al. Hematopoietic Stem Cell Transplantation for XIAP Deficiency in Japan. *J Clin Immunol*. 2016.
313. Yamaguchi K, Shirakabe K, Shibuya H, et al. Identification of a member of the MAPKKK family as a potential mediator of TGF-beta signal transduction. *Science*. 1995 Dec 22;270(5244):2008-11.
314. Wang C, Deng L, Hong M, Akkaraju GR, Inoue JI, Chen ZJ. TAK1 is a ubiquitin-dependent kinase of MKK and IKK. *Nature*. 2001;412(6844):346-351.
315. Lu M, Lin SC, Huang Y, et al. XIAP Induces NF- κ B Activation via the BIR1/TAB1 Interaction and BIR1 Dimerization. *Mol Cell*. 2007;26(5):689-702.
316. Hofer-Warbinek R, Schmid JA, Stehlik C, Binder BR, Lipp J, De Martin R. Activation of NF- κ B by XIAP, the X chromosome-linked inhibitor of apoptosis, in endothelial cells involves TAK1. *J Biol Chem*. 2000;275(29):22064-22068.
317. Hirata Y, Takahashi M, Morishita T, Noguchi T, Matsuzawa A. Post-translational modifications of the TAK1-TAB complex. *Int J Mol Sci*. 2017;18(1):1-17.
318. Hsieh W, Chuang Y, Chiang IH, et al. Inability to resolve specific infection generates innate immunodeficiency syndrome in *Xiap*^{-/-} mice. *Blood*. 2014 Oct 30;124(18):2847-57.
319. Taylor PR, Tsoni SV, Willment JA, et al. Dectin-1 is required for β -glucan recognition and control of fungal infection. *Nat Immunol*. 2007;8(1):31-38.
320. Zhou H, Wertz I, Rourke KO, et al. Bcl10 activates the NF- κ B pathway through ubiquitination of NEMO. *Nature*. 2004 Jan 8;427(6970):167-71.
321. Latour S, Aguilar C. XIAP deficiency syndrome in humans. *Semin Cell Dev Biol*. 2015;39:115-123.
322. Krieg A, Correa RG, Garrison JB, et al. XIAP mediates NOD signaling via interaction with RIP2. *Proc Natl Acad Sci USA*. 2009 Aug 25;106(34):14524-9.

323. Damgaard RB, Nachbur U, Yabal M, et al. The Ubiquitin Ligase XIAP Recruits LUBAC for NOD2 Signaling in Inflammation and Innate Immunity. *Mol Cell*. 2012;46(6):746-758.
324. Damgaard RB, Fiil BK, Speckmann C, et al. Disease-causing mutations in the XIAP BIR2 domain impair NOD2-dependent immune signalling. *EMBO Mol Med*. 2013;5(8):1278-1295.
325. Bauler LD, Duckett CS, O’Riordan MXD. XIAP regulates cytosol-specific innate immunity to listeria infection. *PLoS Pathog*. 2008;4(8).
326. Hsu YS, Zhang Y, You Y, et al. The adaptor protein CARD9 is required for innate immune responses to intracellular pathogens. *Nat Immunol*. 2007;8(2):198-205.
327. Prakash H, Albrecht M, Becker D, Kuhlmann T, Rudel T. Deficiency of XIAP leads to sensitization for Chlamydomydia pneumoniae pulmonary infection and dysregulation of innate immune response in mice. *J Biol Chem*. 2010;285(26):20291-20302.
328. Gérard S, Sibérel S, Martin E, et al. Human iNKT and MAIT cells exhibit a PLZF-dependent proapoptotic propensity that is counterbalanced by XIAP. *Blood*. 2013;121(4):614-623.
329. Marsh RA, Villanueva J, Kim M, et al. Patients with X-linked lymphoproliferative disease due to BIRC4 mutation have normal invariant natural killer T-cell populations. *Clin Immunol*. 2009 Jul;132(1):116-23.
330. Marsh R a, Rao K, Satwani P, et al. Allogeneic hematopoietic cell transplantation for XIAP deficiency: an international survey reveals poor outcomes. *Blood*. 2013;121(6):877-883.
331. Harlin H, Harlin H, Reffey SB, et al. Characterization of XIAP-deficient mice. *Mol Cell Biol*. 2001;21(10):3604-3608.
332. Pfeffer K, Matsuyama T, Kundig TM, et al. Mice deficient for the 55kd tumor necrosis factor receptor are resistant to endotoxic shock yet succumb to L. monocytogenes infection. *Cell*. 1993;73:457-467.
333. Mombaerts P, Iacomini J, Johnson RS, Herrup K, Tonegawa S, Papaioannou VE. RAG-1-deficient mice have no mature B and T lymphocytes. *Cell*. 1992;68(5):869-877.
334. Newton K, Sun X, Dixit VM. Kinase RIP3 is dispensable for normal NF-kappa Bs, signaling by the B-cell and T-cell receptors, tumor necrosis factor receptor 1, and Toll-like receptors 2 and 4. *Mol Cell Biol*. 2004;24(4):1464-1469.
335. Andree M, Seeger JM, Schüll S, et al. BID-dependent release of mitochondrial SMAC dampens XIAP-mediated immunity against Shigella. *EMBO J*.

2014;33(19):2171-2187.

336. Madison BB, Dunbar L, Qiao XT, Braunstein K, Braunstein E, Gumucio DL. Cis Elements of the Villin Gene Control Expression in Restricted Domains of the Vertical (Crypt) and Horizontal (Duodenum, Cecum) Axes of the Intestine. *J Biol Chem*. 2002;277(36):33275-33283.

337. Clausen BE, Burkhardt C, Reith W, Renkawitz R, Förster I. Conditional gene targeting in macrophages and granulocytes using LysMcre mice. *Transgenic Res*. 1999;8(4):265-277.

338. Watson AJM, Chu S, Sieck L, et al. Epithelial barrier function in vivo is sustained despite gaps in epithelial layers. *Gastroenterology*. 2005;129(3):902-912.

339. Wirtz S, Neufert C, Weigmann B, Neurath MF. Chemically induced mouse models of intestinal inflammation. *Nat Protoc*. 2007;2(3):541-546.

340. Zeissig S, Murata K, Sweet L, et al. Hepatitis B virus–induced lipid alterations contribute to natural killer T cell–dependent protective immunity. *Nat Med*. 2012;18(7):1060-1068.

341. Bjerknes M, Cheng H. Methods for the isolation of intact epithelium from the mouse intestine. *Anat Rec*. 1981;199(4):565-574.

342. Danielle C. In vitro cDNA amplification from individual intestinal crypts. *Exp Cell Res*. 1993;208:344-349.

343. Ayabe T, Ashida T, Kohgo Y, Kono T. The role of Paneth cells and their antimicrobial peptides in innate host defense. *Trends Microbiol*. 2004 Aug;12(8):394-8.

344. Kozich JJ, Westcott SL, Baxter NT, Highlander SK, Schloss PD. Development of a dual-index sequencing strategy and curation pipeline for analyzing amplicon sequence data on the miseq illumina sequencing platform. *Appl Environ Microbiol*. 2013;79(17):5112-5120.

345. Magoč T, Salzberg SL. FLASH: Fast length adjustment of short reads to improve genome assemblies. *Bioinformatics*. 2011;27(21):2957-2963.

346. Edgar RC. UPARSE: Highly accurate OTU sequences from microbial amplicon reads. *Nat Methods*. 2013;10(10):996-998.

347. Wang Q, Garrity GM, Tiedje JM, Cole JR. Naïve Bayesian classifier for rapid assignment of rRNA sequences into the new bacterial taxonomy. *Appl Environ Microbiol*. 2007;73(16):5261-5267.

348. Edgar RC. Search and clustering orders of magnitude faster than BLAST.

- Bioinformatics*. 2010;26(19):2460-2461.
349. Dixon P. VEGAN, a package of R functions for community ecology. *J Veg Sci*. 2003;14(6):927-930.
350. Durand A, Donahue B, Peignon G, et al. Functional intestinal stem cells after Paneth cell ablation induced by the loss of transcription factor Math1 (Atoh1). *Proc Natl Acad Sci USA*. 2012;109(23):8965-8970.
351. Kim T-H, Escudero S, Shivdasani RA. Intact function of Lgr5 receptor-expressing intestinal stem cells in the absence of Paneth cells. *Proc Natl Acad Sci USA*. 2012;109(10):3932-3937.
352. Hörnle M, Peters N, Thayaparasingham B, Vörsmann H, Kashkar H, Kulms D. Caspase-3 cleaves XIAP in a positive feedback loop to sensitize melanoma cells to TRAIL-induced apoptosis. *Oncogene*. 2011;30(5):575-587.
353. Srinivasula SM, Hegde R, Saleh A, et al. A conserved XIAP-interaction motif in caspase-9 and Smac/DIABLO regulates caspase activity and apoptosis. *Nature*. 2001;410(6824):112-116.
354. Vince JE, Wong WWL, Gentle I, et al. Inhibitor of Apoptosis Proteins Limit RIP3 Kinase-Dependent Interleukin-1 Activation. *Immunity*. 2012;36(2):215-227.
355. Couturier-Maillard A, Secher T, Rehman A, et al. NOD2-mediated dysbiosis predisposes mice to transmissible colitis and colorectal cancer. *J Clin Invest*. 2013;123(2):700-711.
356. Shi J, Aono S, Lu W, et al. A Novel Role for Defensins in Intestinal Homeostasis: Regulation of IL-1B Secretion. *J Immunol*. 2007;179(2):1245-1253.
357. Laroui H, Ingersoll SA, Liu HC, et al. Dextran sodium sulfate (dss) induces colitis in mice by forming nano-lipocomplexes with medium-chain-length fatty acids in the colon. *PLoS One*. 2012;7(3).
358. Chassaing B, Aitken JD, Malleshappa M, Vijay-Kumar M. Dextran sulfate sodium (DSS)-induced colitis in mice. *Curr Protoc Immunol*. 2014;(SUPPL.104):1-14.
359. Axelsson LG, Landstrom E, Goldschmidt TJ, Gronberg A, Bylund-Fellenius AC. Dextran sulfate sodium (DSS) induced experimental colitis in immunodeficient mice: effects in CD4(+) -cell depleted, athymic and NK- cell depleted SCID mice. *Inflamm Res*. 1996;45(4):181-191.
360. Liu T-C, Gurram B, Baldridge MT, et al. Paneth cell defects in Crohn's disease patients promote dysbiosis. *JCI Insight*. 2016;1(8):1-15.
361. Simms LA, Doecke JD, Walsh MD, Huang N, Fowler E V, Radford-Smith GL.

- Reduced α -defensin expression is associated with inflammation and not NOD2 mutation status in ileal Crohn's disease. *Gut*. 2008;57(7):903-910.
362. Kontoyiannis D, Pasparakis M, Pizarro TT, Cominelli F, Kollias G. Impaired On/Off Regulation of TNF Biosynthesis in Mice Lacking TNF AU-Rich Elements. *Immunity*. 1999;10(3):387-398.
363. Schaubeck M, Clavel T, Calasan J, et al. Dysbiotic gut microbiota causes transmissible Crohn's disease-like ileitis independent of failure in antimicrobial defence. *Gut*. 2015:1-13.
364. Hampe J, Cuthbert A, Croucher PJ. Association between insertion mutation in NOD2 gene and Crohn's disease in German and British population. *Lancet*. 2001;357:1925-1928.
365. Vince JE, Wong WWL, Gentle I, et al. Inhibitor of Apoptosis Proteins Limit RIP3 Kinase-Dependent Interleukin-1 Activation. *Immunity*. 2012;36(2):215-227.
366. Powell N, Walker AW, Stolarczyk E, et al. The Transcription Factor T-bet Regulates Intestinal Inflammation Mediated by Interleukin-7 Receptor+ Innate Lymphoid Cells. *Immunity*. 2012;37(4):674-684.
367. Waidmann M, Bechtold O, Frick JS, et al. *Bacteroides vulgatus* protects against *Escherichia coli*-induced colitis in gnotobiotic interleukin-2-deficient mice. *Gastroenterology*. 2003;125(1):162-177.
368. Schultz M, Tonkonogy SL, Sellon RK, et al. IL-2-deficient mice raised under germfree conditions develop delayed mild focal intestinal inflammation. *Am J Physiol*. 1999;276(6):G1461 LP-G1472.
369. Kaser A, Lee AH, Franke A, et al. XBP1 Links ER Stress to Intestinal Inflammation and Confers Genetic Risk for Human Inflammatory Bowel Disease. *Cell*. 2008;134(5):743-756.
370. Sugimoto K. Role of STAT3 in inflammatory bowel disease. *World J Gastroenterol*. 2008;14(33):5110-5114.
371. Yamamoto M, Yoshizaki K, Kishimoto T, Ito H. IL-6 Is Required for the Development of Th1 Cell-Mediated Murine Colitis. *J Immunol*. 2000;164(9):4878-4882.
372. Carey R, Jurickova I, Ballard E, et al. Activation of an IL-6:STAT3-dependent transcriptome in pediatric-onset inflammatory bowel disease. *Inflamm Bowel Dis*. 2008;14(4):446-457.
373. Reinecker H-C, Loh EY, Ringler DJ, Mehta A, Rombeau JL, MacDermott RP. Monocyte-chemoattractant protein 1 gene expression in intestinal epithelial cells and

- inflammatory bowel disease mucosa. *Gastroenterology*. 1995;108(1):40-50.
374. Khan WI, Motomura Y, Wang H, et al. Critical role of MCP-1 in the pathogenesis of experimental colitis in the context of immune and enterochromaffin cells. *Am J Physiol Liver Physiol*. 2006;291(5):G803-G811.
375. Amininejad L, Charlotheaux B, Theatre E, et al. Analysis of Genes Associated with Monogenic Primary Immunodeficiency Identifies Rare Variants in XIAP in Patients With Crohn's disease. *Gastroenterology*. 2018.
376. Yang X, Kanegane H, Nishida N, et al. Clinical and genetic characteristics of XIAP deficiency in Japan. *J Clin Immunol*. 2012;32(3):411-420.

Appendix

List of Abbreviations

ADAM	a disintegrin and metalloproteinase
AMP	antimicrobial peptide
Ang4	angiogenin 4
APC	antigen presenting cell
BIR	baculovirus inhibitor of apoptosis protein repeat
CBC	crypt base columnar cells
CD	Crohn's disease
CEACAM6	carcinoembryonic antigen-related cell adhesion molecule 6
clAP	cellular inhibitor of apoptosis protein
CRAMP	cathelicidin-related antimicrobial peptide
DC	dendritic cells
DCV	dense core vesicles
Defa	α -defensin
Dll4	delta-like canonical notch ligand 4
DNA	deoxyribonucleic acid
DSS	dextran sulfate sodium
EBV	Epstein-Barr virus
EEC	enteroendocrine cells
EGF	epidermal growth factor
ER	endoplasmic reticulum
FAE	follicle-associated epithelium
FISH	fluorescence <i>in situ</i> hybridization
FOXP3	forkhead box P3
GALT	gut-associated lymphoid tissue
GIT	gastrointestinal tract
GF	germ-free
GWAS	genome wide association study
HD	human alpha defensin
IAP	inhibitor of apoptosis protein
IBD	Inflammatory bowel disease
IEC	intestinal epithelial cell

IL-	interleukin
ILC	innate lymphoid cell
iNKT	invariant natural killer T
ISC	intestinal stem cell
Itf	intestinal trefoil factor
Lgr	leucine-rich repeat-containing G-protein coupled receptors
LPS	lipopolysaccharide
LUBAC	linear ubiquitin chain assembly complex
LyzC	lysozyme C
Lyz1	lysozyme C-1
MAMPs	microbe-associated molecular patterns
MAPK	mitogen-activated protein kinase
MATH1	atonal bHLH transcription factor 1
MCP-1	monocyte chemoattractant protein 1
MDP	muramyl dipeptide
MSC	mesenchymal cells
MMP7	matrix metalloproteinase-7
MNV	Murine norovirus
MUC	mucin
MyD88	myeloid differentiation primary response gene 88
NGS	next-generation sequencing
NF- κ B	nuclear factor kappa-light-chain-enhancer of activated B cells
NKT cell	natural killer T cell
NLRs	nucleotide-binding and oligomerization domain (NOD)-like receptors
NOD1/2	nucleotide-binding oligomerization domain-containing protein 1/2
PC	Paneth cell
PRRs	pattern recognition receptors
RA	retinoic acid
RAG1	recombination activating gene 1
REG3 γ	regenerating islet-derived protein 3 γ
RING	really interesting new gene
RIPK	receptor-interacting serine/threonine-protein kinase 1
RNA	ribonucleic acid
SFB	segmented filamentous bacteria

SMAC	second mitochondria-derived activator of caspase
STAT3	signal transducer and activator of transcription 3
TAB1	TAK-binding protein 1
TAK1	transforming growth factor beta-activated kinase 1
TGF α	transforming growth factor beta
TJ	tight junction
TLRs	toll-like receptors
TNF	tumor necrosis factor
TNFR	tumor necrosis factor receptor
TRAF2	tumor necrosis factor receptor-associated factor-2
Tregs	regulatory T cells
UBA	ubiquitin-associated
UC	ulcerative colitis
WNT	Wingless/Int
Xbp1	X-box binding protein 1
XIAP	X-linked inhibitor of apoptosis protein
XLP-2	X-linked lymphoproliferative syndrome 2

List of figures

Figure 1.1 The intestinal epithelium _____	4
Figure 1.2 PC functions in the gut _____	13
Figure 1.3 Schematic representation of the different domains of XIAP _____	25
Figure 1.4 TNFR1-dependent cell survival pathway _____	26
Figure 1.5 TNFR1-dependent cell death pathway _____	27
Figure 1.6 XIAP- dependent control of the ripoptosome _____	29
Figure 1.7 XIAP-dependent control of caspase-mediated apoptosis _____	31
Figure 1.8 XIAP-dependent control of the inflammasome pathway _____	33
Figure 1.9 XIAP-dependent regulation of TGF- β and BMP signaling _____	34
Figure 1.10 XIAP-dependent control of the fungal infections _____	35
Figure 1.11 XIAP-dependent control of the NOD1/2 signaling pathway _____	36
Figure 2.1 Acute and chronic infection models of <i>H. hepaticus</i> infection _____	50
Figure 2.2 Acute and chronic infection models of DSS-induced colitis _____	55
Figure 3.1 XIAP regulates PC homeostasis _____	58
Figure 3.2 Unaltered numbers of goblet cells and enteroendocrine cells in <i>Xiap</i> ^{-/-} mice _____	59
Figure 3.3 Unaltered stem cell numbers in in <i>Xiap</i> ^{-/-} mice _____	60
Figure 3.4 Increased PC apoptosis in in <i>Xiap</i> ^{-/-} mice _____	61
Figure 3.5 PC death in in <i>Xiap</i> ^{-/-} mice is abrogated by the deletion of <i>Tnfr1</i> _____	62
Figure 3.6 PC defects in in <i>Xiap</i> ^{-/-} mice are mediated by RIPK3 signaling pathway _____	63
Figure 3.7 PC death in <i>Xiap</i> ^{-/-} mice is mediated by the commensal microbiota _____	64
Figure 3.8 XIAP-dependent regulation of microbial abundance in the gut _____	65
Figure 3.9 XIAP-dependent regulation of intestinal microbial composition _____	67
Figure 3.10 Absence of spontaneous inflammation in the ileum of <i>Xiap</i> ^{-/-} mice _____	68
Figure 3.11 Absence of spontaneous inflammation in the colon of <i>Xiap</i> ^{-/-} mice _____	68
Figure 3.12 No evidence of small intestinal inflammation in <i>Xiap</i> ^{-/-} mice _____	69
Figure 3.13 Granulomatous ileitis in <i>Xiap</i> ^{-/-} mice but not WT mice exposed to <i>H. hepaticus</i> _____	71
Figure 3.14 Increased susceptibility to DSS-induced colitis in <i>Xiap</i> ^{-/-} mice _____	73
Figure 3.15 XIAP-dependent susceptibility to DSS-induced colitis is mediated by the innate immune system _____	74
Figure 3.16 Absence of PC loss in mice with PC-, IEC- and myeloid cell-specific deletion of <i>Xiap</i> _____	76

Figure 3.17 No increase in susceptibility to DSS colitis in <i>Xiap</i> ^{ΔIEC} mice	77
Figure 3.18 No increase in susceptibility to DSS colitis in <i>Xiap</i> ^{ΔPC} mice	78
Figure 3.19 No increase in susceptibility to DSS colitis in <i>Xiap</i> ^{ΔMYE} mice	79
Figure 4.1 Model of XIAP-dependent regulation of PC homeostasis and the commensal microbiota	80

List of tables

Table 1.1 Types of PC-AMP	8
Table 2.1 List of antibodies	39
Table 2.2 List of probes and primers	40
Table 2.3 Dehydration steps for staining	50

Declaration

I hereby declare the following:

1. Other than the guidance and advice offered by my supervisor Prof. Sebastian Zeissig, the research work was performed and the dissertation was written independently by me.
2. The thesis has not been submitted either partially or wholly as part of a doctoral degree to any another examining body. Moreover, the current work has neither been published nor submitted for publication.
3. The research work was performed according to the rules of good scientific practice of the German Research Foundation.

Dresden, June 2018

Shreya Gopalakrishnan

Curriculum Vitae

Personal details

Date of birth	02/06/1991
Place of birth	Chennai, India
Citizenship	Indian
Current residence	Hildebrandstrasse 7, apartment nr. 1103, 01219 Dresden, Germany

Education

University Education

Dec 2013- current	Doctoral studies in Immunology Thesis title: <i>“The role of X-linked inhibitor of apoptosis protein (XIAP) in intestinal homeostasis and the pathogenesis of Inflammatory bowel disease (IBD)”</i> Team: Prof. Dr. med. Sebastian Zeissig, DFG-Center for Regenerative Therapies Dresden, Germany
Sept 2012- Sept 2013:	Master of Science (MSc) Infection and Immunity Thesis title: <i>“Studies on Crohn’s disease associated molecule ADAMDEC-1”</i> Team: Prof. Anthony W. Segal, Center for Molecular Medicine, University

Sept 2008- July 2012:

College London (UCL), London, United Kingdom

Bachelor of Technology (B.Tech) in Biotechnology

Thesis title: "*Studies on Haemolysin isolated from Bacillus cereus BFE5400 isolated from Earthworm's gut*"

Team: Prof. Muthukumaran Sivanandham, SVCE, Anna University, Chennai, India

School Education

1995-2008

SBOA School & Junior College, Chennai, India

Publication

Philipp Rausch, Marijana Basic, Arvind Batra, Stephan C. Bischoff, Michael Blaut, Thomas Clavel, Joachim Gläsner, **Shreya Gopalakrishnan**, Guntram A. Grassl, Claudia Günther, Dirk Haller, Misa Hirose, Saleh Ibrahim, Gunnar Loh, Jochen Mattner, Stefan Nagel, Oliver Pabst, Franziska Schmidt, Britta Siegmund, Till Strowig, Valentina Volynets, Stefan Wirtz, Sebastian Zeissig, Yvonne Zeissig, André Bleich, John F. Baines, **Analysis of factors contributing to variation in the C57BL/6J fecal microbiota across German animal facilities. *Int J Med Microbiol.* 2016 Aug;306(5):343-55. doi: 10.1016/j.ijmm.2016.03.004**

Acknowledgements

Firstly, I would like to thank my supervisor Prof. Dr. med. Sebastian Zeissig for giving me an excellent opportunity to carry out my doctoral studies in his laboratory. Thank-you Sebastian, for your constant guidance, advice and great enthusiasm in your supervision. I very much enjoyed our scientific discussions, have learnt so much from you and will continue to look up to you for further guidance and inspiration!

Next, I want to thank Prof. Dr.Dr.h.c. Thomas C. G. Bosch for offering second supervision, Prof. Dr. rer. nat. Heiner Schäfer to have agreed to be an examiner in my disputation and Prof. Stanislav N. Gorb to have agreed to be the chairperson in my disputation.

Further, I would like to thank our collaborators Prof. André Bleich, Dr.rer.nat. Marijana Basic and Ms. Anna Smoczek at Hannover Medical School, Prof. John Baines, Dr. rer. nat. Jun Wang and Mrs. Katja Cloppenburg-Schmidt at Kiel University, and Prof. Michael Muders at University Hospital Bonn for discussions, organization and technical assistance with experiments in the project. I would also like to thank all my lab colleagues for several useful discussions that were very helpful for me during my studies. A special thanks to Dr. Yvonne Zeissig for her supervision and training that she offered me during the initial stages of my doctoral studies. Thanks to our lab manager Mrs. Melanie Jäger for all the help with genotyping the mice for the project. A big thanks to people who spent time reading my thesis- Emilie Huc Claustre, Maren Rudolf, Giuseppina Luzzi and Sandra Segeletz.

Lab life is much nicer with friends who were a lot of fun to work with! Thanks to Emilie, Pina, Marie, Maren, Tohid, Chiara and Yuting for this. I had a fantastic time with all of you.

A special thanks to my best friend Emilie who has always believed in me, supported and advised me in several situations both professionally, and personally. I very much enjoyed our late evening insightful discussions about our projects and life!

Most importantly, I want to thank my mom Sundari, my dad Gopalakrishnan, my brother Krishnan and my cousin sister Anjana for their unconditional love, support and encouragement at all times.

Lastly, I want to thank the person who always brought out the best in me: Dinesh Krishnamoorthy. Thanks, Dinesh, for being very patient with me, a great inspiration, and an amazing partner! You have always encouraged me to do my best in life, and I look very forward to our life together!